NASA TECHNICAL NOTE

NASA TN D-3334

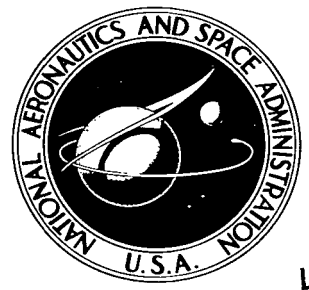

AERODYNAMIC DAMPING AND OSCILLATORY STABILITY IN PITCH AND YAW OF GEMINI CONFIGURATIONS AT MACH NUMBERS FROM 0.50 TO 4.63

by Bruce R. Wright and Robert A. Kilgore

Langley Research Center
Langley Station, Hampton, Va.

NATIONAL AERONAUTICS AND SPACE ADMINISTRATION • WASHINGTON, D. C. • MARCH 1966

ERRATA

NASA Technical Note D-3334

AERODYNAMIC DAMPING AND OSCILLATORY STABILITY IN PITCH AND YAW OF GEMINI CONFIGURATIONS AT MACH NUMBERS FROM 0.50 TO 4.63

By Bruce R. Wright and Robert A. Kilgore

March 1966

Pages 8 and 11: The photographs on pages 8 and 11 were inadvertently misplaced in assembly of this report and, as is obvious from the discussion, photo L-63-1939.1 should be on page 11 and photo L-65-9039 should be on page 8.

NASA-Langley, 1966

Issued 10-19-66

NASA TN D-3334

AERODYNAMIC DAMPING AND OSCILLATORY STABILITY IN PITCH AND YAW OF GEMINI CONFIGURATIONS AT MACH NUMBERS FROM 0.50 TO 4.63

By Bruce R. Wright and Robert A. Kilgore

Langley Research Center
Langley Station, Hampton, Va.

NATIONAL AERONAUTICS AND SPACE ADMINISTRATION

For sale by the Clearinghouse for Federal Scientific and Technical Information
Springfield, Virginia 22151 – Price $1.05

AERODYNAMIC DAMPING AND OSCILLATORY STABILITY IN PITCH AND YAW OF GEMINI CONFIGURATIONS AT MACH NUMBERS FROM 0.50 TO 4.63

By Bruce R. Wright and Robert A. Kilgore
Langley Research Center

SUMMARY

Wind-tunnel measurements of the aerodynamic damping and oscillatory stability in pitch and yaw for 0.10-scale models of proposed Gemini abort and reentry configurations have been made at Mach numbers from 0.50 to 4.63 by using a 2° amplitude forced-oscillation mechanism. The damping and oscillatory-stability parameters in pitch were obtained at mean angles of attack in the approximate ranges of $\pm 45^{\circ}$ from 0° and $\pm 45^{\circ}$ from 180° with the models at an angle of sideslip of 0°. (Both angle of attack and angle of sideslip are defined as 0° when the antenna housing points into the wind.) The damping and oscillatory-stability parameters in yaw were determined at mean angles of sideslip near 0° and 180° with the models at an angle of attack of 0°. Tests were made to determine the effect of canting the front face of the antenna housing 18°.

Both the abort and reentry configurations with the antenna housing forward (mean angles of attack from about -50° to 50°) generally exhibit positive or near-zero damping in pitch for all Mach numbers, but the abort configuration exhibits negative damping at the higher mean angles of attack for low supersonic Mach numbers. Canting the face of the antenna housing to an angle of 18° has little effect on the damping for the abort configuration or the reentry configuration with the antenna housing forward.

Both the abort and reentry configurations with the antenna housing forward are unstable throughout the range of mean angle of attack at the lowest test Mach number but stable throughout the range of mean angle of attack at the higher test Mach numbers. For the intermediate Mach numbers, regions of stability are present at the lower positive and negative mean angles of attack. Canting the face of the antenna housing to an angle of 18° for the reentry configuration with the antenna housing forward decreases the stability near 0° mean angle of attack at all Mach numbers; however, canting the face of the antenna housing of the abort configuration with the antenna housing forward has little effect on the stability.

The abort and reentry configurations with the antenna housing rearward generally exhibit negative or zero damping in pitch over a varying range of mean angle of attack near 180°. Both configurations are generally stable up to about $\pm 25^{\circ}$ from 180°.

In general, the yawing characteristics are very similar to the pitching characteristics for both the abort and reentry configurations.

INTRODUCTION

In order to predict accurately the behavior of the Gemini abort and reentry configurations in the atmosphere, both the static- and dynamic-stability parameters for the two configurations must be known. Although stability parameters for simple bodies may at times be obtained by theoretical methods, an experimental approach is usually necessary for complicated bodies, such as Gemini, because of unpredictable airflow behavior. Therefore, an experimental research program has been conducted by the National Aeronautics and Space Administration to determine the aerodynamic parameters of proposed Gemini configurations. As a part of this program, wind-tunnel tests have been made to measure the aerodynamic-damping and oscillatory-stability parameters in pitch and in yaw for 0.10-scale models of proposed Gemini abort and reentry configurations. The results of these tests are presented herein.

Because of the asymmetry in the Gemini configurations with respect to the XY-plane produced by the offset center of mass and asymmetrically located deep-set observation windows, it was considered necessary to measure the aerodynamic damping and oscillatory stability in pitch through both a positive and a negative range of angle of attack. Therefore, the tests in pitch were made at mean angles of attack in the approximate ranges of $\pm 45^{\circ}$ from 0° and $\pm 45^{\circ}$ from 180° at an angle of sideslip of 0°. Measurements of the damping and oscillatory stability in yaw were made through an angle-of-sideslip range. Inasmuch as the configurations are generally symmetrical with respect to the XZ-plane, the tests in yaw were made through either a positive or a negative range of mean angle of sideslip near 0° and 180° with the models at an angle of attack of 0°.

Limited space within the model did not permit the oscillation axis of the balance to be located at the proposed center-of-mass location for the reentry configuration at mean angles of attack near 30°. The model of the reentry configuration, therefore, was tested with the oscillation axis at the abort center-of-mass location for mean angles of attack near 30°. In order to determine whether the data so obtained might be applicable to the reentry configuration, tests were also made of the reentry configuration with the oscillation axis located at both the reentry and the abort center-of-mass locations for mean angles of attack near 0°, -30°, and 180°.

Canting the front face of the antenna housing 18° was considered as a means of making the reentry configuration with the antenna housing forward longitudinally unstable in order to insure heat-shield-forward orientation during reentry. However, the destabilizing effect of the cant must not cause instability of the abort configuration. Therefore,

the tests in pitch were made with 0^{o} and 18^{o} cant for the abort configuration as well as for the reentry configuration.

The data were obtained at selected Mach numbers from 0.50 to 4.63 by using a 2^{o} amplitude forced-oscillation mechanism. The Reynolds number, based on the diameter of the heat shield, varied from about 1.6×10^{6} to 3.4×10^{6}. The reduced-frequency parameter varied from 0.0045 to 0.0795 for the tests in pitch and from 0.0090 to 0.0775 for the tests in yaw.

SYMBOLS

Measurements for this investigation are given in the International System of Units (SI). Equivalent values are indicated herein parenthetically in U.S. Customary Units. Details concerning the use of SI, together with physical constants and conversion factors, are given in reference 1.

The aerodynamic parameters are referred to the body system of axes, as shown in sketch (a), in which the coefficients, angles, and angular velocities are shown in the positive sense.

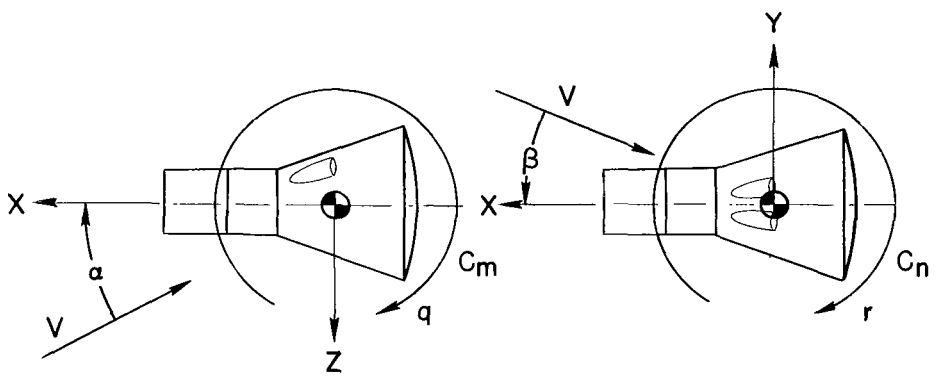

Sketch (a)

These axes originate at the centers of oscillation of the models, as shown in sketches (b) and (c) presented in the section on "Models." The equations which were used to reduce the dimensional aerodynamic parameters of the model to nondimensional aerodynamic parameters are presented in the section on "Measurements and Reduction of Data."

A reference area, $\pi\left(\frac{d}{2}\right)^{2}$, 0.0411 meter^{2} $\left(0.442 \text{ foot}^{2}\right)$

C_m pitching-moment coefficient, $\frac{\text{Pitching moment}}{q_\infty Ad}$ (see sketch (a))

$C_{m_q} = \frac{\partial C_m}{\partial\left(\frac{qd}{V}\right)}$ per radian

$C_{m_{\dot{q}}} = \frac{\partial C_m}{\partial\left(\frac{\dot{q}d^2}{V^2}\right)}$ per radian

$C_{m_\alpha} = \frac{\partial C_m}{\partial \alpha}$ per radian

$C_{m_{\dot{\alpha}}} = \frac{\partial C_m}{\partial\left(\frac{\dot{\alpha}d}{V}\right)}$ per radian

$C_{m_q} + C_{m_{\dot{\alpha}}}$ damping-in-pitch parameter, per radian

$C_{m_\alpha} - k^2 C_{m_{\dot{q}}}$ oscillatory-longitudinal-stability parameter, per radian

C_n yawing-moment coefficient, $\frac{\text{Yawing moment}}{q_\infty Ad}$ (see sketch (a))

$C_{n_r} = \frac{\partial C_n}{\partial\left(\frac{rd}{V}\right)}$ per radian

$C_{n_{\dot{r}}} = \frac{\partial C_n}{\partial\left(\frac{\dot{r}d^2}{V^2}\right)}$ per radian

$C_{n_\beta} = \frac{\partial C_n}{\partial \beta}$ per radian

$C_{n_{\dot{\beta}}} = \frac{\partial C_n}{\partial\left(\frac{\dot{\beta}d}{V}\right)}$ per radian

$C_{n_r} - C_{n_{\dot{\beta}}} \cos \alpha$ damping-in-yaw parameter, per radian

$C_{n_\beta} \cos \alpha + k^2 C_{n_{\dot{r}}}$ oscillatory-directional-stability parameter, per radian

d reference length, diameter of heat shield, 0.2286 meter (0.750 foot)

f frequency of oscillation, cycles/second

k	reduced-frequency parameter, $\frac{\omega d}{V}$, radians
M	free-stream Mach number
q	angular velocity of model about Y-axis, radians/second (see sketch (a))
q_∞	free-stream dynamic pressure, newtons/meter^2 (pounds/foot^2)
R	Reynolds number based on d
r	angular velocity of model about Z-axis, radians/second (see sketch (a))
V	free-stream velocity, meters/second (feet/second)
X,Y,Z	body system of axes
α	angle of attack, degrees or radians or mean angle of attack, degrees (see sketch (a))
β	angle of sideslip, degrees or radians or mean angle of sideslip, degrees (see sketch (a))
ω	angular velocity, $2\pi f$, radians/second

A dot over a quantity denotes the first derivative with respect to time. The expression $\cos \alpha$ appears in the damping-in-yaw and oscillatory-directional-stability parameters because these parameters are expressed in the body system of axes.

APPARATUS

Models

The Gemini abort configuration consists of the antenna housing, the cabin section, and the abort-stabilization and retro-rocket module. The more important design dimensions of the 0.10-scale model of the Gemini abort configuration are given in sketch (b). Linear dimensions are in meters. This configuration is shown with the antenna housing having an uncanted front face, which is hereinafter referred to as the 0^o cant. The dashed lines indicate a modification of the antenna housing which was necessary for sting clearance for tests of either the abort or the reentry configuration when either angle of attack or angle of sideslip was near 180^o.

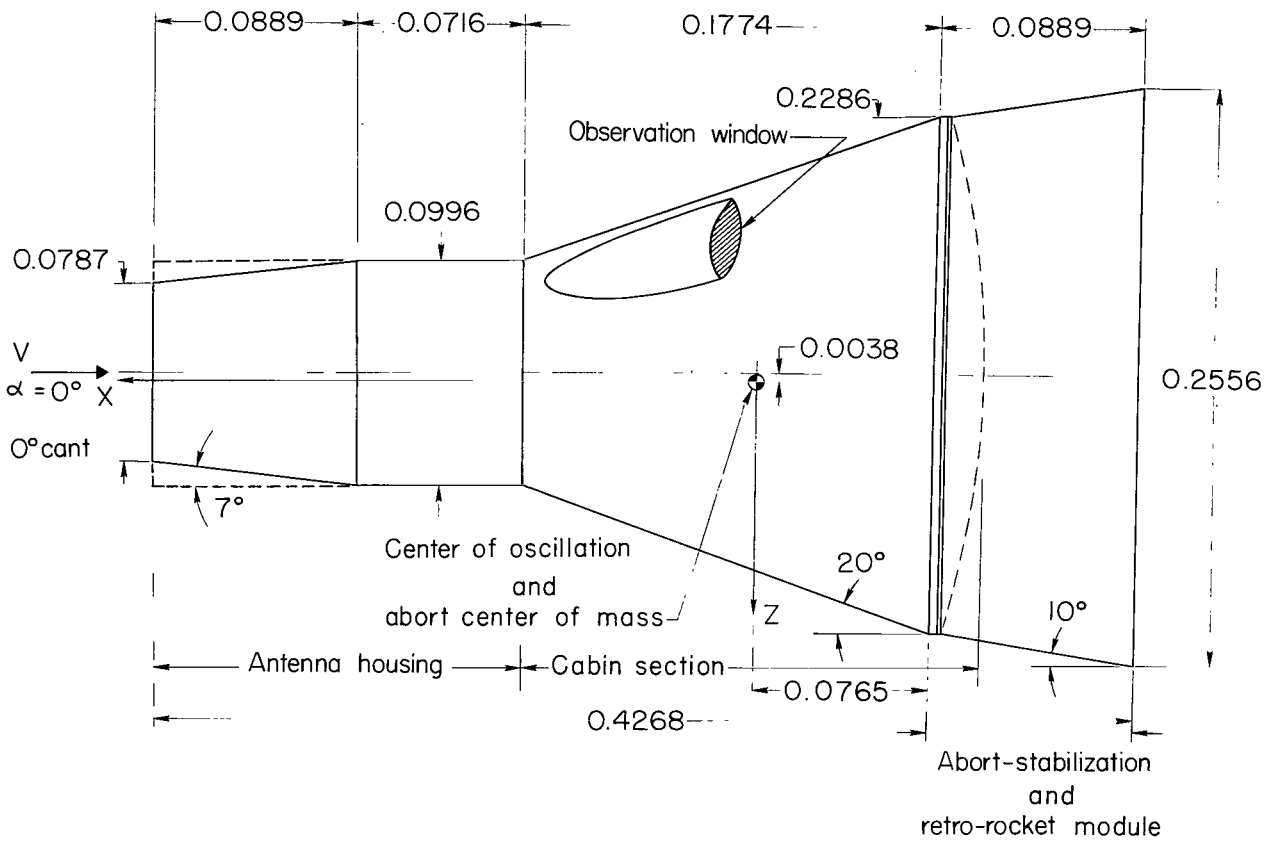

Sketch (b)

The Gemini reentry configuration is identical to the abort configuration except that the abort-stabilization and retro-rocket module is removed. The more important design dimensions of the 0.10-scale model of the Gemini reentry configuration are given in sketch (c). Linear dimensions are in meters. This configuration is shown with the antenna housing having a front face canted 18^{o}, which is hereinafter referred to as the 18^{o} cant.

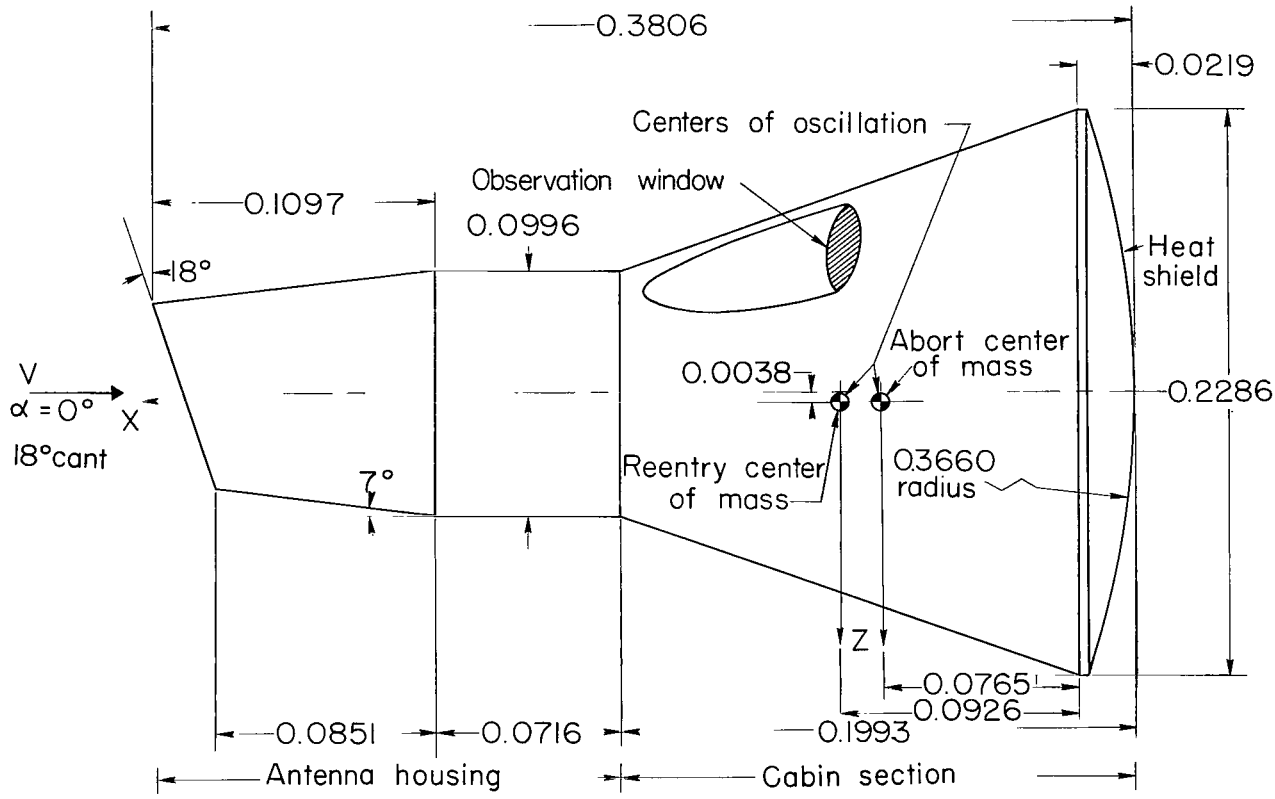

Sketch (c)

The centers of oscillation which correspond to the proposed full-scale center-of-mass locations are shown in sketches (b) and (c) and are located in the XZ-plane. Both the abort and reentry centers of oscillation are presented for the reentry configuration because, as mentioned in the "Introduction," the model of the reentry configuration was oscillated about both the abort and the reentry center-of-mass locations for certain test conditions. The sketches do not show details of the observation windows, docking blocks (located on the antenna housing), retro-rockets, or openings for sting clearance which were incorporated on the models. These details can be seen in the following photographs:

For correct photograph see page 11

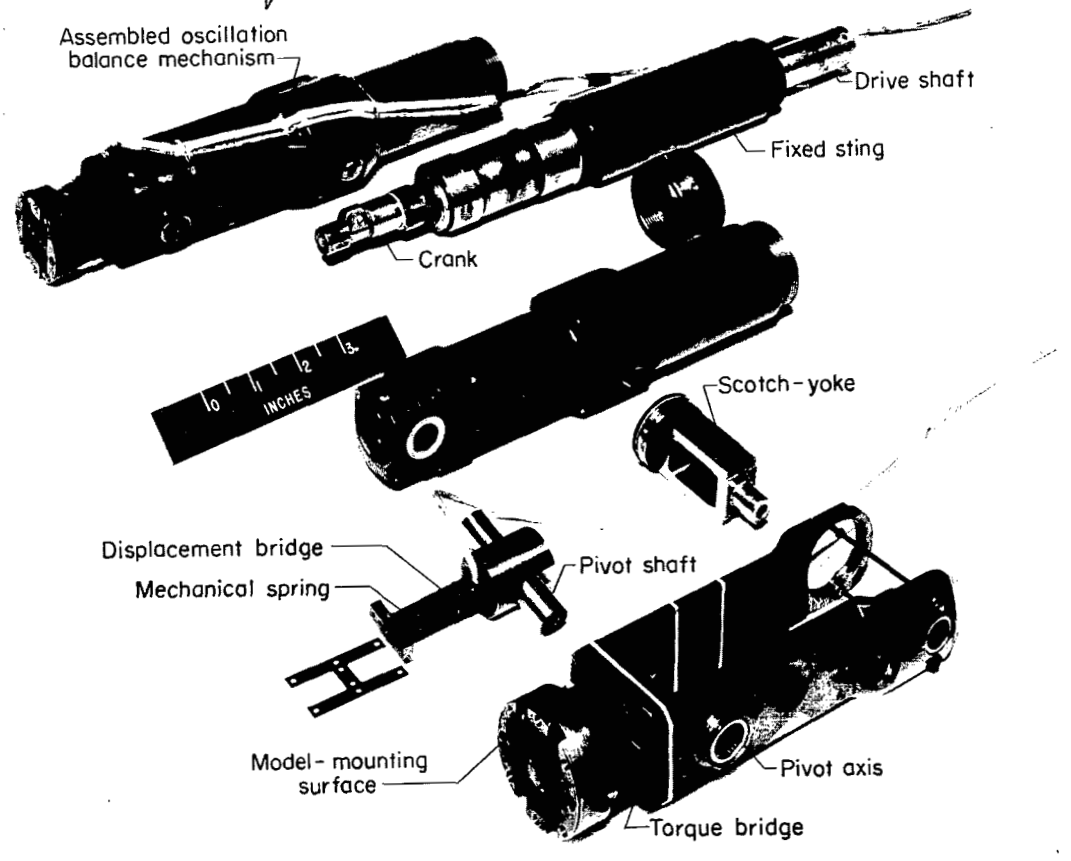

L-63-1939.1

The dummy retro-rockets shown were incorporated on the model of the abort configuration only for tests with the blunt end of the model pointing into the wind. The docking blocks were on the models only for the tests at Mach numbers of 1.50, 1.70, and 2.16. A decision was made after these tests to eliminate the docking blocks from the Gemini configuration. In order to provide the desired angle-of-attack range, the models were mounted at fixed offset angles with respect to the center line of the oscillation-balance mechanism. The model-sting offset angles are shown in sketch (d).

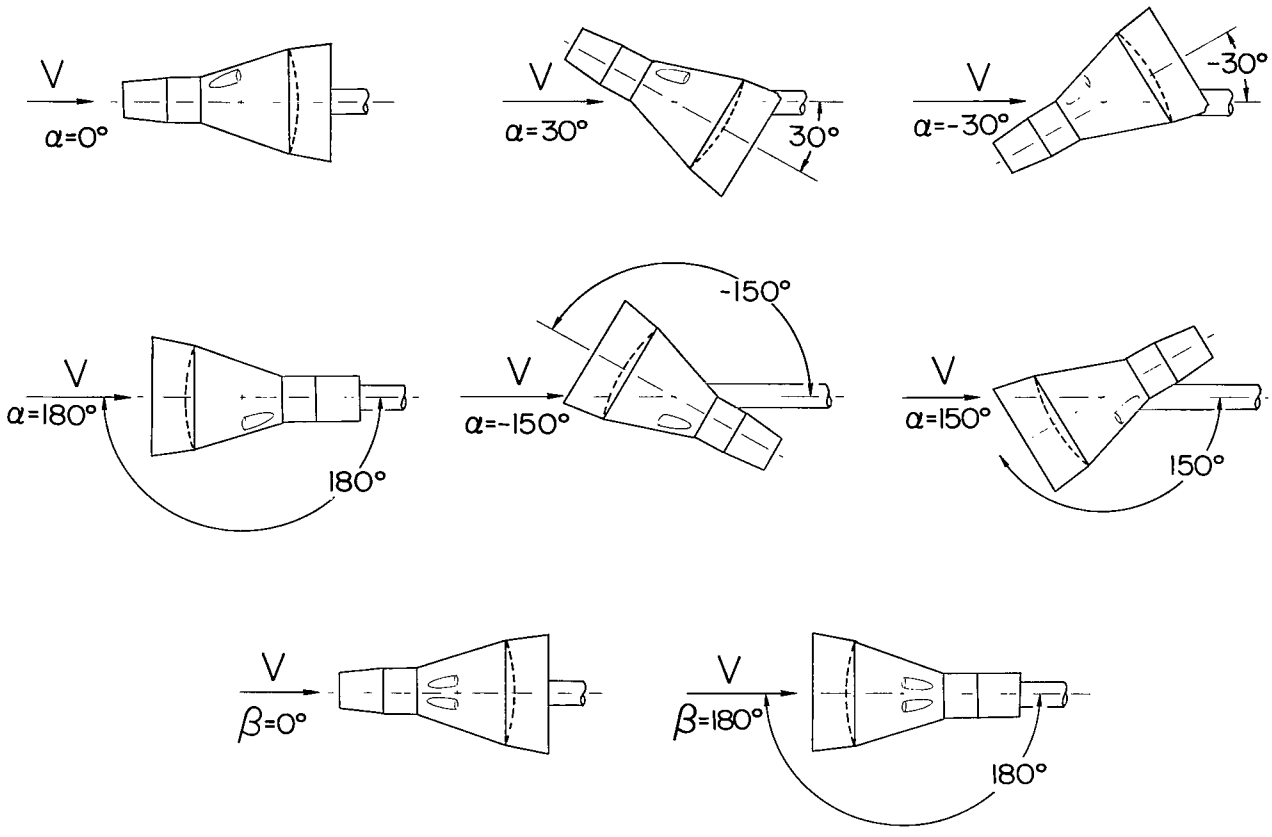

Sketch (d)

Some of the models mounted at various offset angles on the oscillation-balance mechanism are shown in the following photographs:

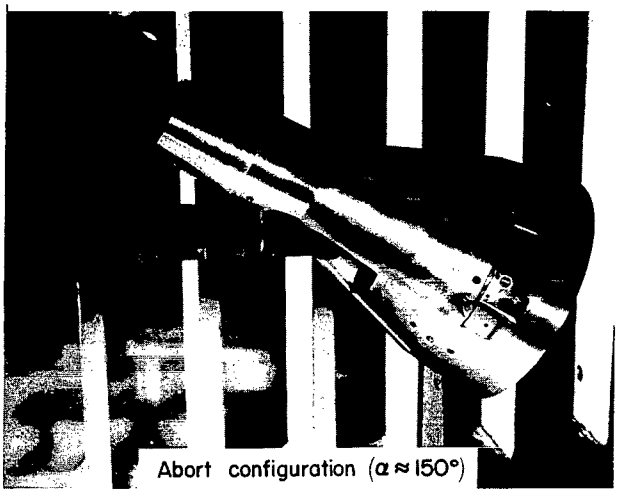

Abort configuration ($\alpha \approx 150°$)

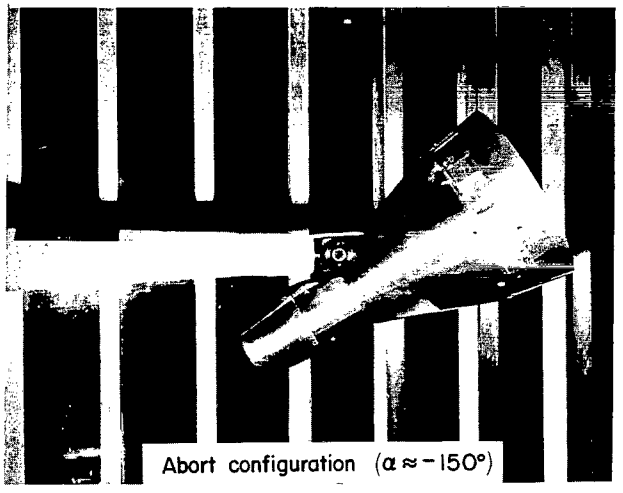

Abort configuration ($\alpha \approx -150°$)

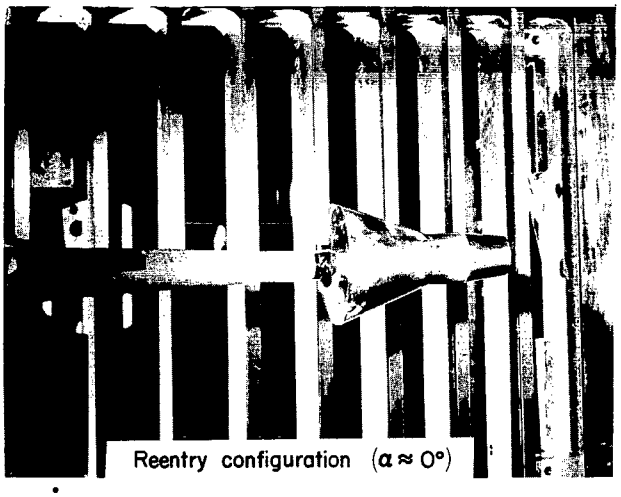

Reentry configuration ($\alpha \approx 0°$)

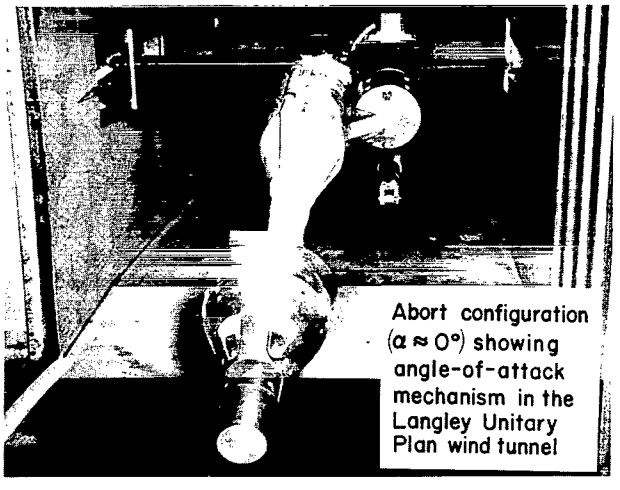

Abort configuration ($\alpha \approx 0°$) showing angle-of-attack mechanism in the Langley Unitary Plan wind tunnel

L-65-9040

The models were made of aluminum with aerodynamically smooth surfaces exposed to the airstream.

Oscillation-Balance Mechanism

Exploded and assembled views of the forward portion of the single-component (pitching moment) oscillation-balance mechanism which was used for the present investigation are presented in the following photograph:

For correct photograph see page 8

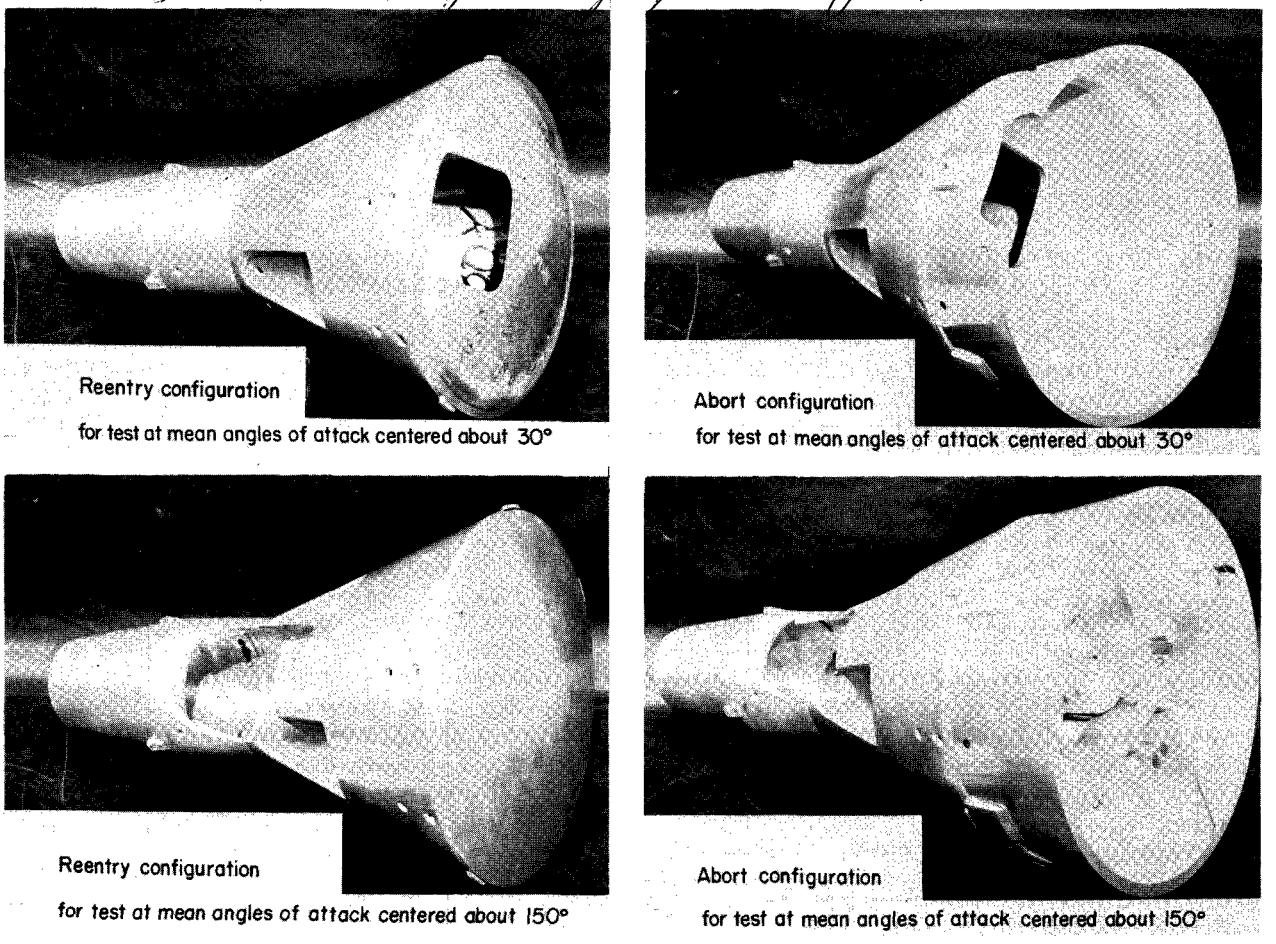

Reentry configuration for test at mean angles of attack centered about 30°

Abort configuration for test at mean angles of attack centered about 30°

Reentry configuration for test at mean angles of attack centered about 150°

Abort configuration for test at mean angles of attack centered about 150°

L-65-9039

Since the amplitude of the forced oscillation is small, the rotary motion of an electric motor is used to provide essentially sinusoidal motion to the balance through the crank and Scotch-yoke mechanism. A 2^{o} oscillation amplitude was used for all the tests reported herein. The oscillatory motion is about the pivot axis, which is usually located at the proposed center-of-mass location of the configuration being tested.

The strain-gage bridge used to measure the torque required to oscillate the model is located between the model-mounting surface and the pivot axis. This bridge location eliminates the pivot-friction characteristics from the model system and thereby eliminates the need to correct the data for varying pivot friction associated with changing

aerodynamic load. Although the torque bridge is physically forward of the pivot axis, all torques are measured with respect to the pivot axis.

The mechanical spring shown in the photograph is installed between the model-mounting surface and the fixed sting. The strain-gage bridge which is attached to the mechanical spring is used to determine the amplitude of the model angular displacement with respect to the fixed sting. The mechanical spring allows the model system to be oscillated at velocity resonance. Although the models may be oscillated at frequencies from about 1 to 30 cycles per second with the forced-oscillation balance, as mentioned in reference 2 the damping coefficient is obtained most accurately by operating at velocity resonance. The oscillation frequency varied from 1.52 to 16.93 cycles per second for the tests reported herein.

Wind Tunnels

Two wind tunnels were used to obtain the data presented herein. Both tunnels are equipped for control of relative humidity and total temperature of the air in the tunnel in order to minimize the effects of condensation shocks and for control of total pressure in order to obtain the test Reynolds number.

Langley 8-foot transonic pressure tunnel.- The data for Mach numbers of 0.50, 0.80, 0.95, and 1.20 were obtained in the Langley 8-foot transonic pressure tunnel. The test section of this single-return closed-circuit wind tunnel is about 2.2 meters square (about 7.1 feet square) with slotted upper and lower walls to permit continuous operation through the transonic speed range. Test-section Mach numbers from near 0 to 1.30 can be obtained and kept constant by controlling the speed of the tunnel-fan drive motor. The Mach number distribution is reasonably uniform throughout the test section, with a maximum deviation from the average free-stream Mach number of approximately 0.01 at the higher Mach numbers.

The sting-support strut is designed to keep the model near the center line of the tunnel through a range of sting angle of attack from about -5° to 14° when used with the oscillation-balance mechanism.

Langley Unitary Plan wind tunnel.- The data for Mach numbers of 1.50, 1.70, and 2.16 were obtained in test section number 1 of the Langley Unitary Plan wind tunnel. The data for Mach numbers of 3.00 and 4.63 were obtained in test section number 2 of the same tunnel. Both test sections are about 1.2 meters square (4 feet square) and about 2.1 meters long (7 feet long). Asymmetric sliding blocks which vary the area ratio are used to change the Mach number from about 1.47 to 2.87 in test section number 1 and from about 2.30 to 4.65 in test section number 2. The angle-of-attack mechanism used for this investigation has a total range of about 25° when used with the

oscillation-balance mechanism. A complete description of the Langley Unitary Plan wind tunnel is given in reference 3.

MEASUREMENTS AND REDUCTION OF DATA

The strain-gage bridges used to sense the torque required to oscillate the model and the angular displacement of the model with respect to the sting are powered by 3000-cps carrier voltage. The bridge outputs are proportional to the instantaneous torque and the instantaneous angular displacement. The constant components of the bridge outputs are removed by using conventional bridge-balance circuits. The nonconstant components are amplified and passed through mechanically coupled but electrically independent sine-cosine resolvers which rotate with constant angular velocity at the frequency of model oscillation and resolve each signal into two components. The components are rectified by phase-sensitive demodulators and read on damped digital voltmeters to provide direct-current voltages proportional to the orthogonal components of the amplitude of the torque required to oscillate the model and the amplitude of the angular displacement of the model with respect to the sting. The amplitudes of the torque and displacement are then computed from their respective orthogonal components. The individual resolvers are electrically alined so that the phase angle between the torque and the angular displacement may also be determined from the orthogonal components.

The resolver—damped-voltmeter system acts as an extremely narrow band-pass filter with the center frequency always being the frequency of oscillation of the model. In this way, as explained in reference 2, the effects of random torque inputs due to tunnel turbulence or other causes are eliminated and only the components of torque and angular displacement which occur at the frequency of oscillation are used in computing the dynamic stability characteristics of the model.

The frequency of oscillation is measured by using an electronic counter to determine the number of pulses generated in 1 second by an induction-coil pickup and a 100-tooth gear which is fastened to the shaft of one of the resolvers.

For the pitching tests, measurements are made of the amplitude of the torque required to oscillate the model in pitch T_Y, the amplitude of the angular displacement in pitch of the model with respect to the sting Θ, the phase angle η between T_Y and Θ, and the angular velocity of the forced oscillation ω. The viscous-damping coefficient in pitch for this single-degree-of-freedom system is computed as

$$C_Y = \frac{T_Y \sin \eta}{\omega \Theta} \tag{1}$$

and the spring-inertia parameter in pitch is computed as

$$K_Y - I_Y\omega^2 = \frac{T_Y \cos \eta}{\Theta} \tag{2}$$

where K_Y is the torsional-spring coefficient of the system and I_Y is the moment of inertia of the system about the body Y-axis.

For these tests, the damping-in-pitch parameter was computed as

$$C_{m_q} + C_{m_{\dot{\alpha}}} = -\frac{V}{q_\infty Ad^2}\left[(C_Y)_{\text{wind on}} - (C_Y)_{\text{wind off}}\right] \tag{3}$$

and the oscillatory-longitudinal-stability parameter was computed as

$$C_{m_\alpha} - k^2 C_{m_{\dot{q}}} = -\frac{1}{q_\infty Ad}\left[(K_Y - I_Y\omega^2)_{\text{wind on}} - (K_Y - I_Y\omega^2)_{\text{wind off}}\right] \tag{4}$$

Since the wind-off value of C_Y is not a function of oscillation frequency, it is determined at the frequency of wind-off velocity resonance because C_Y can be determined most accurately at this frequency. The wind-off value of $K_Y - I_Y\omega^2$ is determined at the same frequency as the wind-on value of $K_Y - I_Y\omega^2$ since this parameter is a function of frequency.

For the yawing tests, measurements are made of the amplitude of the torque required to oscillate the model in yaw T_Z, the amplitude of the angular displacement in yaw of the model with respect to the sting Ψ, the phase angle λ between T_Z and Ψ, and the angular velocity of the forced oscillation ω. The viscous-damping coefficient in yaw for this single-degree-of-freedom system is computed as

$$C_Z = \frac{T_Z \sin \lambda}{\omega\Psi} \tag{5}$$

and the spring-inertia parameter in yaw is computed as

$$K_Z - I_Z\omega^2 = \frac{T_Z \cos \lambda}{\Psi} \tag{6}$$

where K_Z is the torsional-spring coefficient of the system and I_Y is the moment of inertia of the system about the body Y-axis.

For these tests, the damping-in-yaw parameter was computed as

$$C_{n_r} - C_{n_{\dot{\beta}}} \cos \alpha = -\frac{V}{q_\infty Ad^2}\left[(C_Z)_{\text{wind on}} - (C_Z)_{\text{wind off}}\right] \tag{7}$$

and the oscillatory-directional-stability parameter was computed as

$$C_{n_\beta} \cos \alpha + k^2 C_{n_{\dot{r}}} = \frac{1}{q_\infty A d}\left[\left(K_Z - I_Z\omega^2\right)_{\text{wind on}} - \left(K_Z - I_Z\omega^2\right)_{\text{wind off}}\right] \quad (8)$$

The wind-off value of C_Z is determined at the frequency of wind-off velocity resonance, and the wind-off and wind-on values of $K_Z - I_Z\omega^2$ are determined at the same frequency.

TESTS AND PRESENTATION OF RESULTS

The tests were made at selected Mach numbers from 0.50 to 4.63 by using a 2° amplitude forced-oscillation mechanism. The damping and oscillatory-stability parameters in pitch were obtained at mean angles of attack in the approximate ranges of $\pm 45^\circ$ from 0° and $\pm 45^\circ$ from 180° with the models at an angle of sideslip of 0°. The damping and oscillatory-stability parameters in yaw were determined at mean angles of sideslip near 0° and 180° with the models at an angle of attack of 0°. The Reynolds number, based on the diameter of the heat shield, varied from about 1.6×10^6 to 3.4×10^6. The Reynolds number equaled the anticipated full-scale Reynolds number at all Mach numbers except 1.50, 1.70, and 2.16. At these Mach numbers, the full-scale Reynolds number could not be obtained because of insufficient model load limits. The reduced-frequency parameter varied from about 0.0045 to 0.0795 for the tests in pitch and from about 0.0090 to 0.0775 for the tests in yaw. These values of reduced-frequency parameter are representative of the anticipated full-scale values.

The basic dynamic-stability data are presented in the following figures:

RESULTS AND DISCUSSION

Longitudinal Stability

Explanation of longitudinal-stability parameters.- The damping-in-pitch parameter $C_{m_q} + C_{m_{\dot{\alpha}}}$ is a measure of the effective damping experienced by the model while being forced to oscillate through an angle-of-attack range from $\alpha - \Theta$ to $\alpha + \Theta$, where α is the mean angle of attack and Θ is the amplitude of the forced oscillation. Since Θ is small, the value of $C_{m_q} + C_{m_{\dot{\alpha}}}$ is essentially a measure of the damping at a discrete angle of attack. A negative value of $C_{m_q} + C_{m_{\dot{\alpha}}}$ at any mean angle of attack α indicates that the model experiences a net positive aerodynamic damping in pitch during the oscillations about that α.

The oscillatory-longitudinal-stability parameter $C_{m_\alpha} - k^2 C_{m_{\dot{q}}}$ is a function of the variation of oscillatory pitching moment with angle of attack through the angle-of-attack range from $\alpha - \Theta$ to $\alpha + \Theta$. A negative value of this parameter at any mean angle of attack α indicates that the oscillating model is aerodynamically stable with respect to that α.

Abort configuration with antenna housing forward (α centered around 0°).- The data in figure 1 show that positive or near-zero damping in pitch is generally exhibited for the abort configuration with the antenna housing forward at all Mach numbers except 1.70 and 2.16, where appreciable negative damping is present for mean angles of attack greater than about $\pm 30^\circ$. The stability parameter is very dependent upon both Mach number and mean angle of attack. At the lowest Mach number, 0.50, the Gemini abort configuration with the antenna housing forward is unstable at all mean angles of attack, whereas the configuration generally is stable at all mean angles of attack at the higher Mach numbers of 3.00 and 4.63. At the intermediate Mach numbers, regions of stability are present at the smaller positive and negative mean angles of attack. At a Mach number of 2.16 at the positive mean angles of attack near 30°, the discontinuity in the data is associated with an abrupt change in the flow over the body due to changing boundary-layer separation. Canting the face of the antenna housing to an angle of 18° has, in general, little effect on the damping and oscillatory stability in pitch for the abort configuration with the antenna housing forward.

The general symmetry about 0° mean angle of attack of both the damping and the stability data for the abort configuration with the antenna housing forward indicates that the offset center of mass and the external asymmetry of the model do not appreciably affect the damping and stability characteristics in pitch.

Abort configuration with antenna housing rearward (α centered around 180°).- The Gemini abort configuration with the antenna housing rearward generally has negative

damping in pitch at mean angles of attack near 180°, as can be seen in figure 2. However, the damping in pitch generally becomes positive at mean angles of attack about 5° from 180° at the higher supersonic Mach numbers and about 30° from 180° at Mach numbers of 1.20 and below.

At Mach number 1.20 and below, this configuration is generally stable for mean angles of attack within about 25° of 180°. Although reflected shock waves prevented data from being obtained throughout the entire range of mean angle of attack at Mach numbers greater than 1.20, the abort configuration appears to be stable at mean angles of attack within about 10° or 15° of 180° at a Mach number of 2.16 and above.

Reentry configuration with antenna housing forward (α centered around 0°).- As mentioned in the "Introduction," canting the face of the antenna housing 18° was considered as a means of making the reentry configuration with the antenna housing forward longitudinally unstable near 0° angle of attack in order to insure that this configuration would orient itself with the heat shield forward during reentry rather than with the antenna housing forward. The configuration with the face of the antenna housing canted 18° is less stable than the configuration with 0° cant near 0° mean angle of attack at all Mach numbers, as can be seen from the data in figure 3. However, only at Mach numbers of 1.20 and below does this decrease in stability appear significant since only at these Mach numbers is the decrease in stability sufficient to cause the stable configuration to become unstable near $\alpha = 0°$. Canting the face of the antenna housing has little effect on the damping in pitch, which is positive or near zero throughout the Mach number and mean-angle-of-attack ranges.

In general, the trends of the damping and stability parameters for the reentry configuration with the antenna housing forward are very similar to those for the abort configuration with the antenna housing forward. As mentioned in the "Introduction," the model of the reentry configuration with the antenna housing forward was tested with the oscillation axis at the abort center-of-mass location for mean angles of attack near 30° because of space limitations within the model. In order to determine whether the data so obtained might be applicable to the reentry configuration with the oscillation axis at the reentry center-of-mass location for mean angles of attack near 30°, tests were also made of this configuration with the oscillation axis at both the reentry and the abort center-of-mass locations at mean angles of attack near 0°, -30°, and 180°. (The data obtained near $\alpha = 180°$ are presented in figure 4.) Because only slight differences were obtained in the damping characteristics about the two center-of-mass locations, the data near $\alpha = 30°$ for the reentry configuration oscillating about the abort center-of-mass location should be applicable to the reentry configuration oscillating about the reentry center of mass. As would be expected, the configuration is less stable at the more rearward center-of-mass location (abort center of mass).

Reentry configuration with antenna housing rearward (α centered around 180°).- The Gemini reentry configuration with the antenna housing rearward generally exhibits negative or near-zero damping in pitch at mean angles of attack near 180° at all Mach numbers, as can be seen from the data in figure 4. However, the damping in pitch becomes positive for mean angles of attack more than about 30° from 180°. The data obtained at the two center-of-mass locations show very little effect of oscillation center on the damping-in-pitch parameter. Although regions of instability are present at Mach numbers of 1.70 and below, this configuration is generally stable at mean angles of attack within about ±30° of 180° at a Mach number of 1.70 and at all values of α at Mach numbers of 2.16 and above.

Directional Stability

Explanation of directional-stability parameters.- The interpretation of the directional-stability parameters, presented in figures 5 to 8, is analogous to the interpretation of the longitudinal-stability parameters. A negative value of the damping-in-yaw parameter $C_{n_r} - C_{n_{\dot{\beta}}} \cos \alpha$ at any mean angle of sideslip β indicates that the model experiences a net positive aerodynamic damping in yaw during the oscillations about that β. A positive value of the oscillatory-directional-stability parameter $C_{n_\beta} \cos \alpha + k^2 C_{n_{\dot{r}}}$ at any β indicates that the oscillating model is aerodynamically stable with respect to that β.

Abort and reentry configurations.- As previously mentioned, the data in yaw were obtained through an angle-of-sideslip range at $\alpha = 0°$. Therefore, the only differences between the yawing data and the pitching data would be produced by the slight offset of the center-of-mass location and other model asymmetries. The yawing data for the abort configuration are presented in figures 5 and 6, and the data for the reentry configuration, in figures 7 and 8. In general, the pitching and yawing characteristics are very similar for the two configurations. The damping and stability parameters for both pitch and yaw as a function of Mach number are presented in figure 9 for $\alpha = \beta = 0°$ and in figure 10 for $\alpha = \beta = 180°$ to show graphically the similarity between the pitching and yawing results.

CONCLUDING REMARKS

Wind-tunnel measurements of the aerodynamic damping and oscillatory stability in pitch and yaw for 0.10-scale models of proposed Gemini abort and reentry configurations have been made at Mach numbers from 0.50 to 4.63 by using a 2° amplitude forced-oscillation mechanism. The damping and oscillatory-stability parameters in pitch were obtained at mean angles of attack in the approximate ranges of ±45° from 0° and ±45°

from 180° with the models at an angle of sideslip of 0°. (Both angle of attack and angle of sideslip are defined as 0° when the antenna housing points into the wind.) The damping and oscillatory-stability parameters in yaw were determined at mean angles of sideslip near 0° and 180° with the models at an angle of attack of 0°. Tests were made to determine the effect of canting the front face of the antenna housing 18°.

Both the abort and reentry configurations with the antenna housing forward (mean angles of attack from about -50° to 50°) generally exhibit positive or near-zero damping in pitch for all Mach numbers, but the abort configuration exhibits negative damping at the higher mean angles of attack for low supersonic Mach numbers. Canting the face of the antenna housing to an angle of 18° has little effect on the damping for the abort configuration or the reentry configuration with the antenna housing forward.

Both the abort and reentry configurations with the antenna housing forward are unstable throughout the range of mean angle of attack at the lowest test Mach number but stable throughout the range of mean angle of attack at the higher test Mach numbers. For the intermediate Mach numbers, regions of stability are present at the lower positive and negative mean angles of attack. Canting the face of the antenna housing to an angle of 18° for the reentry configuration with the antenna housing forward decreases the stability near 0° mean angle of attack at all Mach numbers; however, canting the face of the antenna housing of the abort configuration with the antenna housing forward has little effect on the stability.

The abort and reentry configurations with the antenna housing rearward generally exhibit negative or zero damping in pitch over a varying range of mean angle of attack near 180°. Both configurations are generally stable up to about ±25° from 180°.

In general, the yawing characteristics are very similar to the pitching characteristics for both the abort and reentry configurations.

Langley Research Center,
National Aeronautics and Space Administration,
Langley Station, Hampton, Va., November 8, 1965.

REFERENCES

1. Mechtly, E. A.: The International System of Units – Physical Constants and Conversion Factors. NASA SP-7012, 1964.

2. Braslow, Albert L.; Wiley, Harleth G.; and Lee, Cullen Q.: A Rigidly Forced Oscillation System for Measuring Dynamic-Stability Parameters in Transonic and Supersonic Wind Tunnels. NASA TN D-1231, 1962. (Supersedes NACA RM L58A28.)

3. Anon.: Manual for Users of the Unitary Plan Wind Tunnel Facilities of the National Advisory Committee for Aeronautics. NACA, 1956.

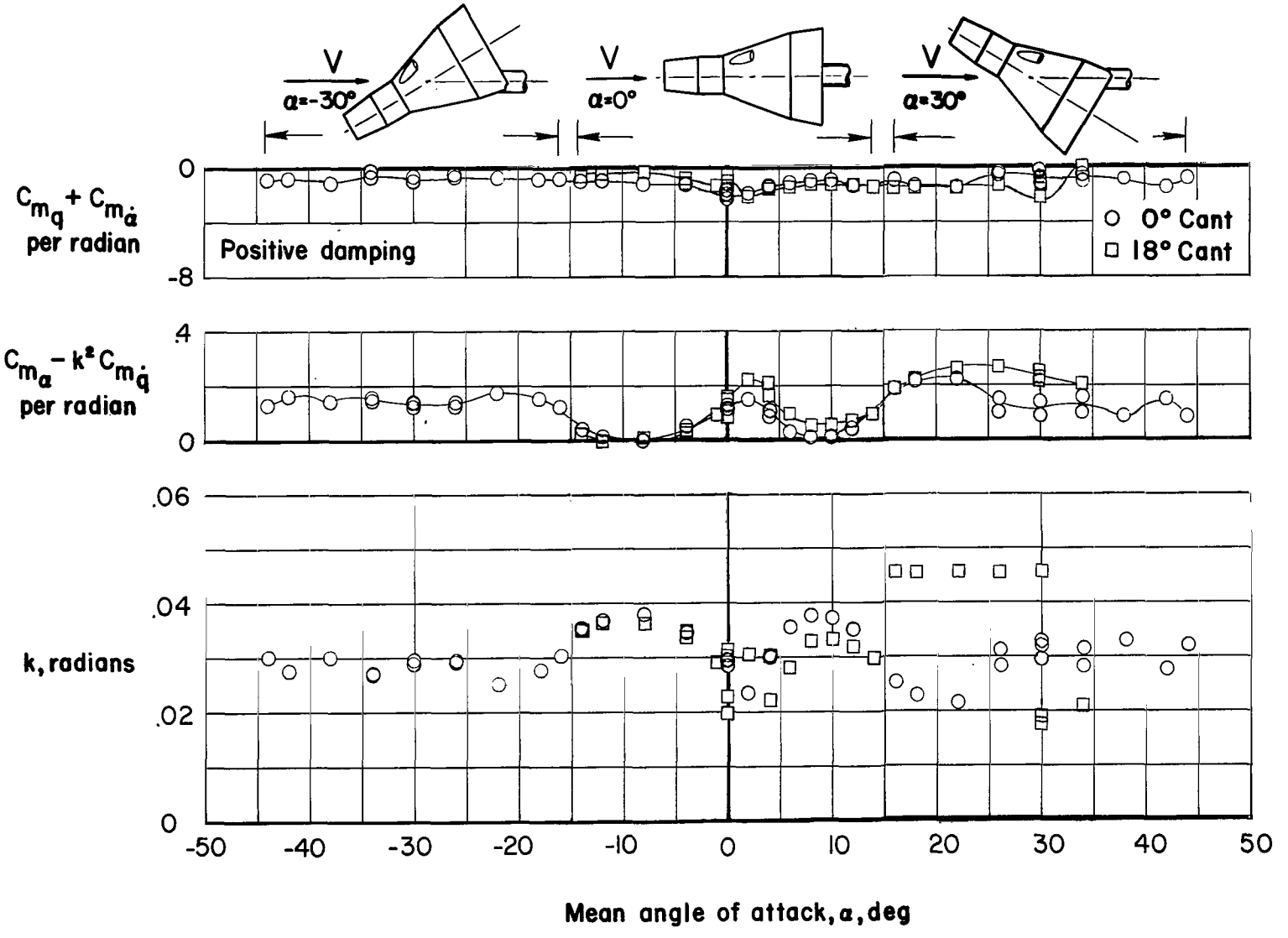

(a) M = 0.50; R = 2.56 × 10^6 to 3.29 × 10^6.

Figure 1.- Variation of damping-in-pitch parameter, oscillatory-longitudinal-stability parameter, and reduced-frequency parameter with mean angle of attack for models of Gemini abort configuration centered around 0^0 angle of attack. $\beta = 0^0$.

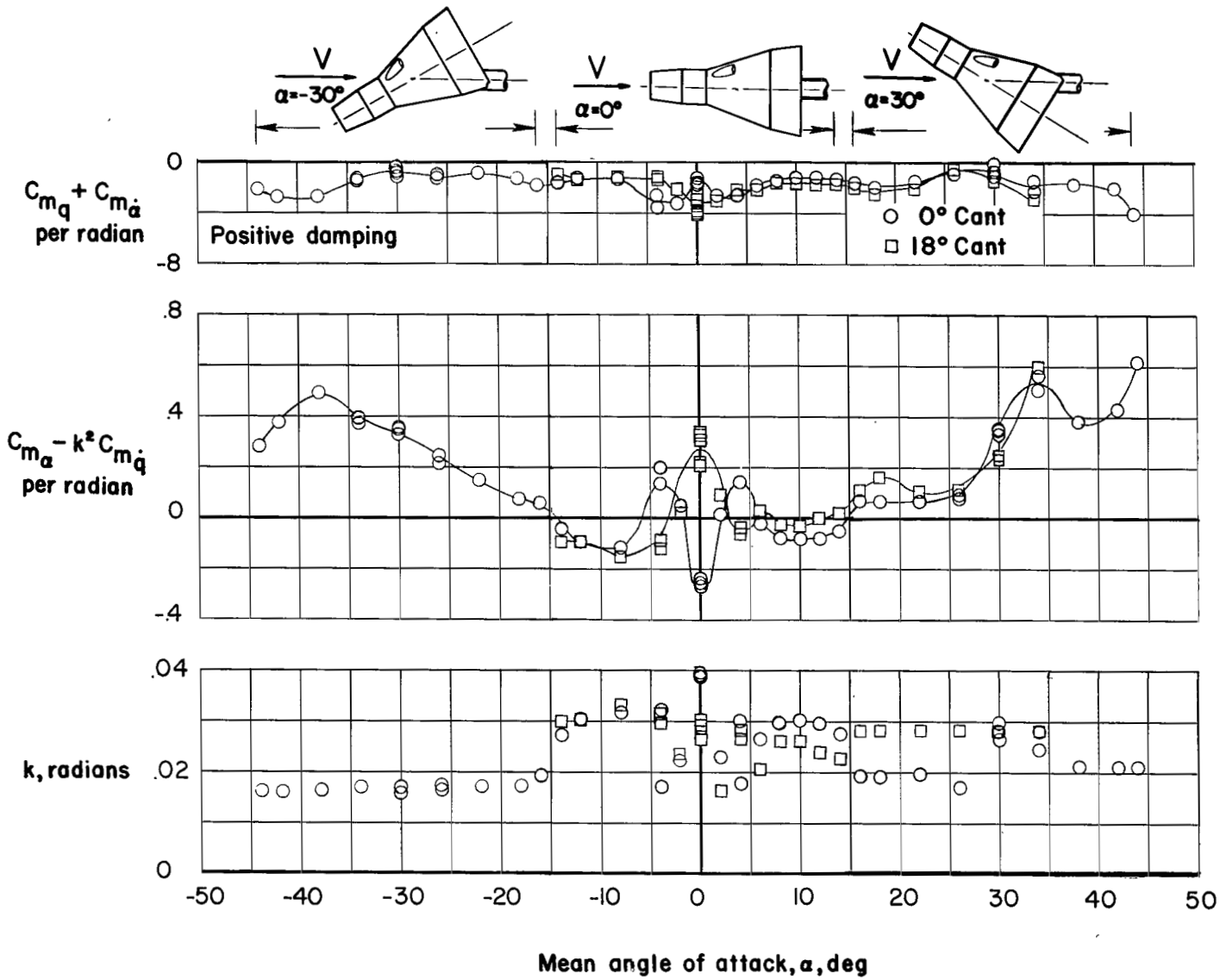

(b) M = 0.80; R = 3.28×10^6.

Figure 1.- Continued.

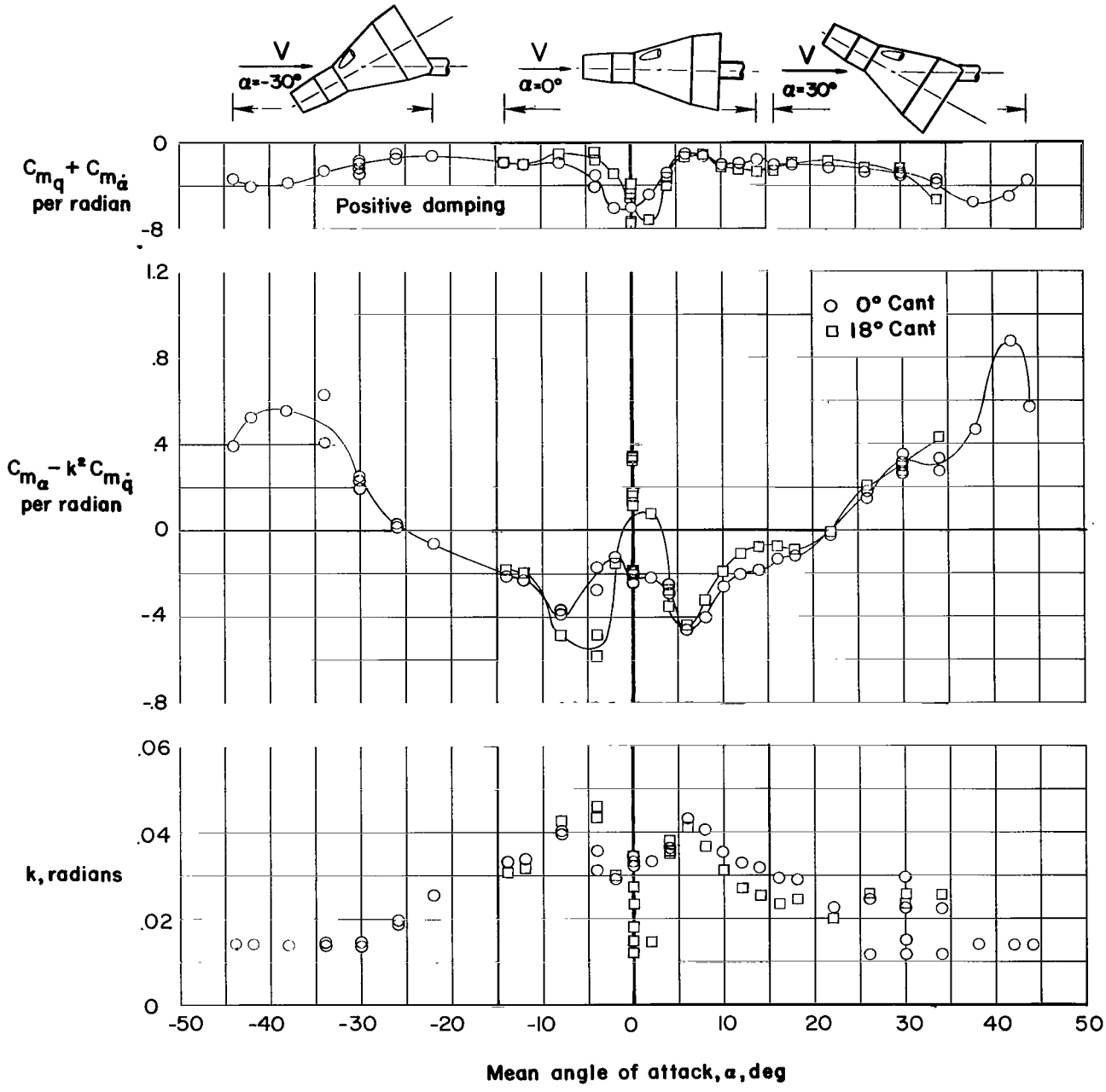

(c) M = 0.95; R = 3.28×10^6.

Figure 1.- Continued.

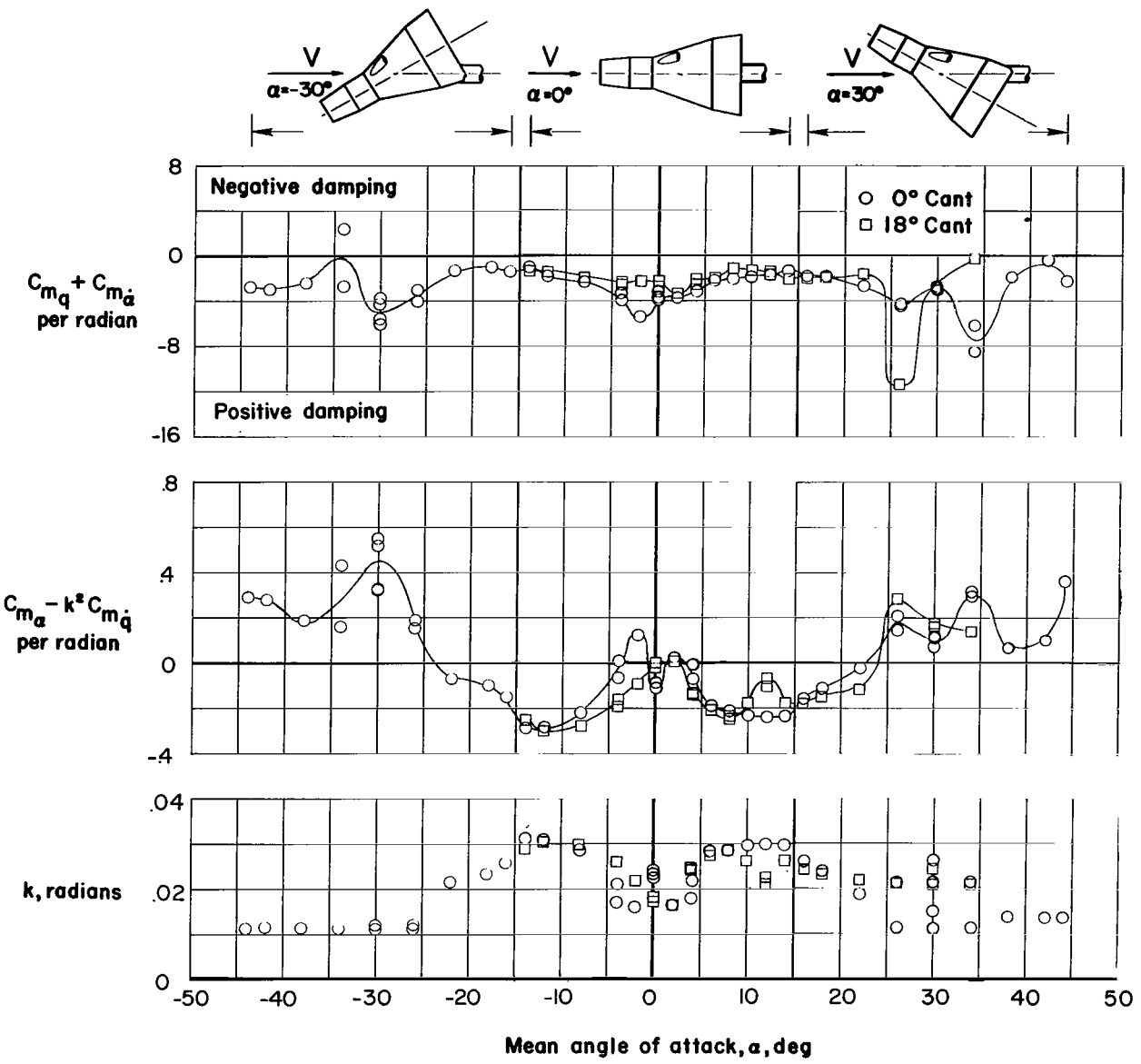

(d) M = 1.20; R = 3.26×10^6.

Figure 1.- Continued.

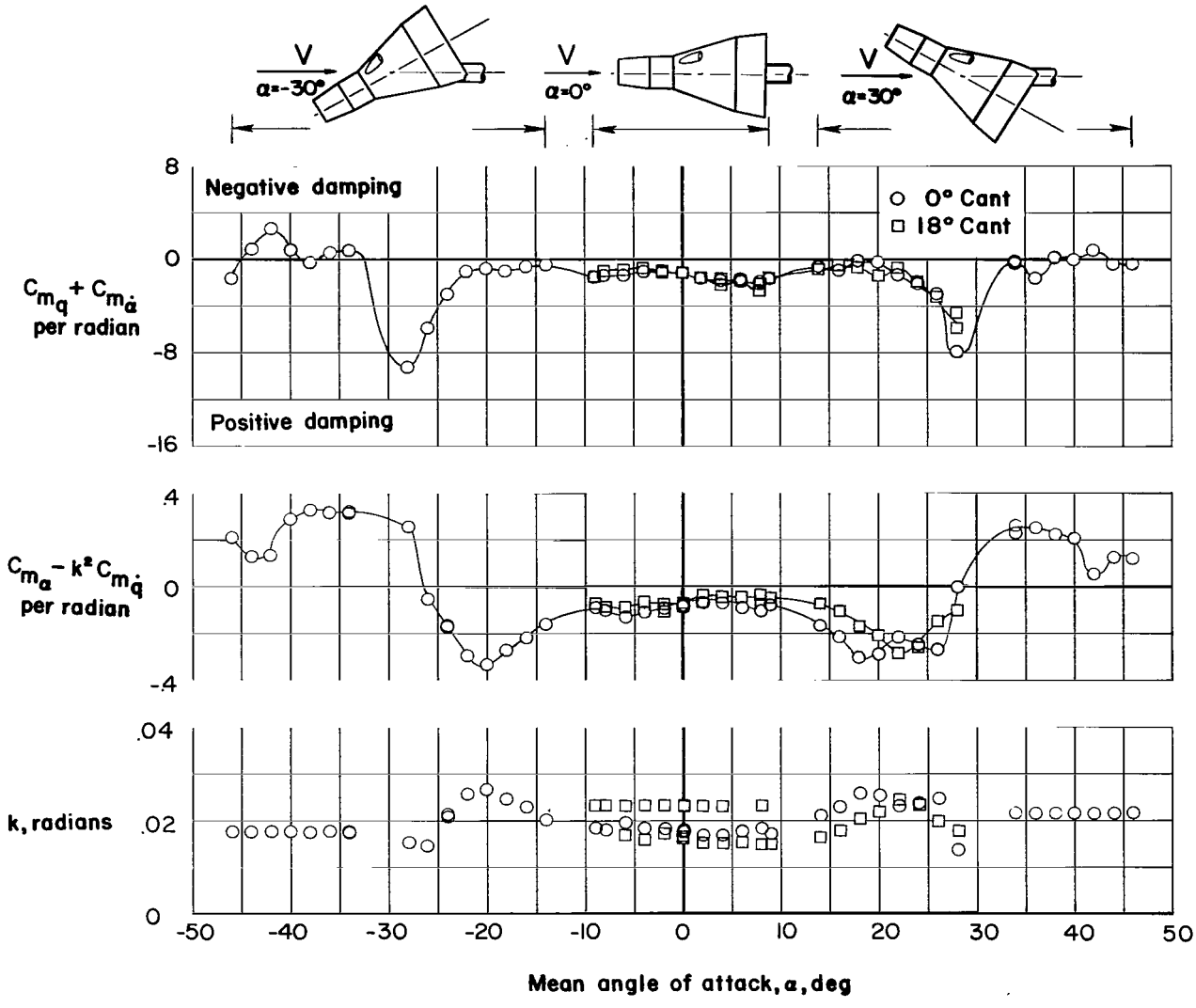

(e) M = 1.70; R = 3.30 × 10^6.

Figure 1.- Continued.

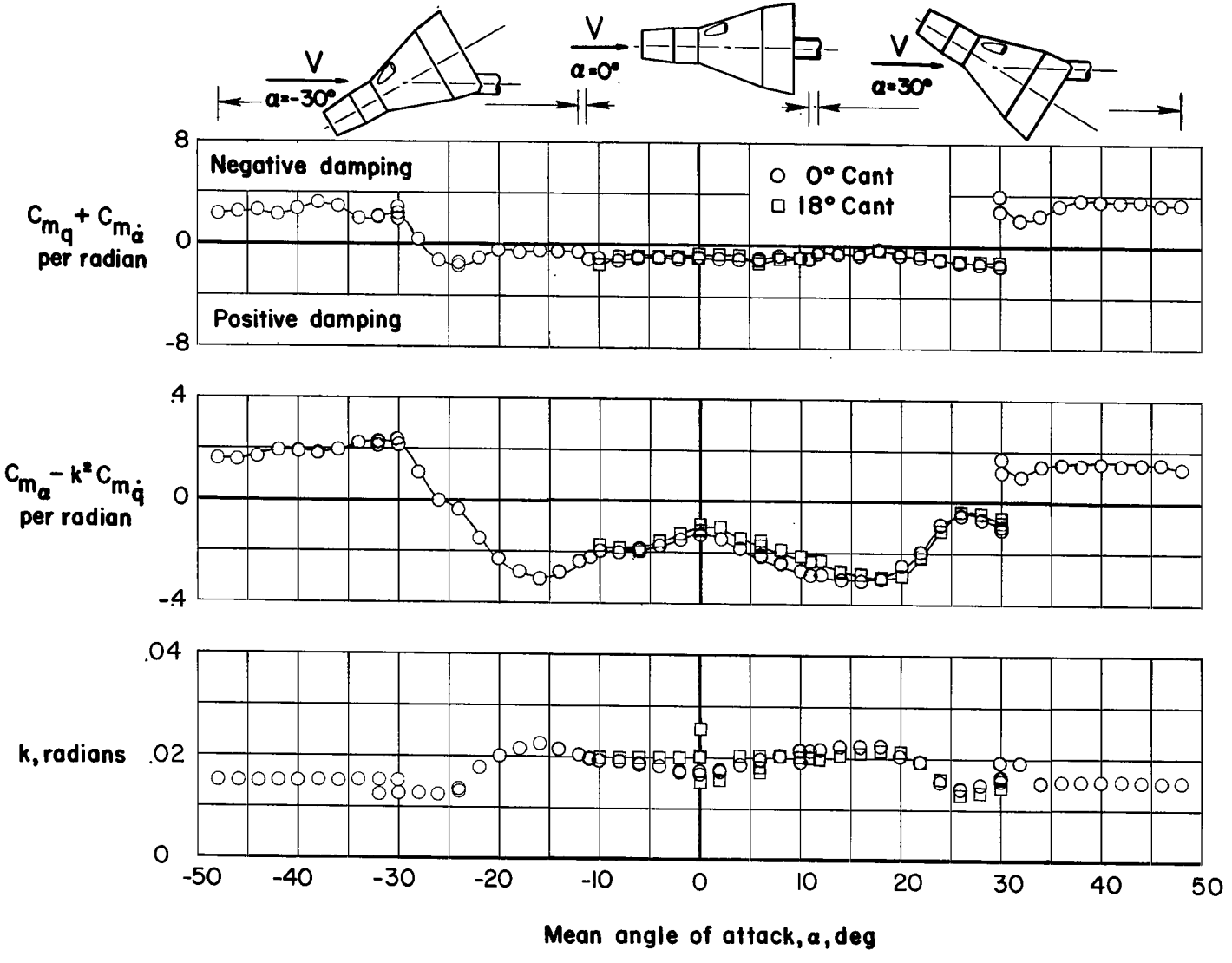

(f) M = 2.16; R = 3.36 × 10^6.

Figure 1.- Continued.

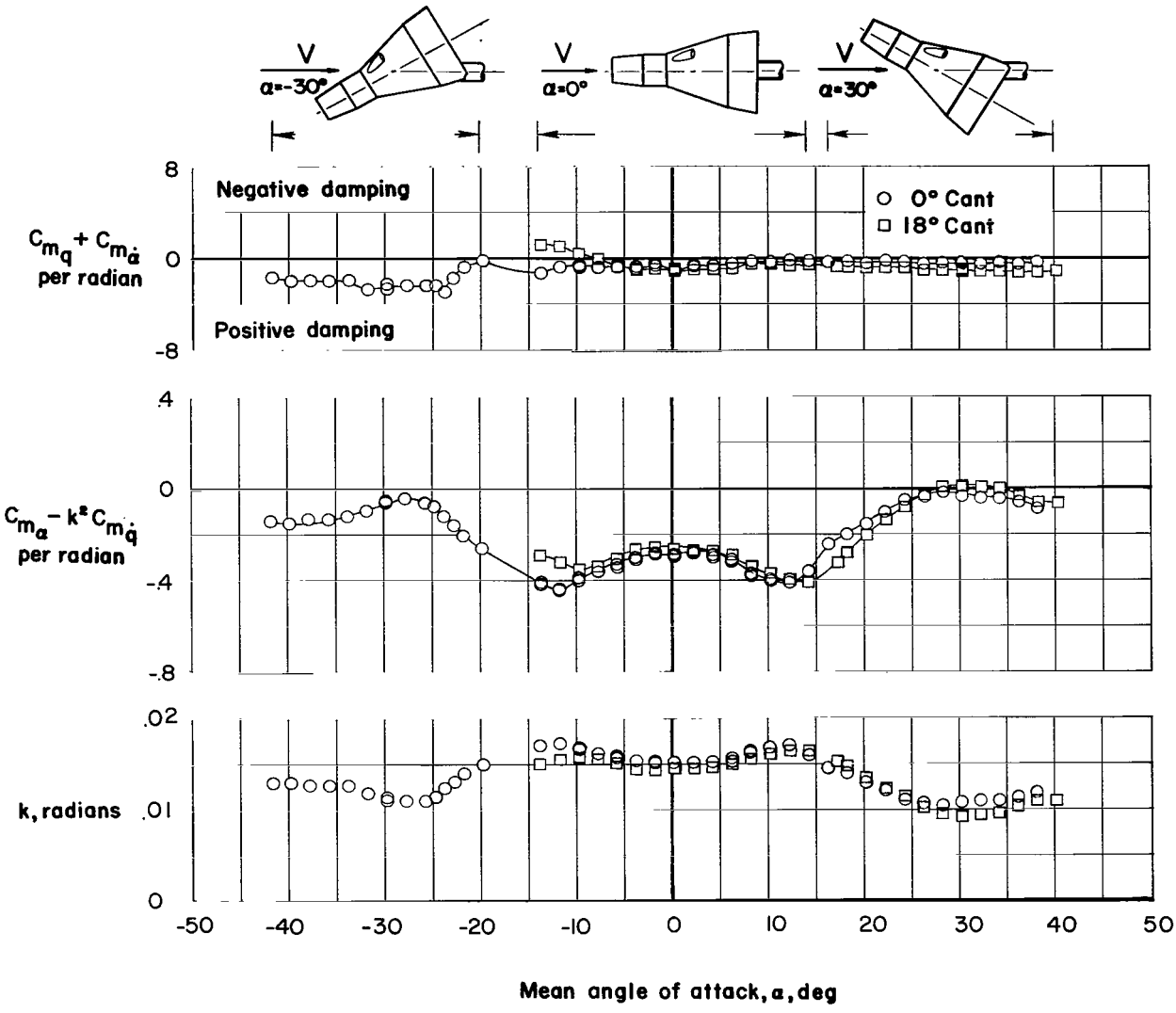

(g) M = 3.00; R = 2.10 × 10^6.

Figure 1.- Continued.

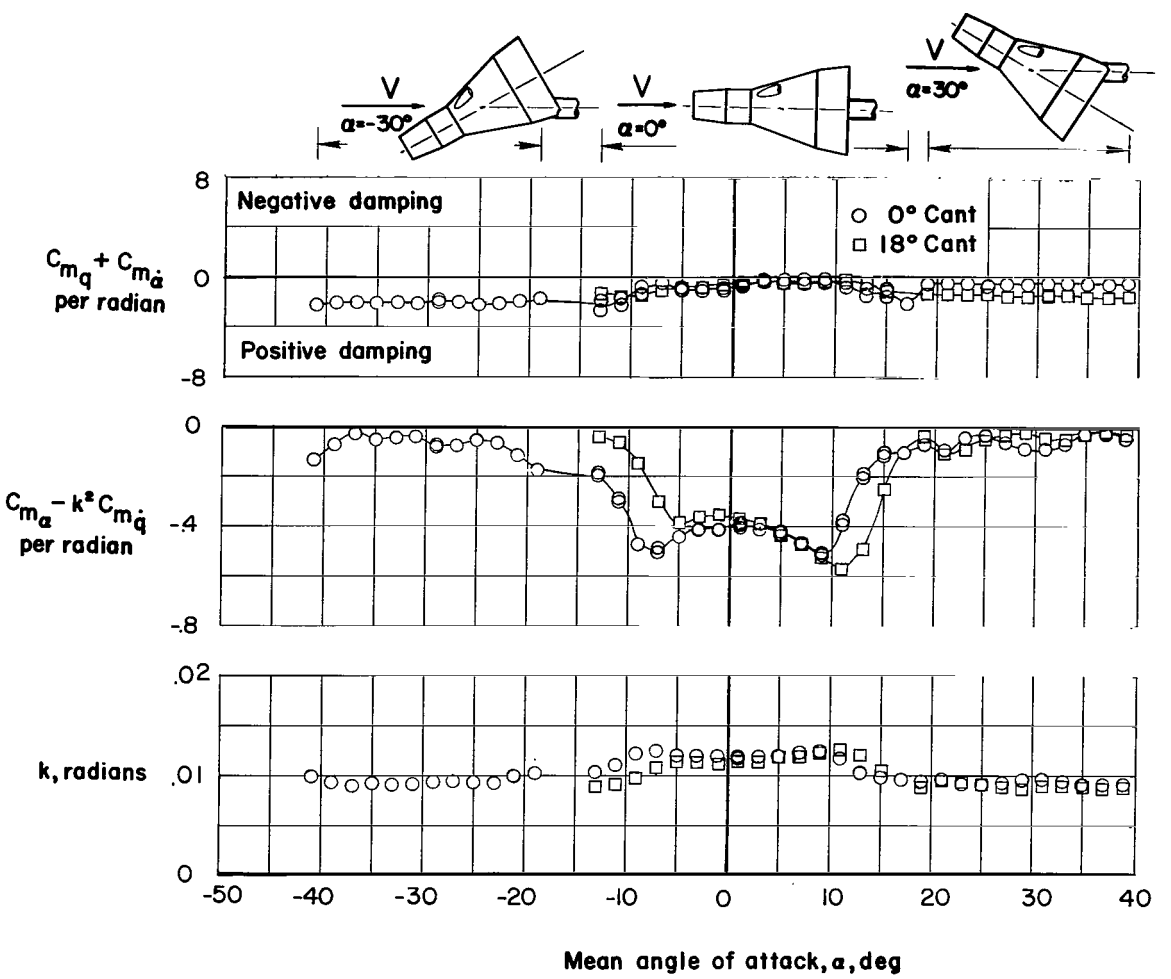

(h) M = 4.63; R = 1.58×10^6.

Figure 1.- Concluded.

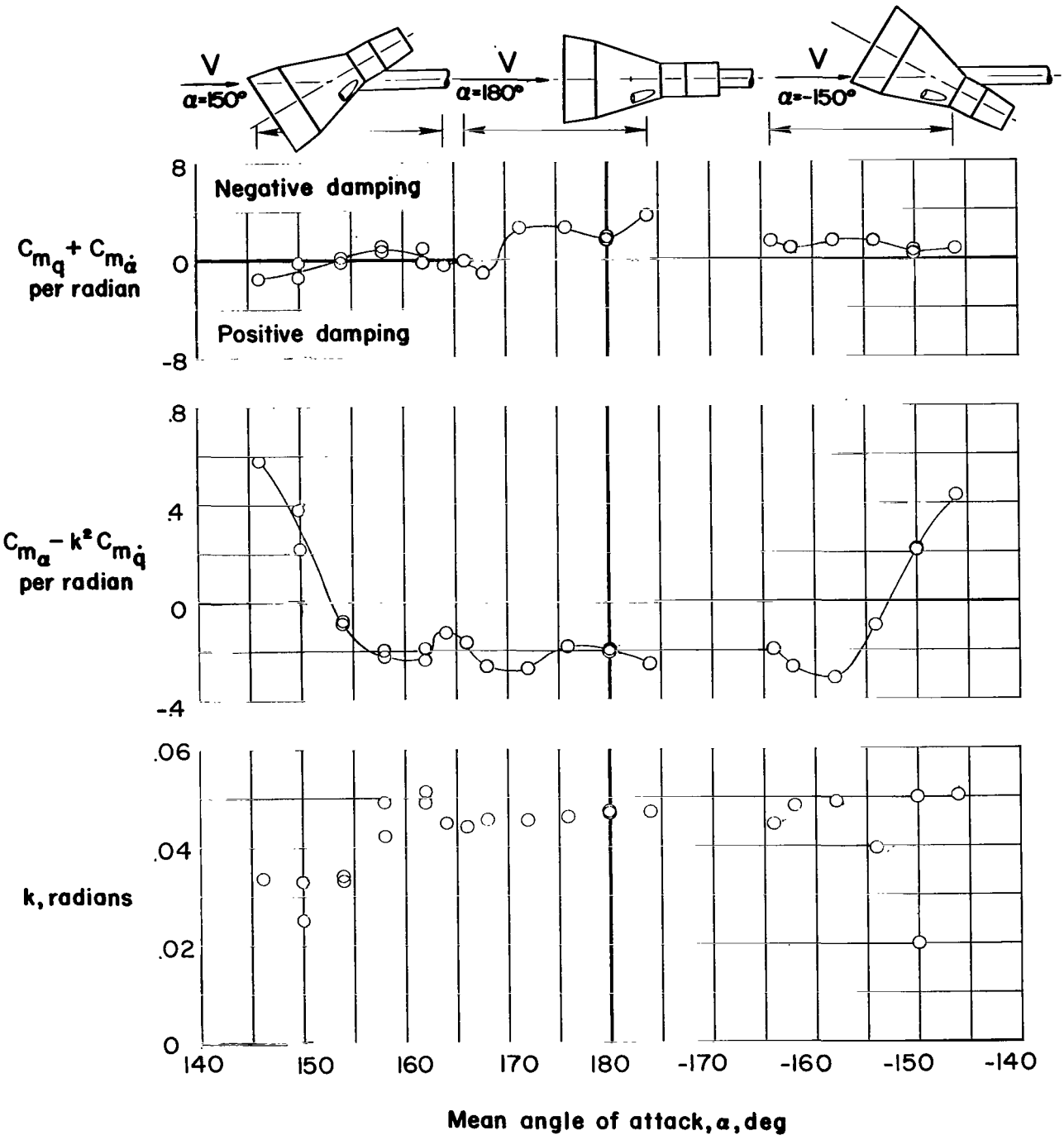

(a) M = 0.50; R = 2.56×10^6 to 3.33×10^6.

Figure 2.- Variation of damping-in-pitch parameter, oscillatory-longitudinal-stability parameter, and reduced-frequency parameter with mean angle of attack for models of Gemini abort configuration centered around 180^0 angle of attack. $\beta = 0^0$.

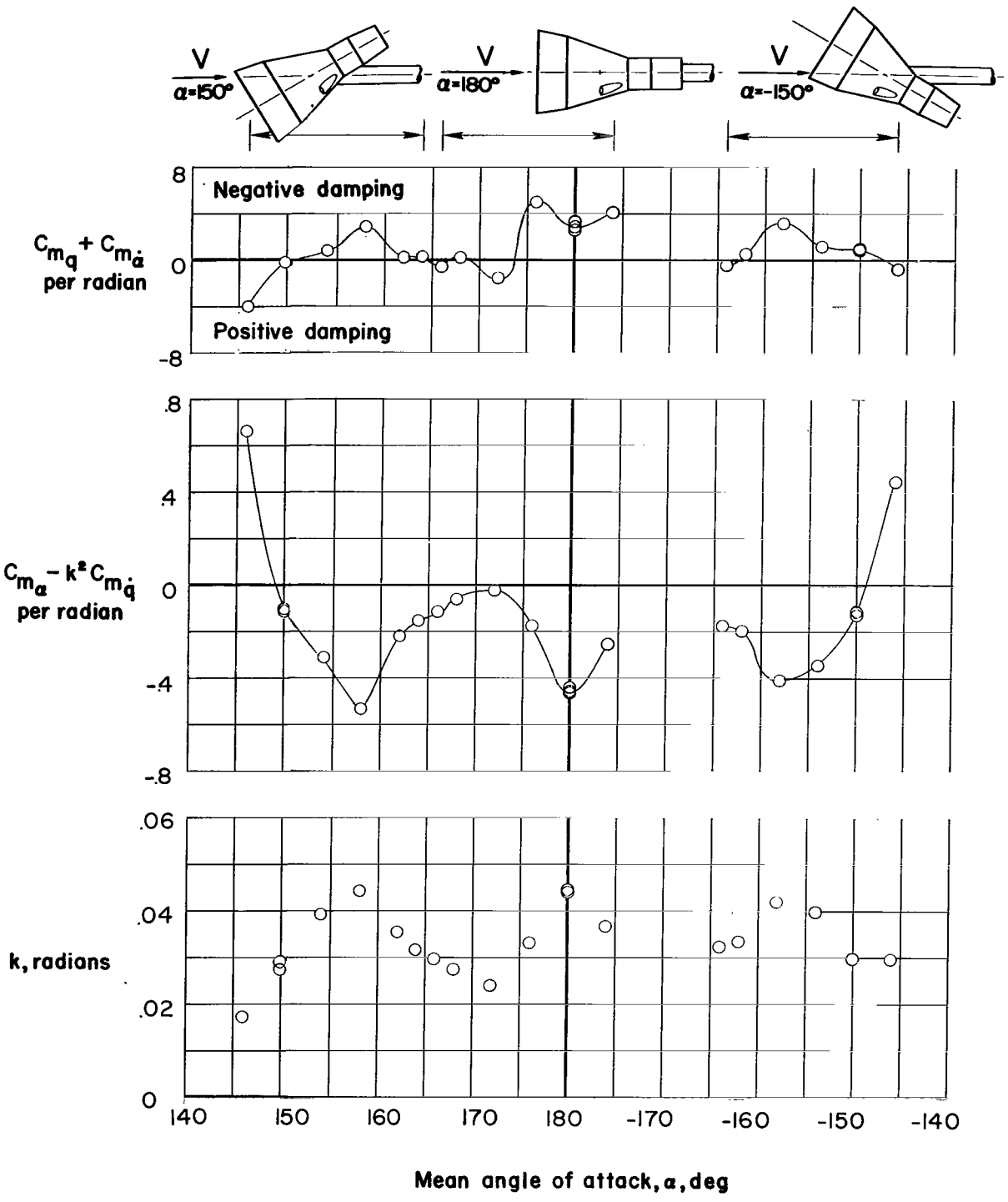

(b) M = 0.80; R = 3.28×10^6.

Figure 2.- Continued.

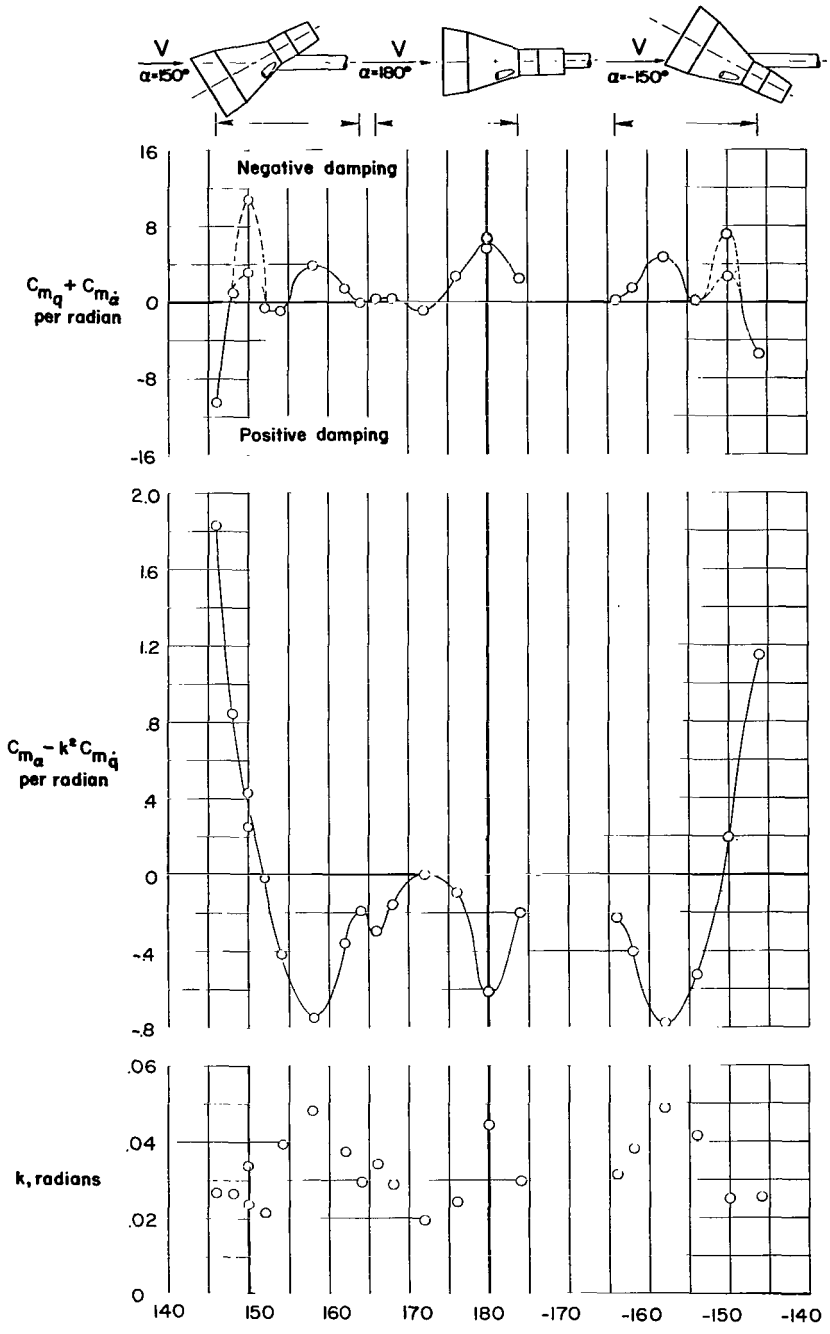

(c) M = 0.95; R = 3.27×10^6.

Figure 2.- Continued.

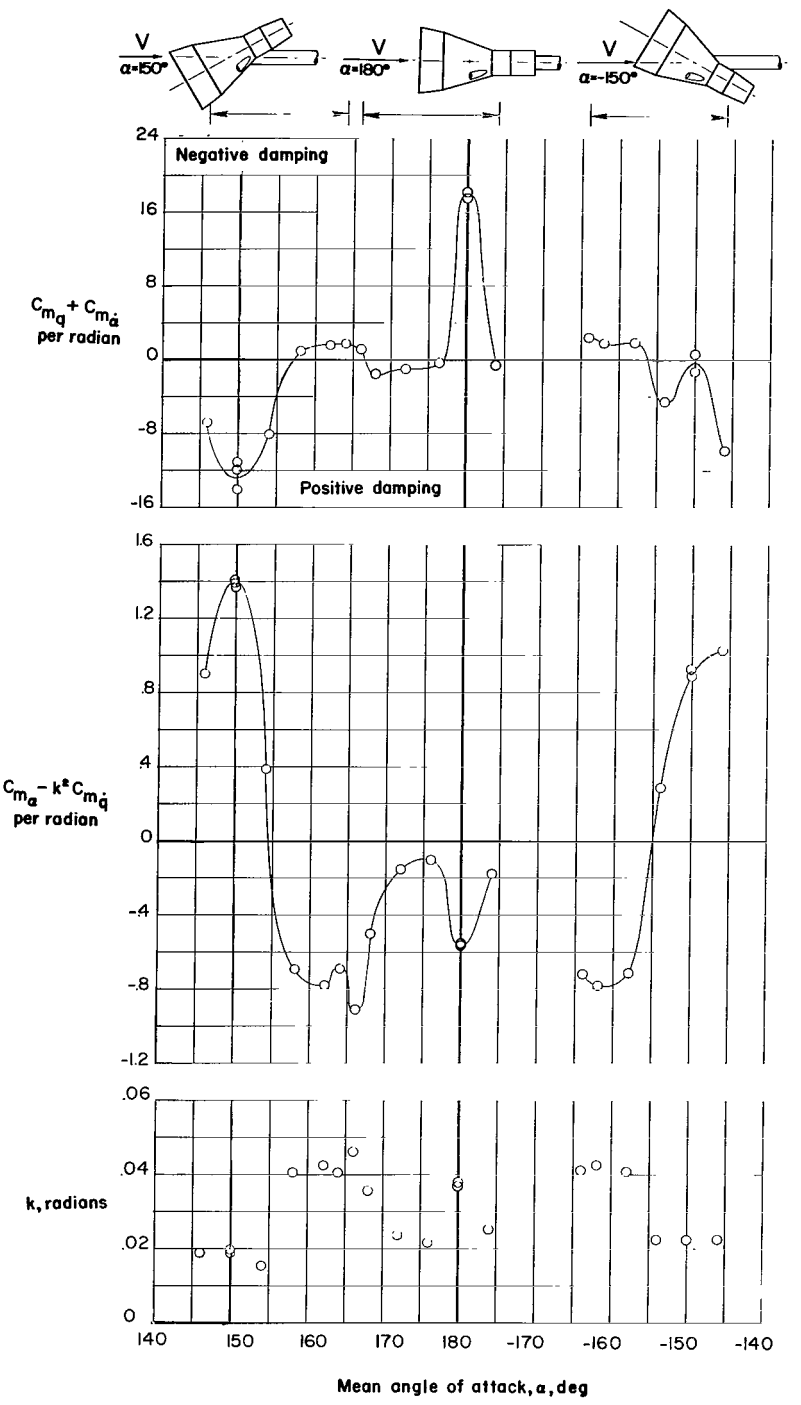

(d) M = 1.20; R = 3.25×10^6.

Figure 2.- Continued.

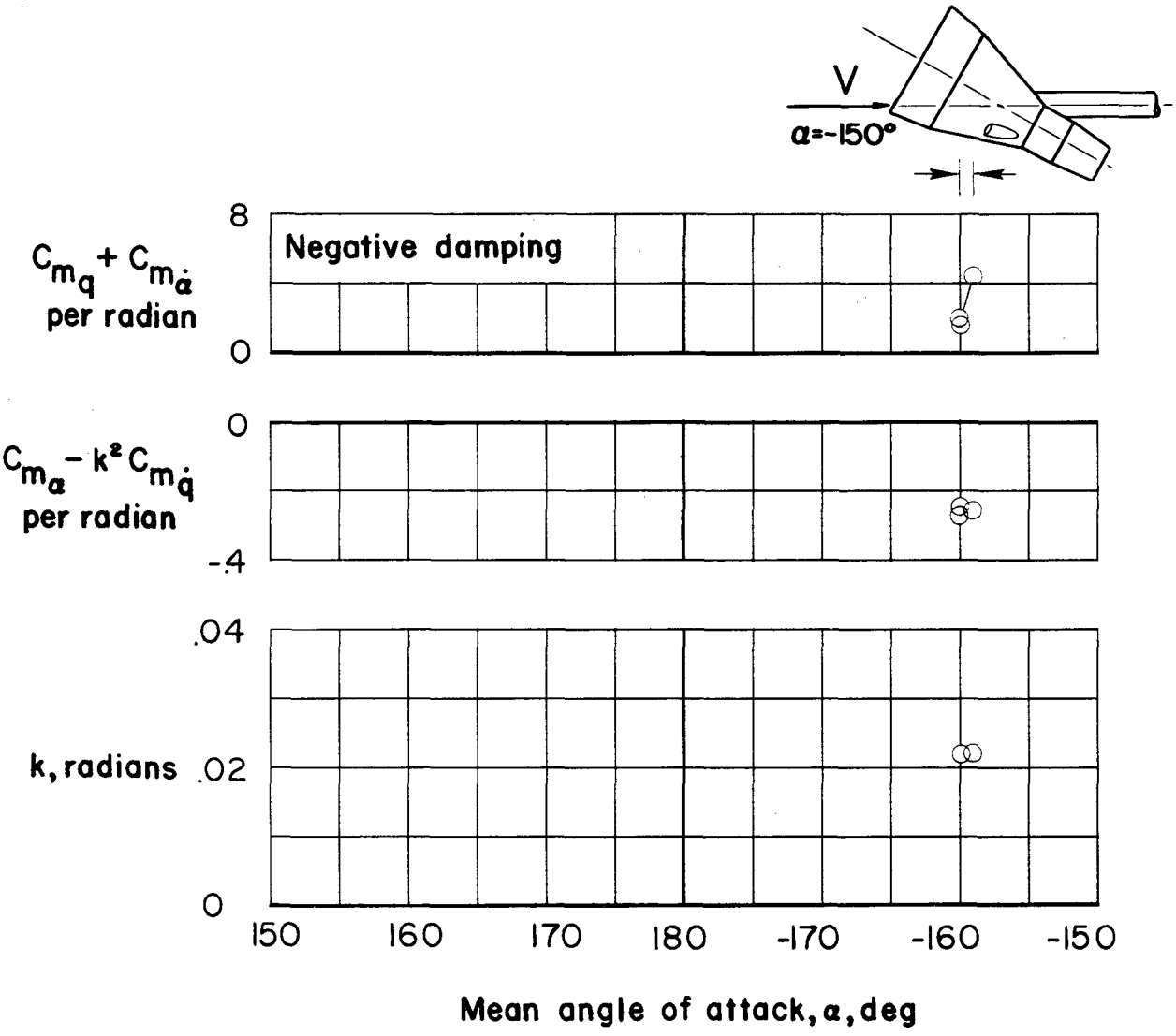

(e) M = 1.70; R = 3.30×10^6.

Figure 2.- Continued.

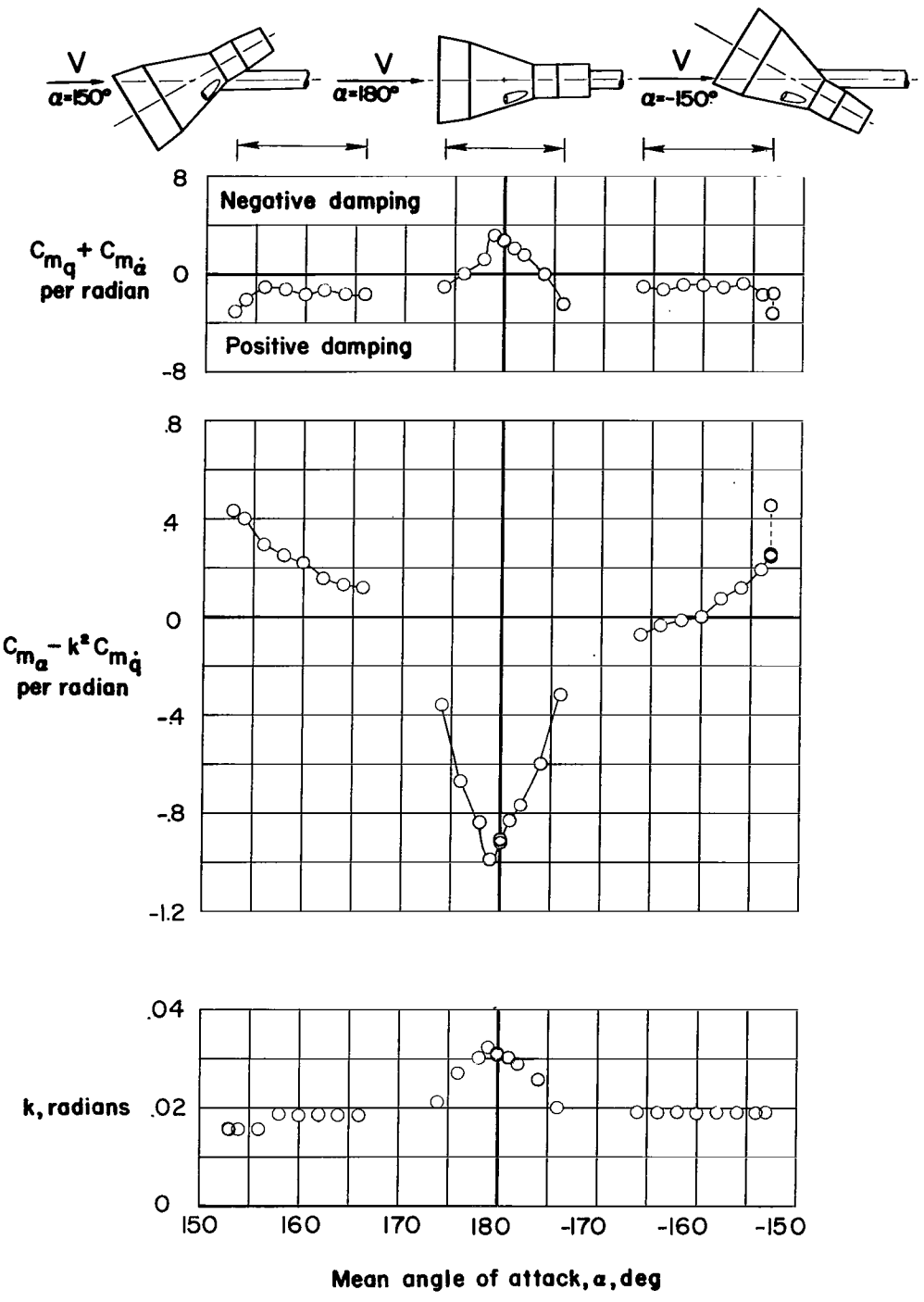

(f) M = 2.16; R = 3.36×10^6.

Figure 2.- Continued.

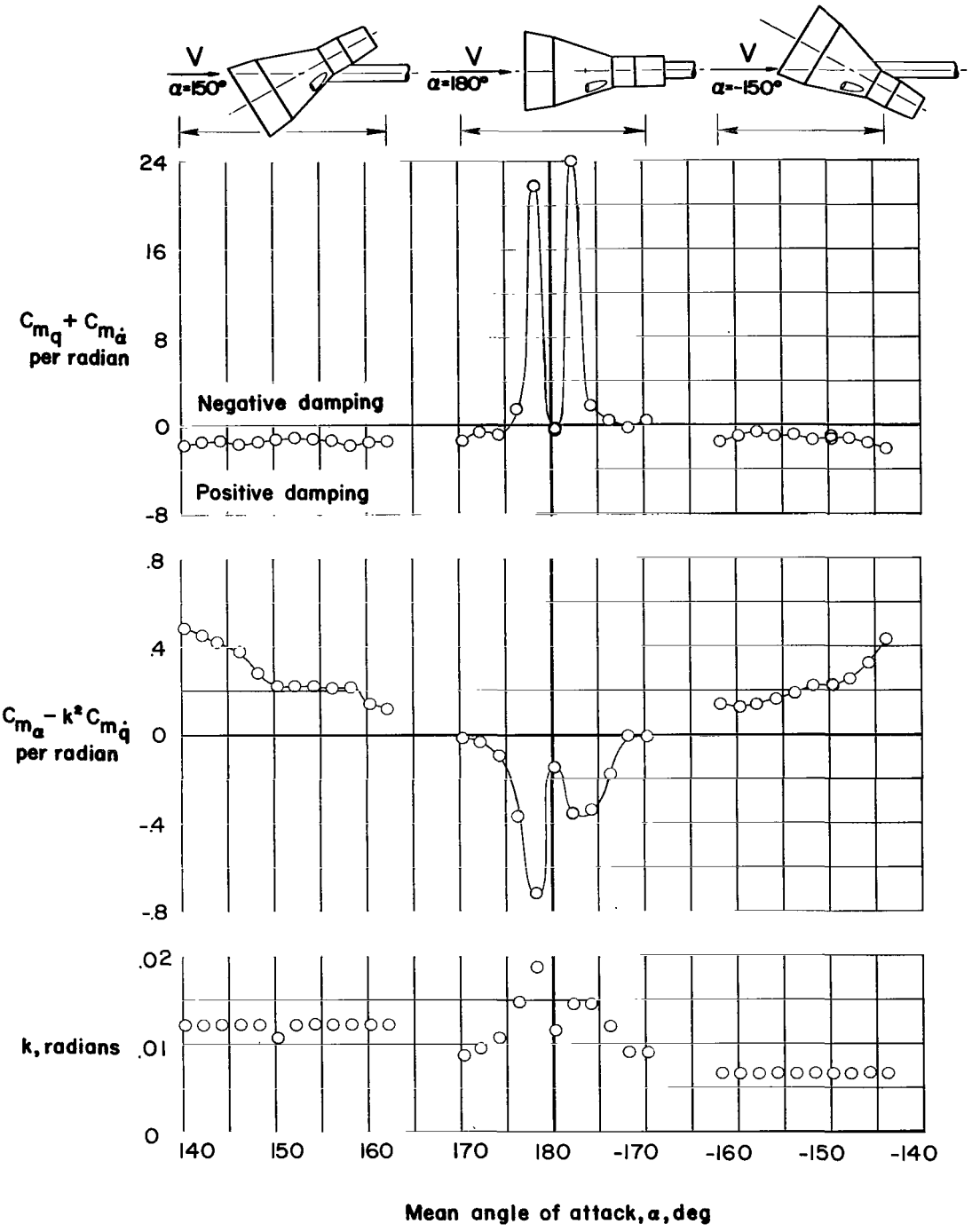

(g) M = 3.00; R = 2.10 × 10^6.

Figure 2.- Continued.

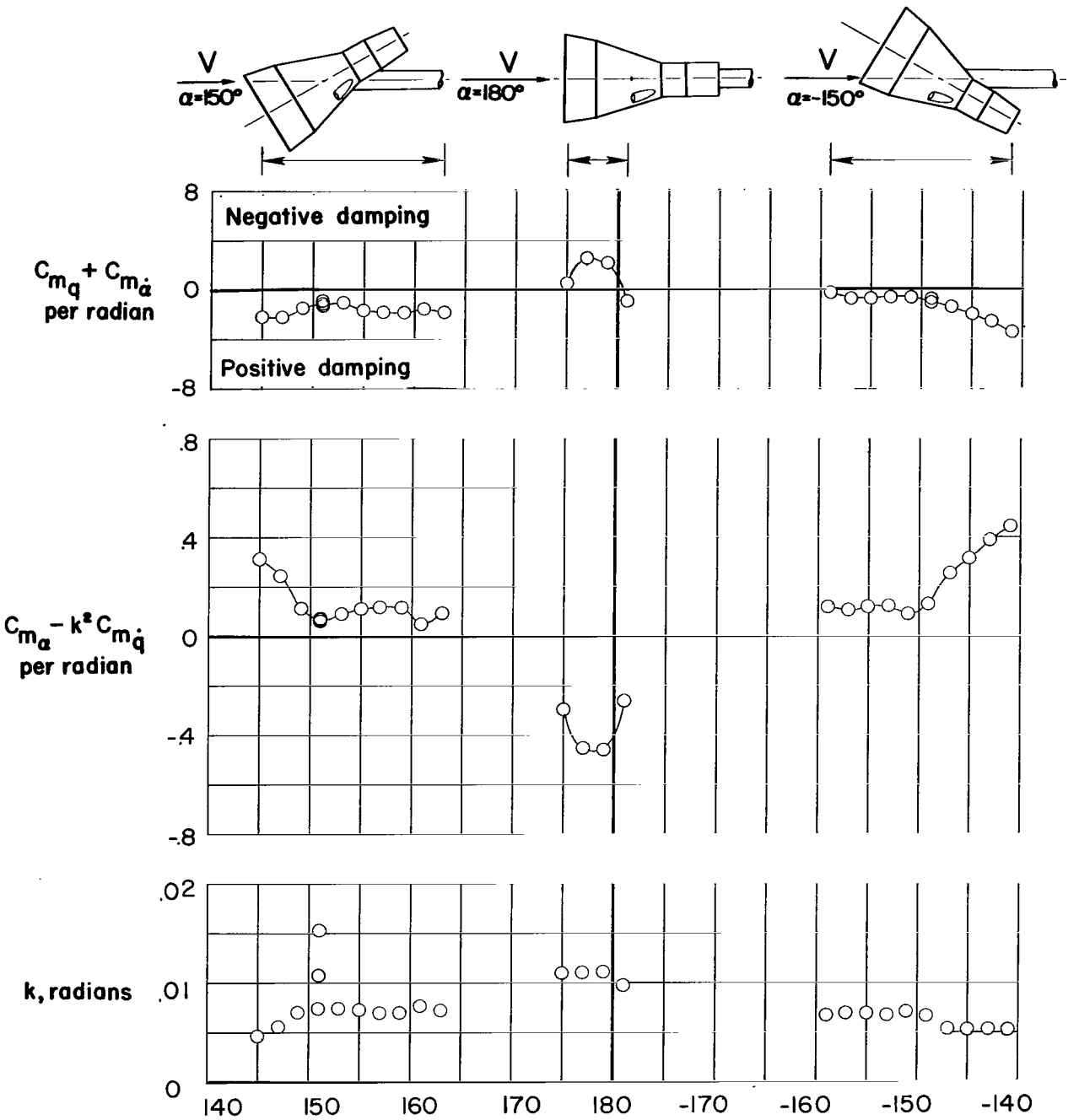

(h) M = 4.63; R = 1.57×10^6.

Figure 2.- Concluded.

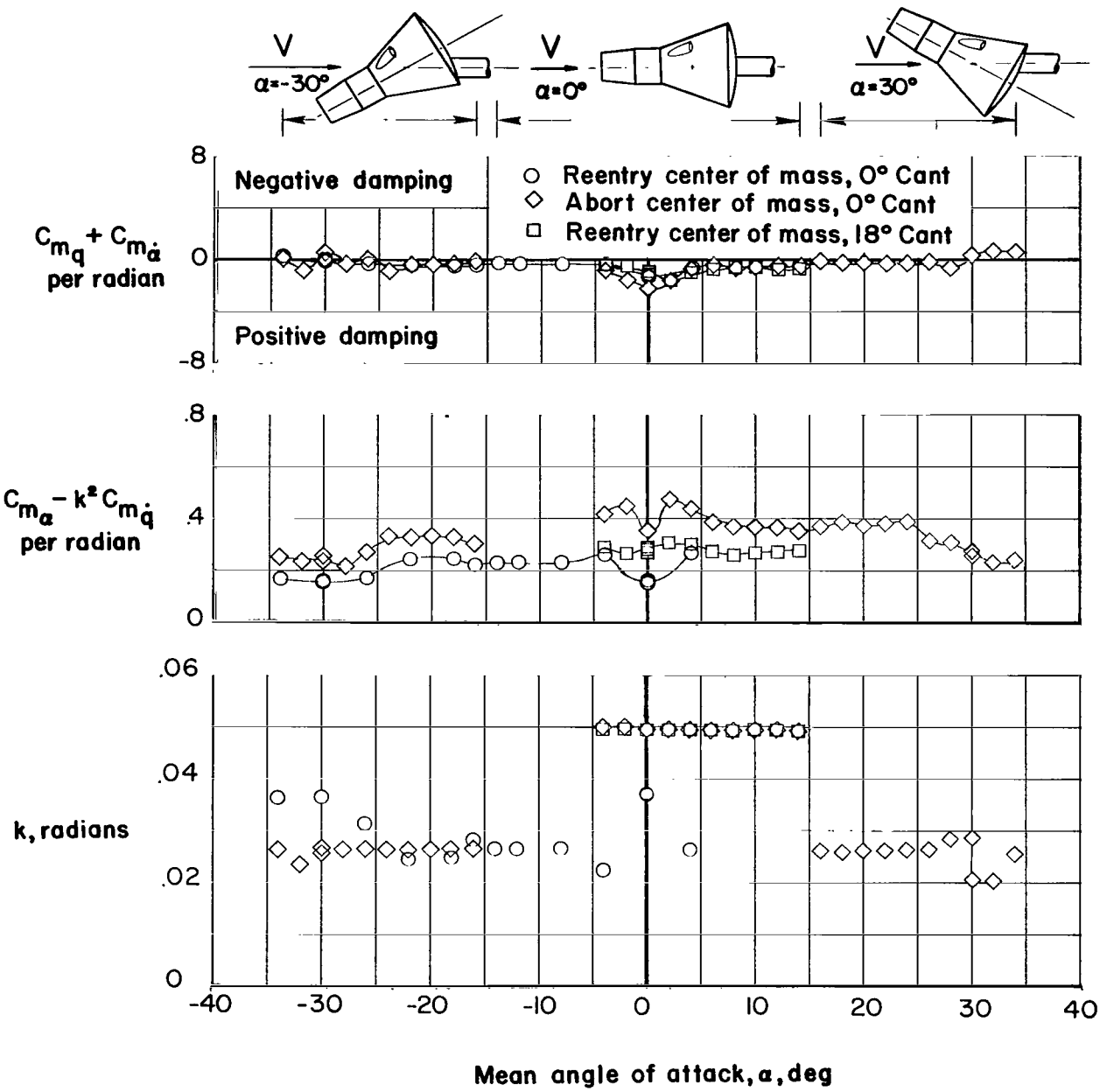

(a) M = 0.50; R = 2.56×10^6 to 3.28×10^6.

Figure 3.- Variation of damping-in-pitch parameter, oscillatory-longitudinal-stability parameter, and reduced-frequency parameter with mean angle of attack for models of Gemini reentry configuration centered around 0^0 angle of attack. $\beta = 0^0$.

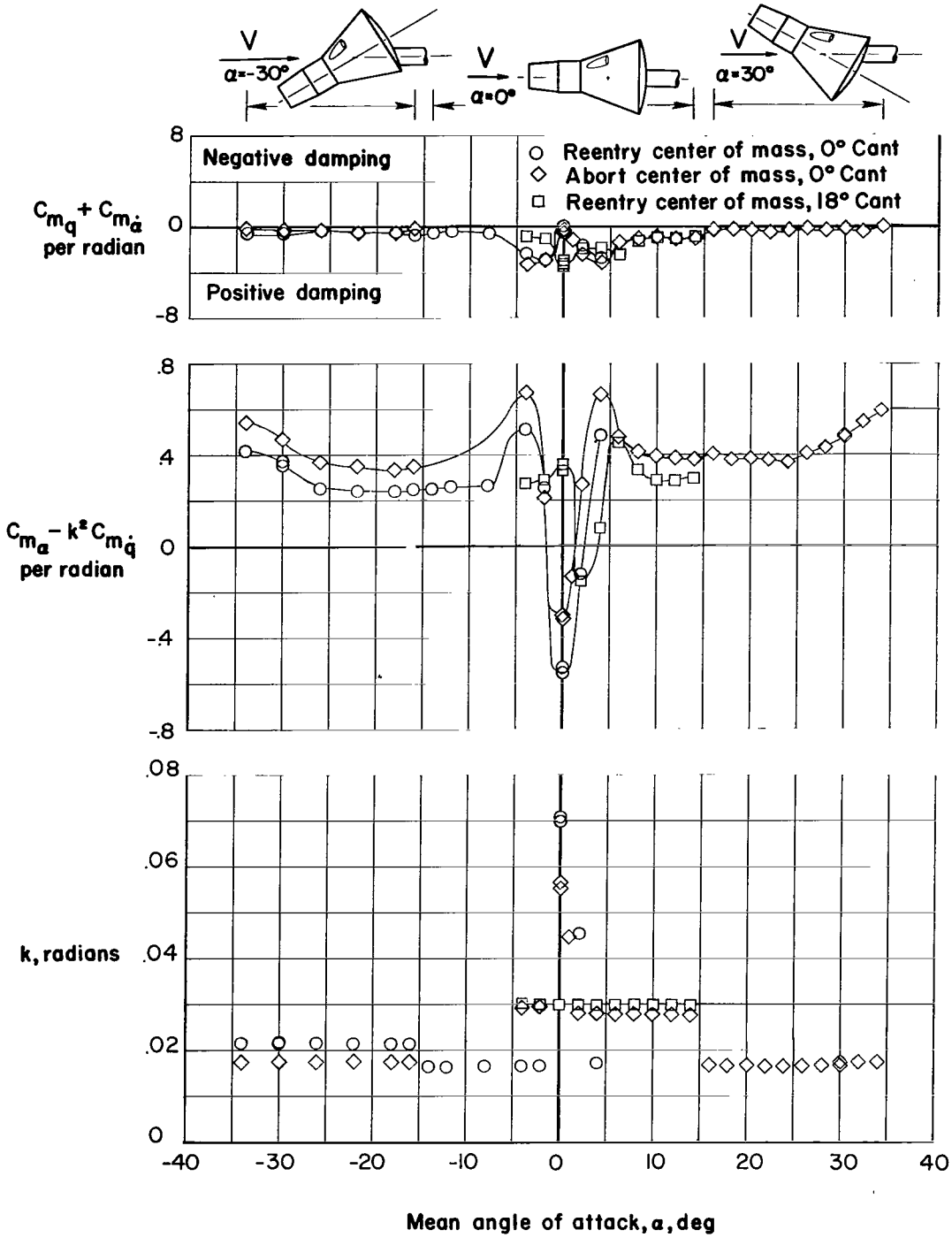

(b) M = 0.80; R = 3.28×10^6.

Figure 3.- Continued.

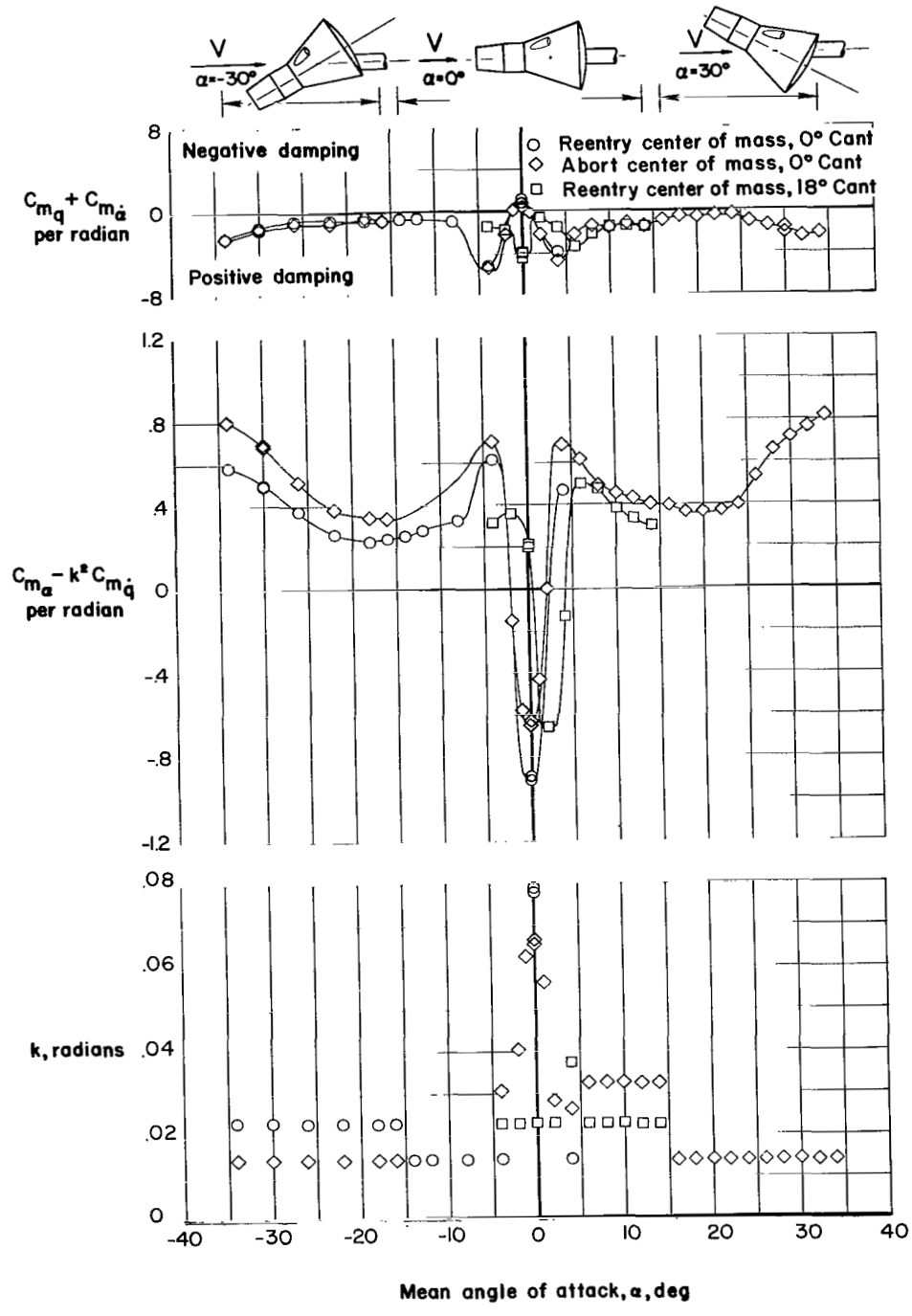

(c) M = 0.95; R = 3.29×10^6.

Figure 3.- Continued.

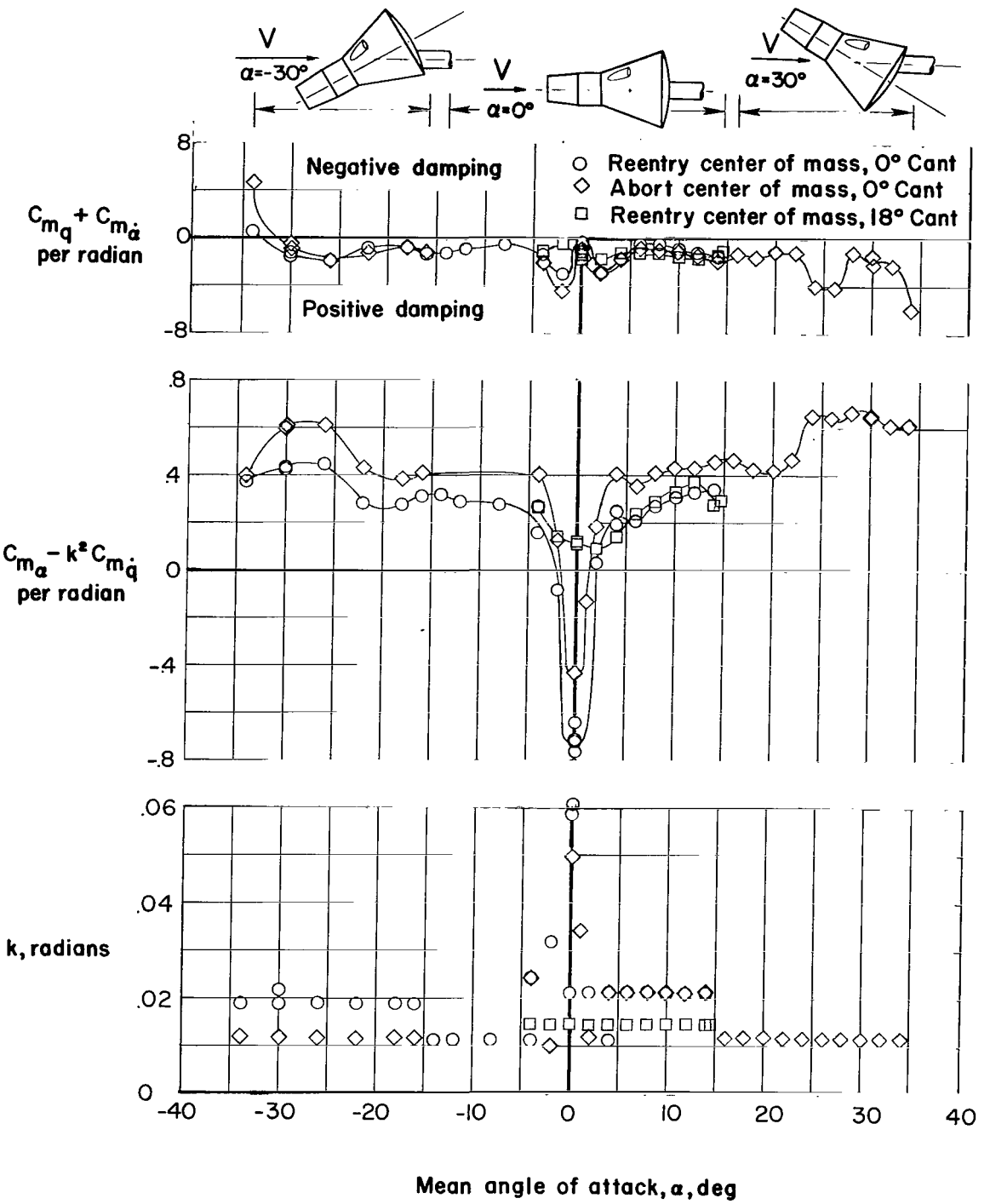

(d) M = 1.20; R = 3.31×10^6.

Figure 3.- Continued.

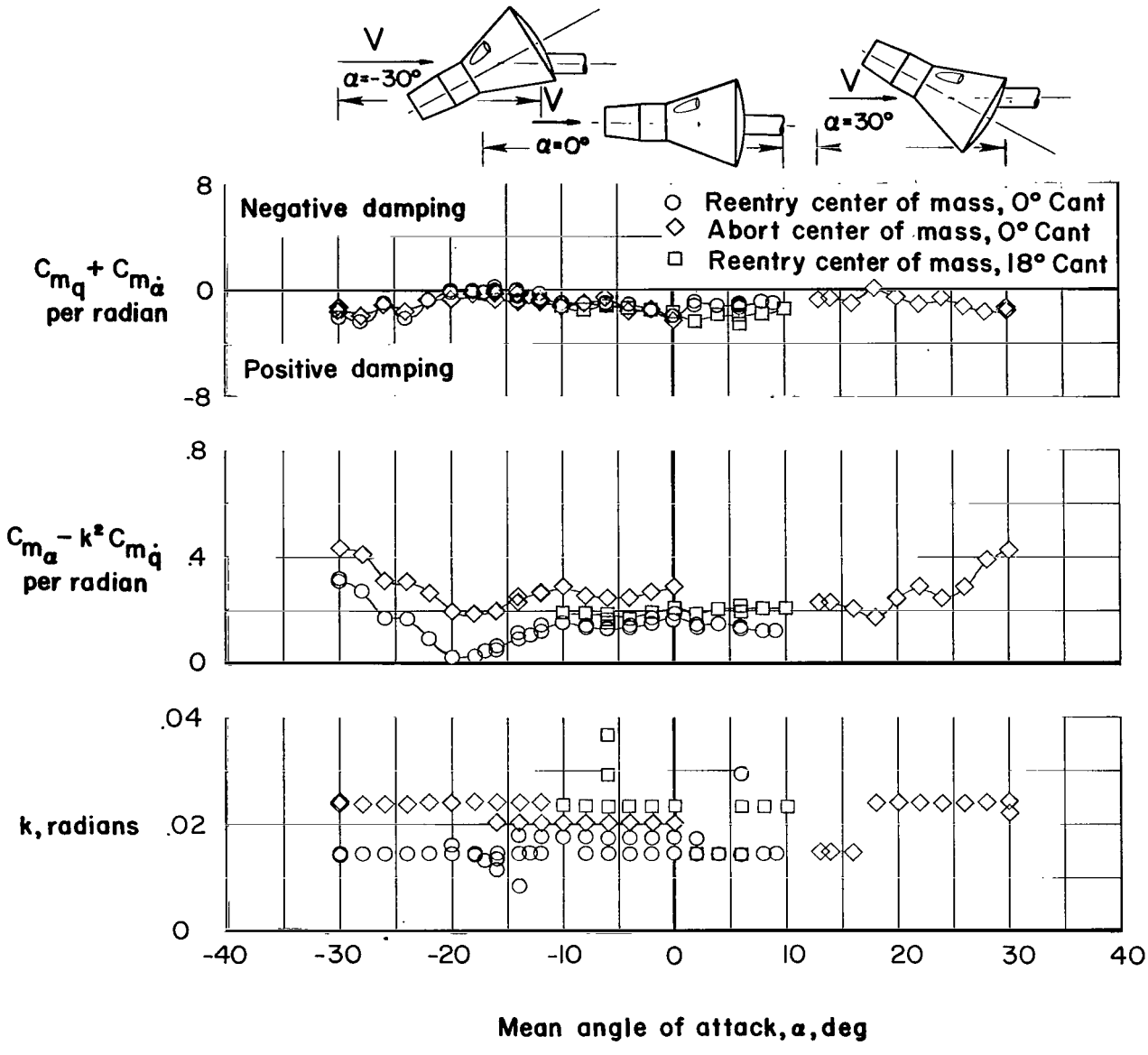

(e) M = 1.70; R = 3.30 × 10^6.

Figure 3.- Continued.

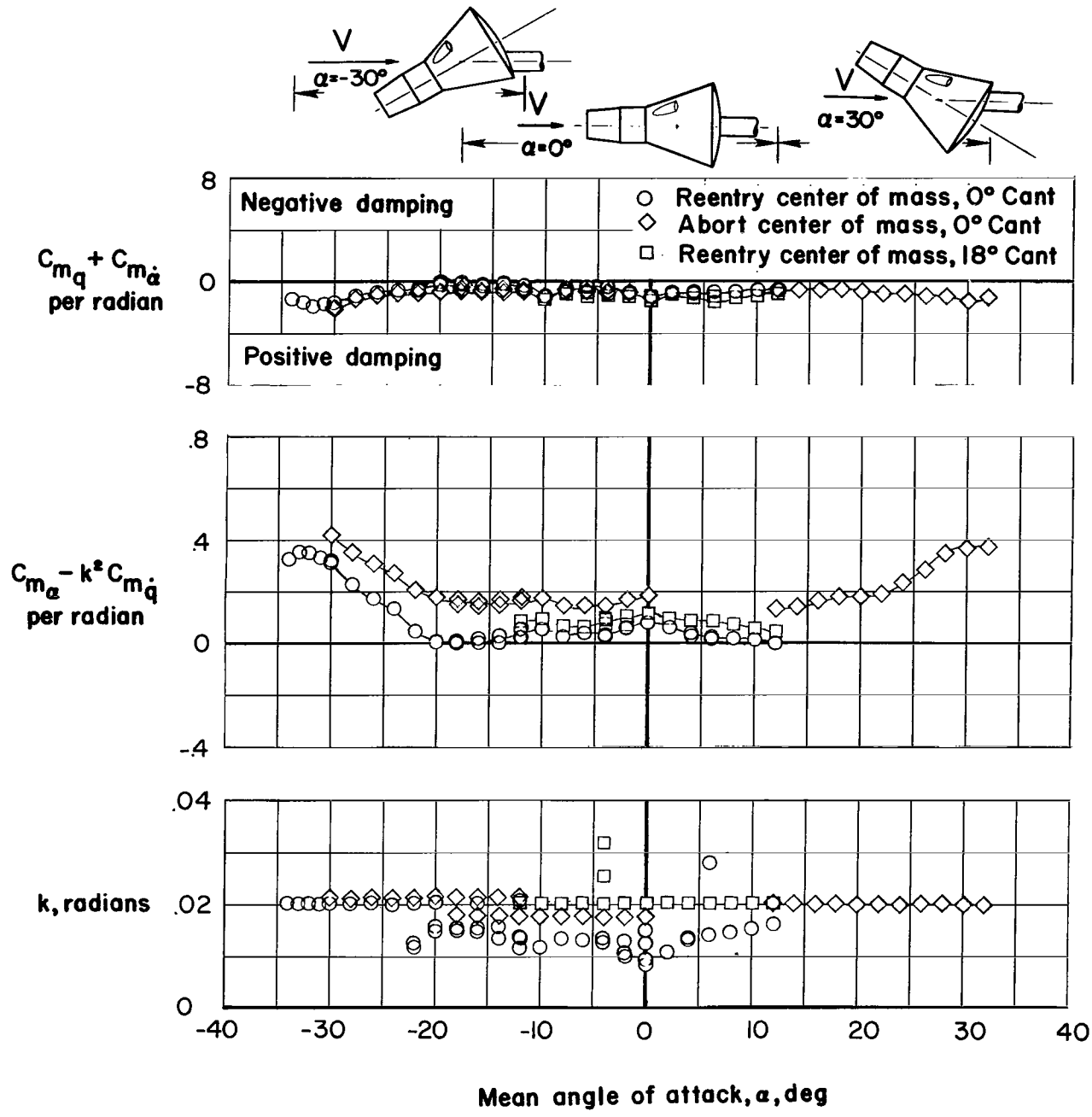

(f) M = 2.16; R = 3.36×10^6.

Figure 3.- Continued.

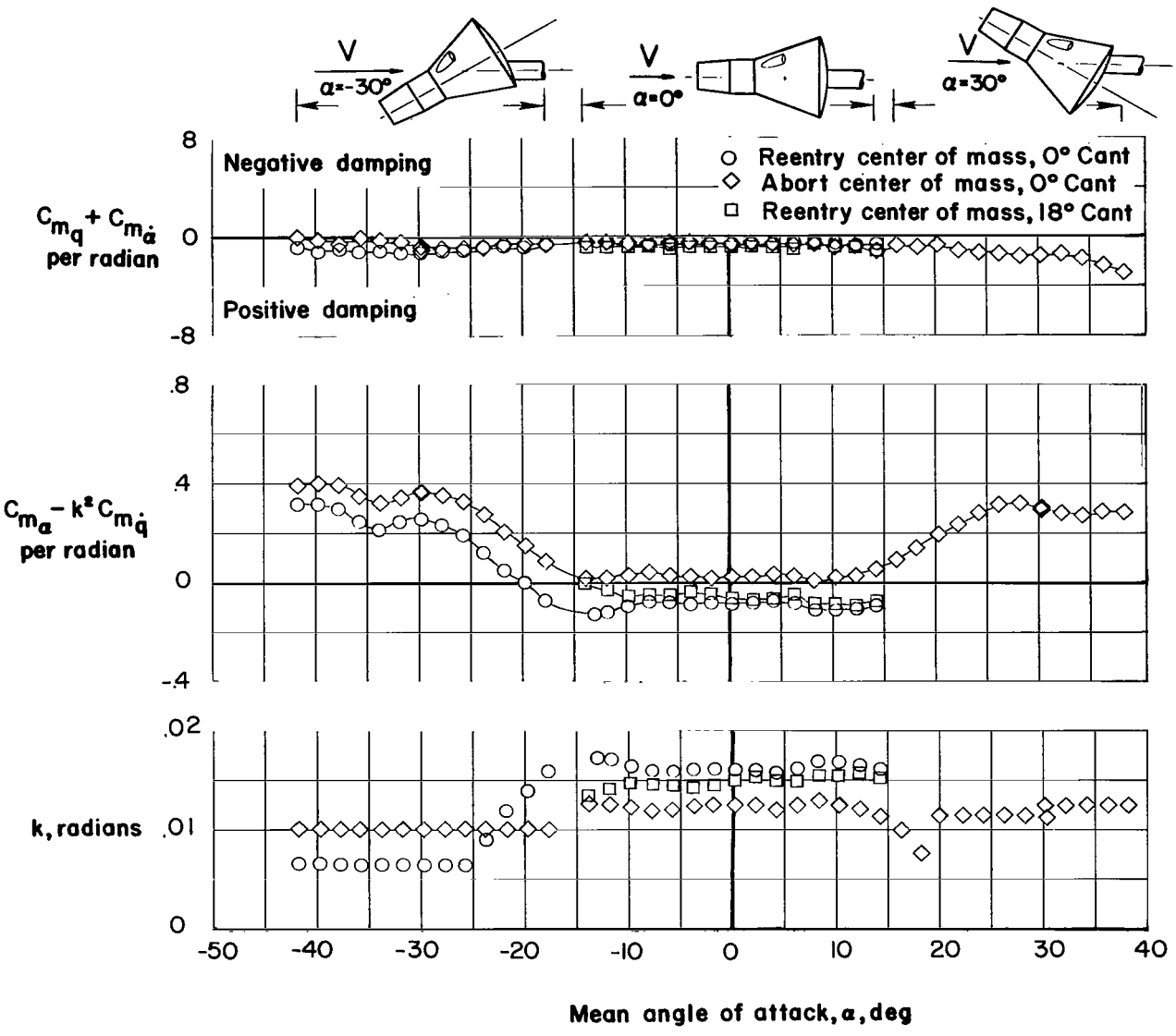

(g) $M = 3.00$; $R = 2.10 \times 10^6$.

Figure 3.- Continued.

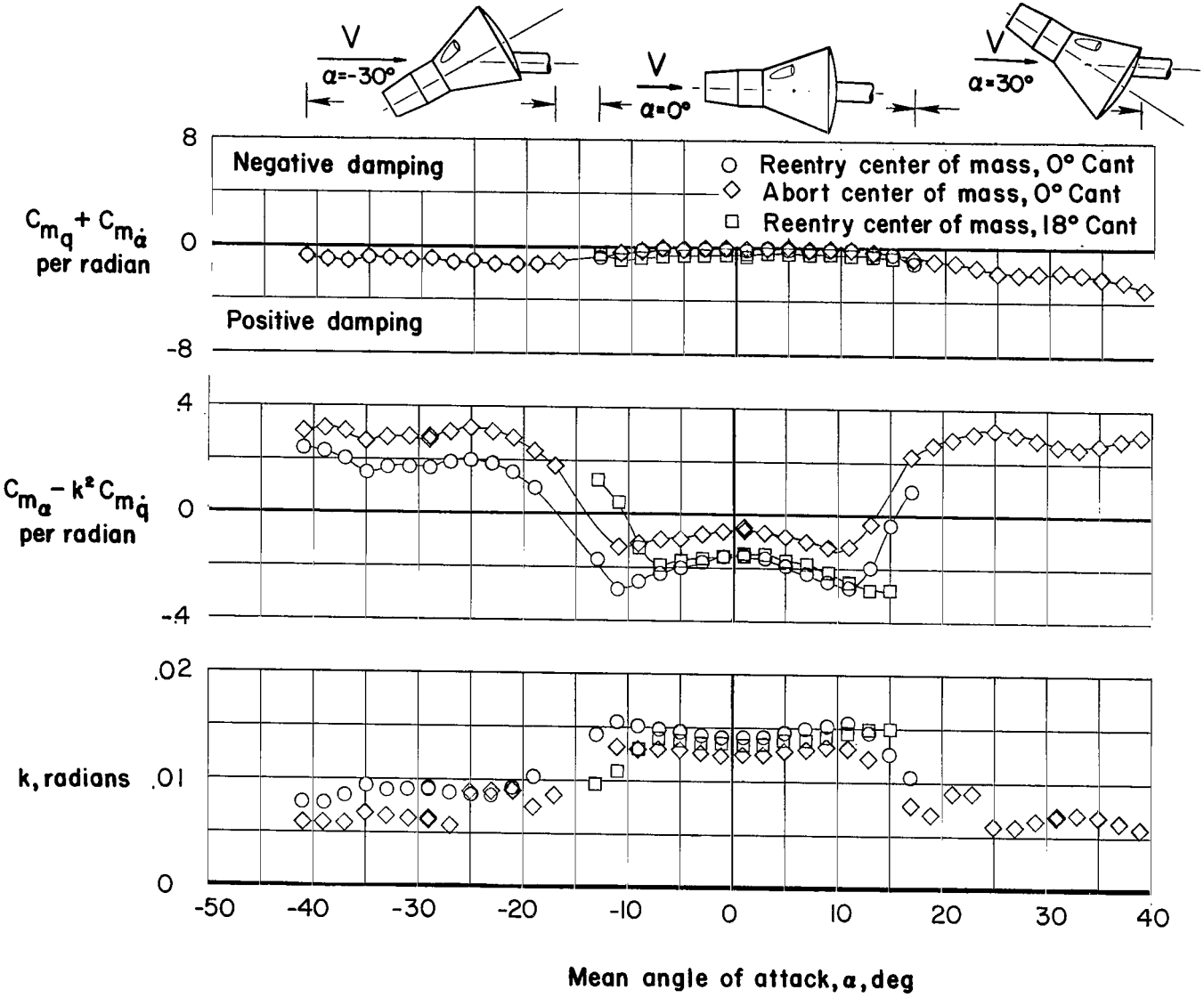

(h) $M = 4.63$; $R = 1.79 \times 10^6$.

Figure 3.- Concluded.

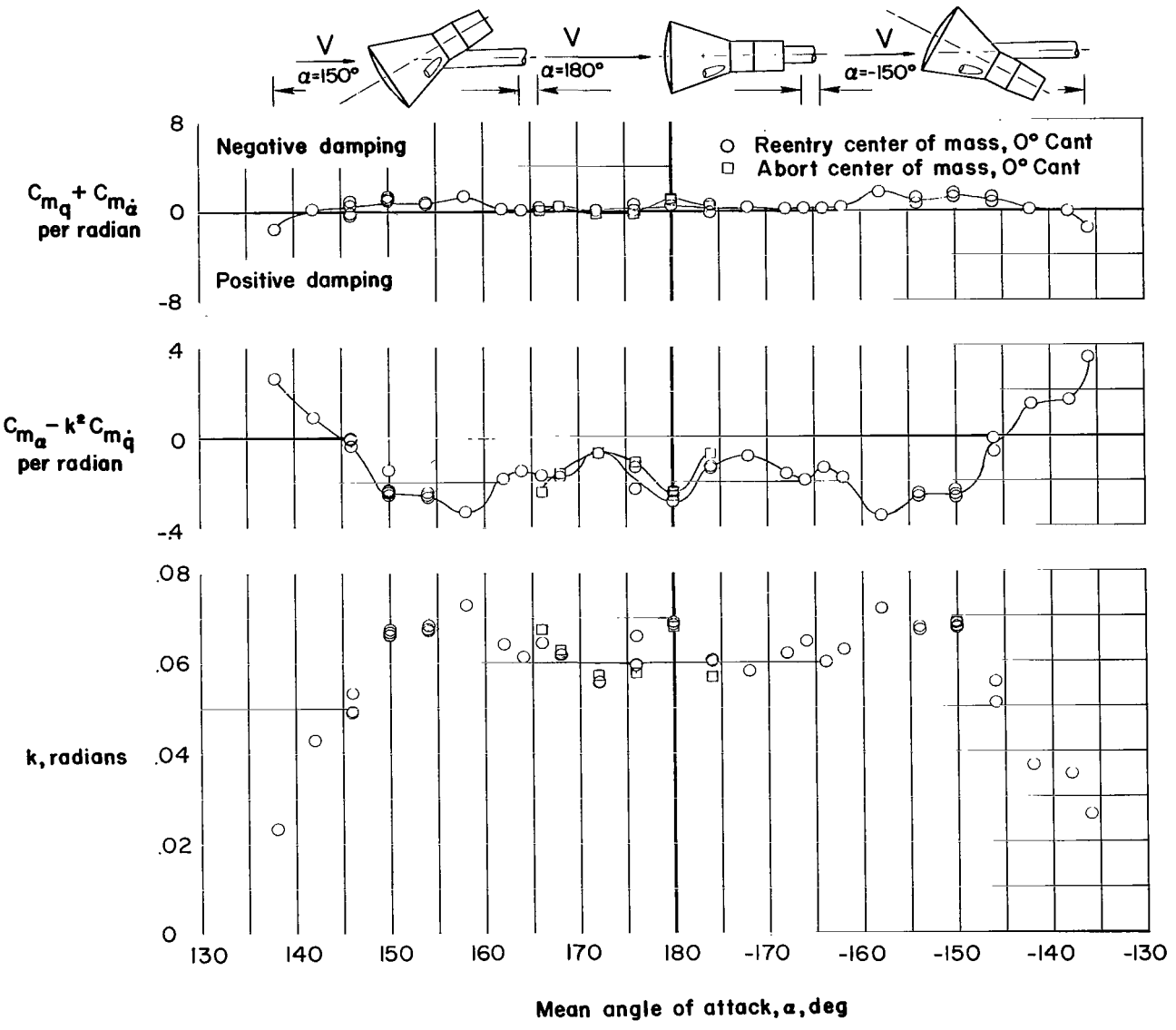

(a) M = 0.50; R = 2.56×10^6.

Figure 4.- Variation of damping-in-pitch parameter, oscillatory-longitudinal-stability parameter, and reduced-frequency parameter with mean angle of attack for models of Gemini reentry configuration centered around 180^0 angle of attack. $\beta = 0^0$.

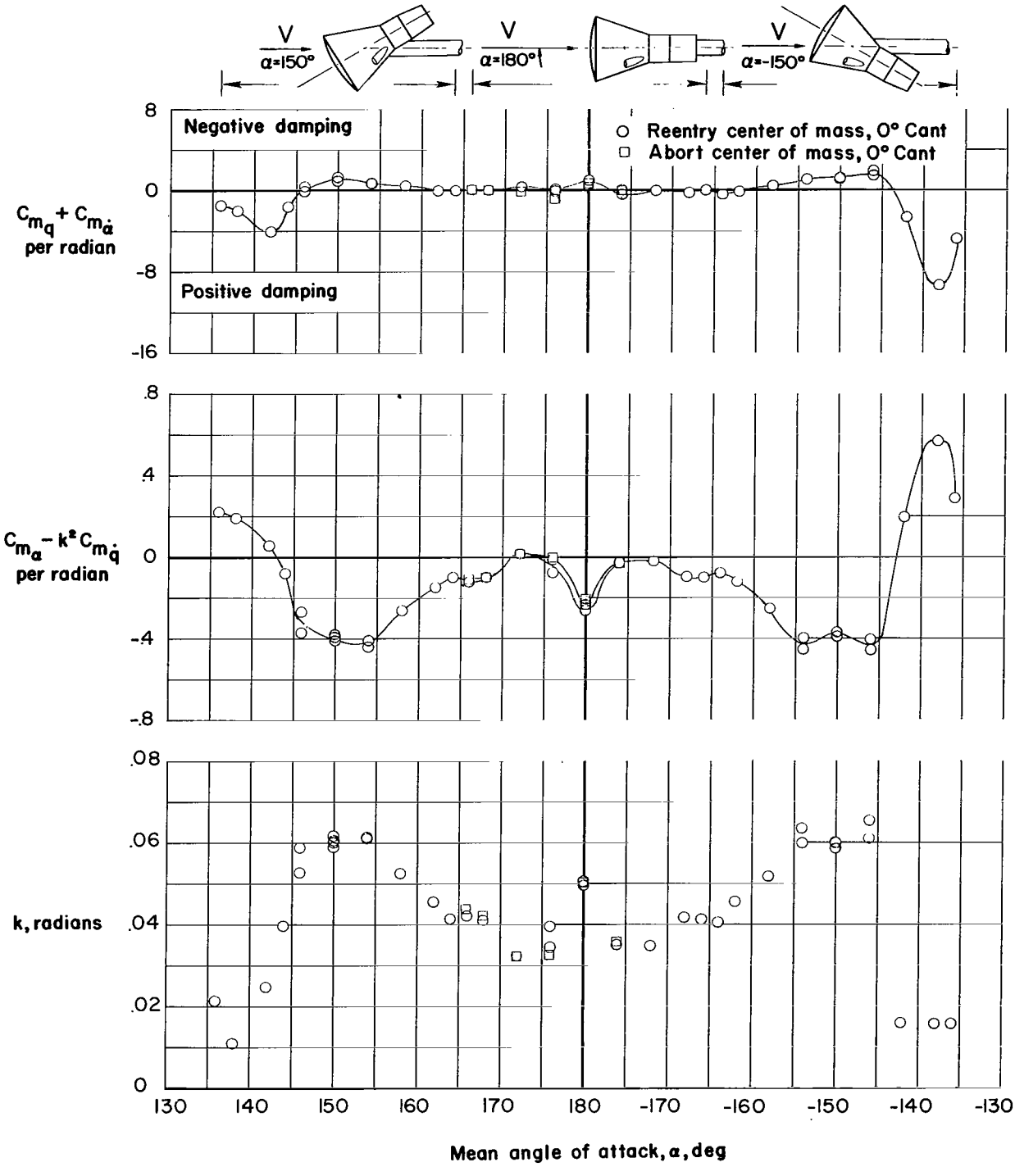

(b) M = 0.80; R = 3.27 × 10^6.

Figure 4.- Continued.

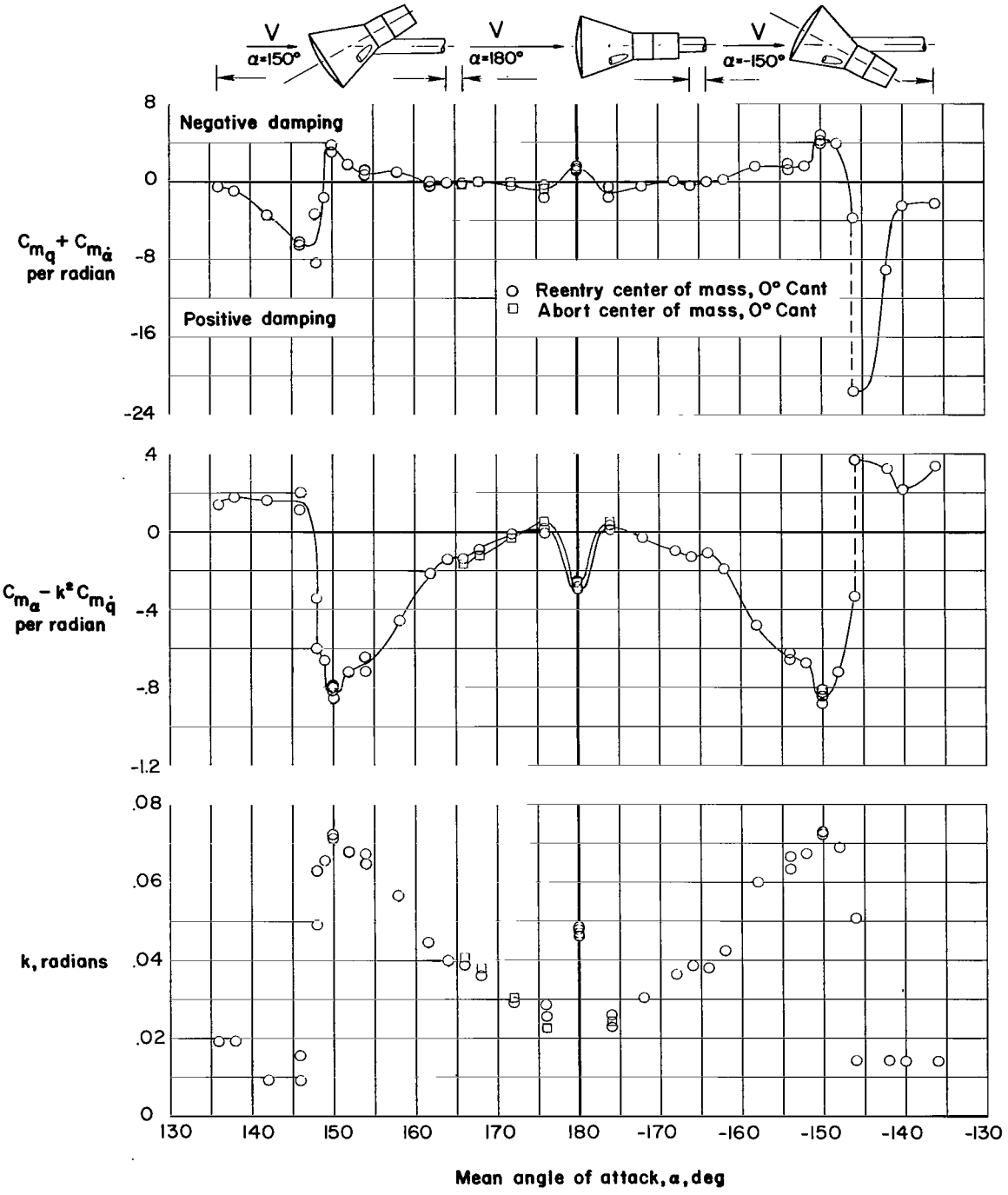

(c) M = 0.95; R = 3.29 × 10^6.

Figure 4.- Continued.

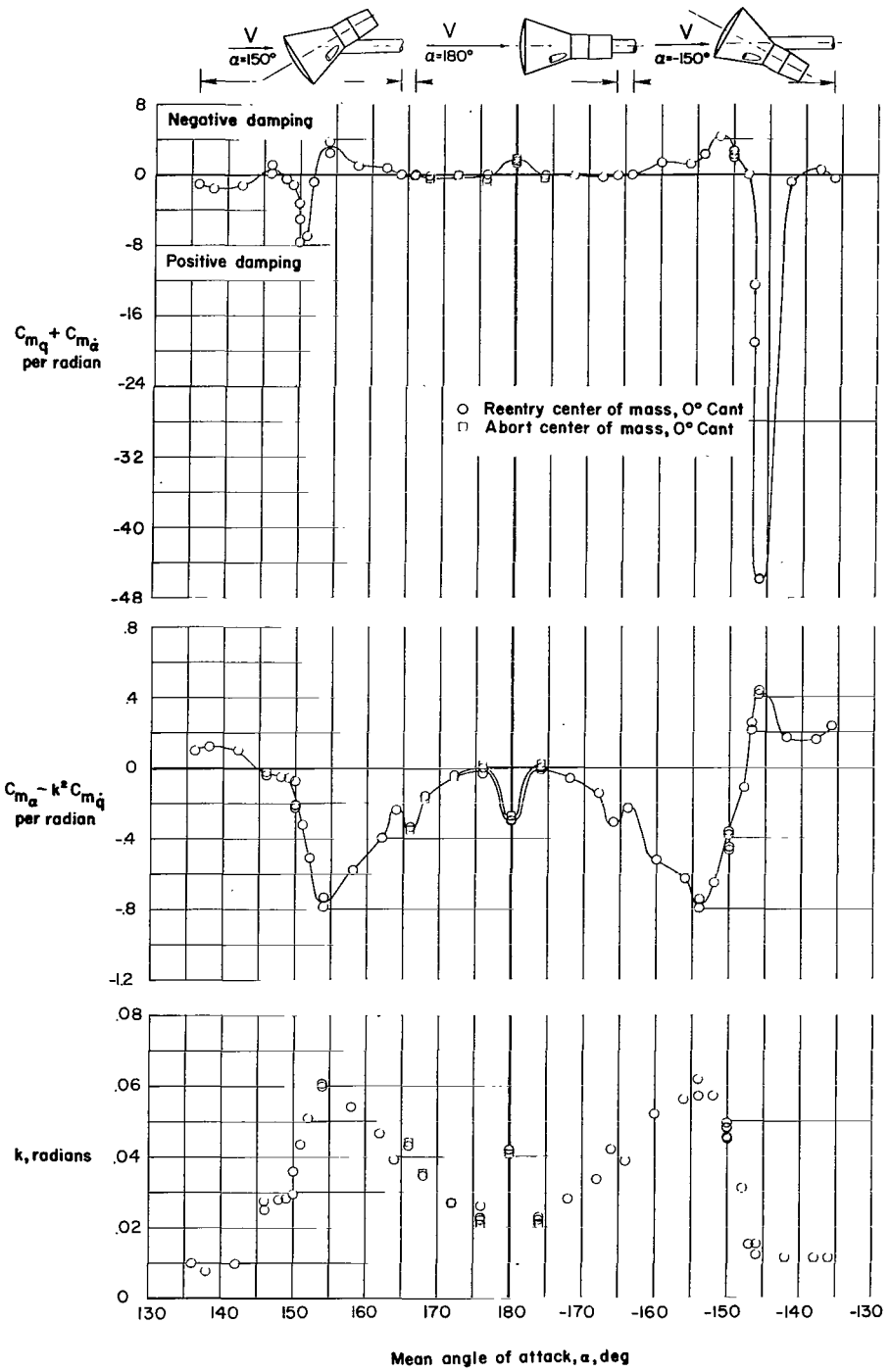

(d) M = 1.20; R = 3.25×10^6.

Figure 4.- Continued.

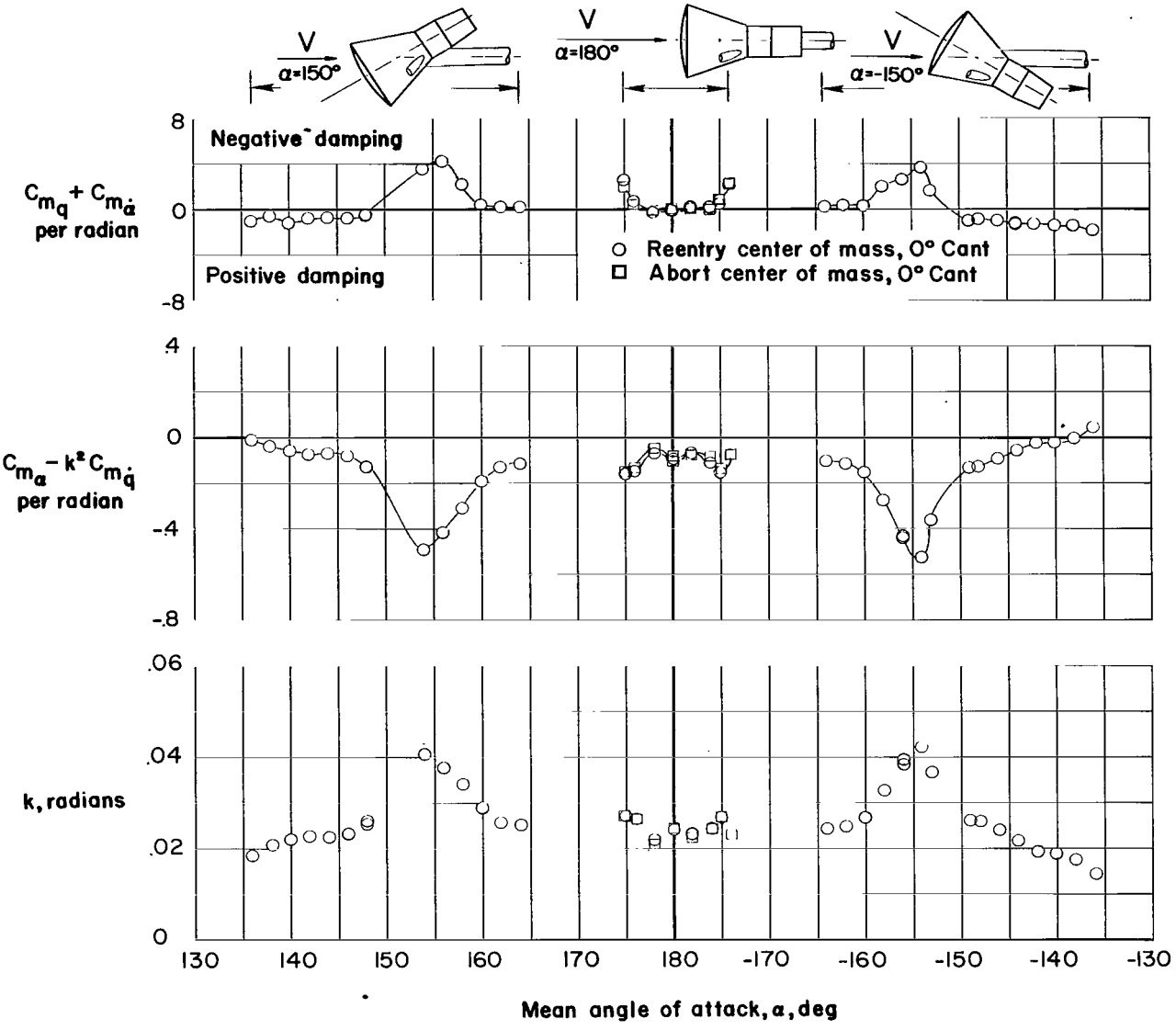

(e) M = 1.70; R = 3.30 × 10^6.

Figure 4.- Continued.

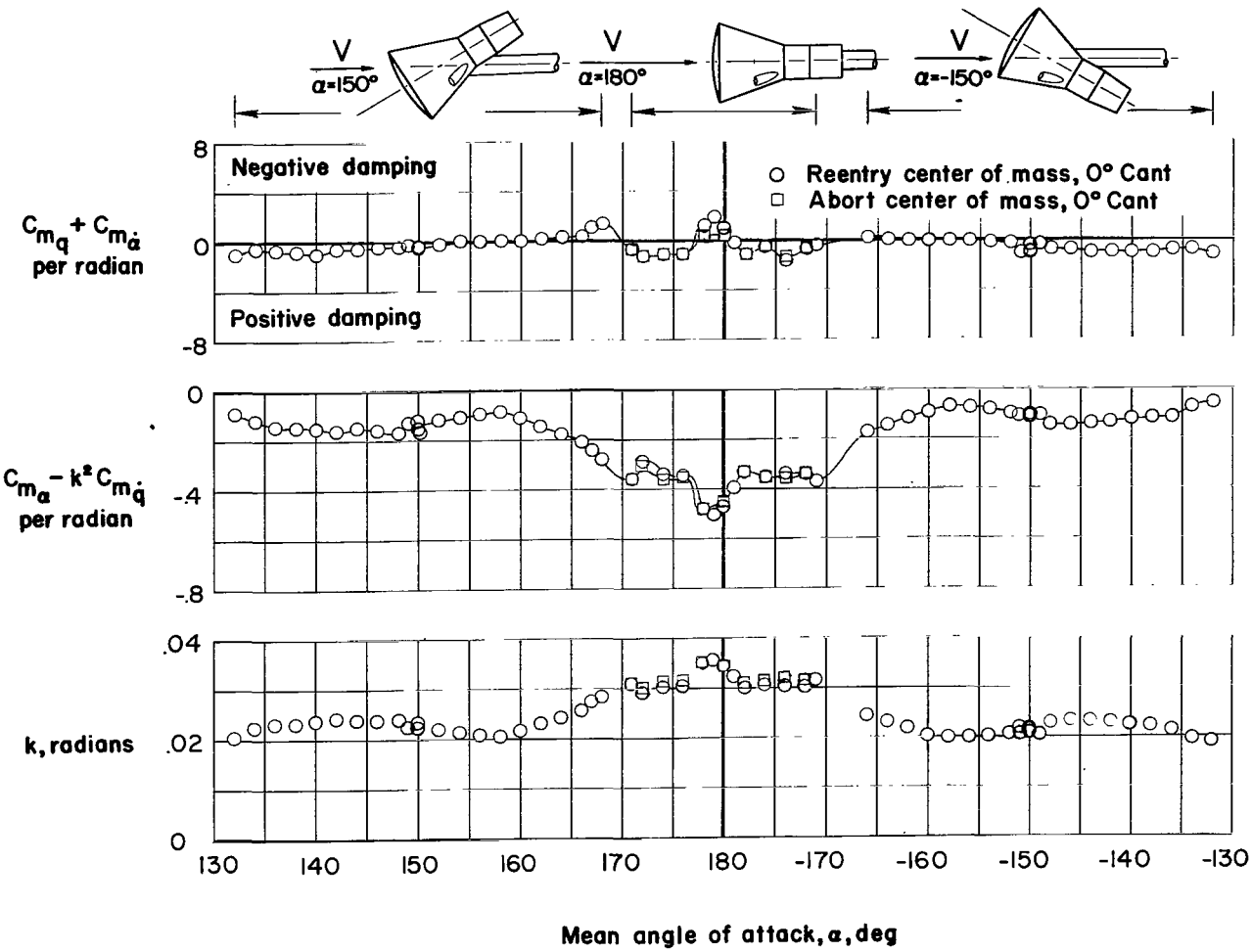

(f) M = 2.16; R = 3.36 × 10^6.

Figure 4.- Continued.

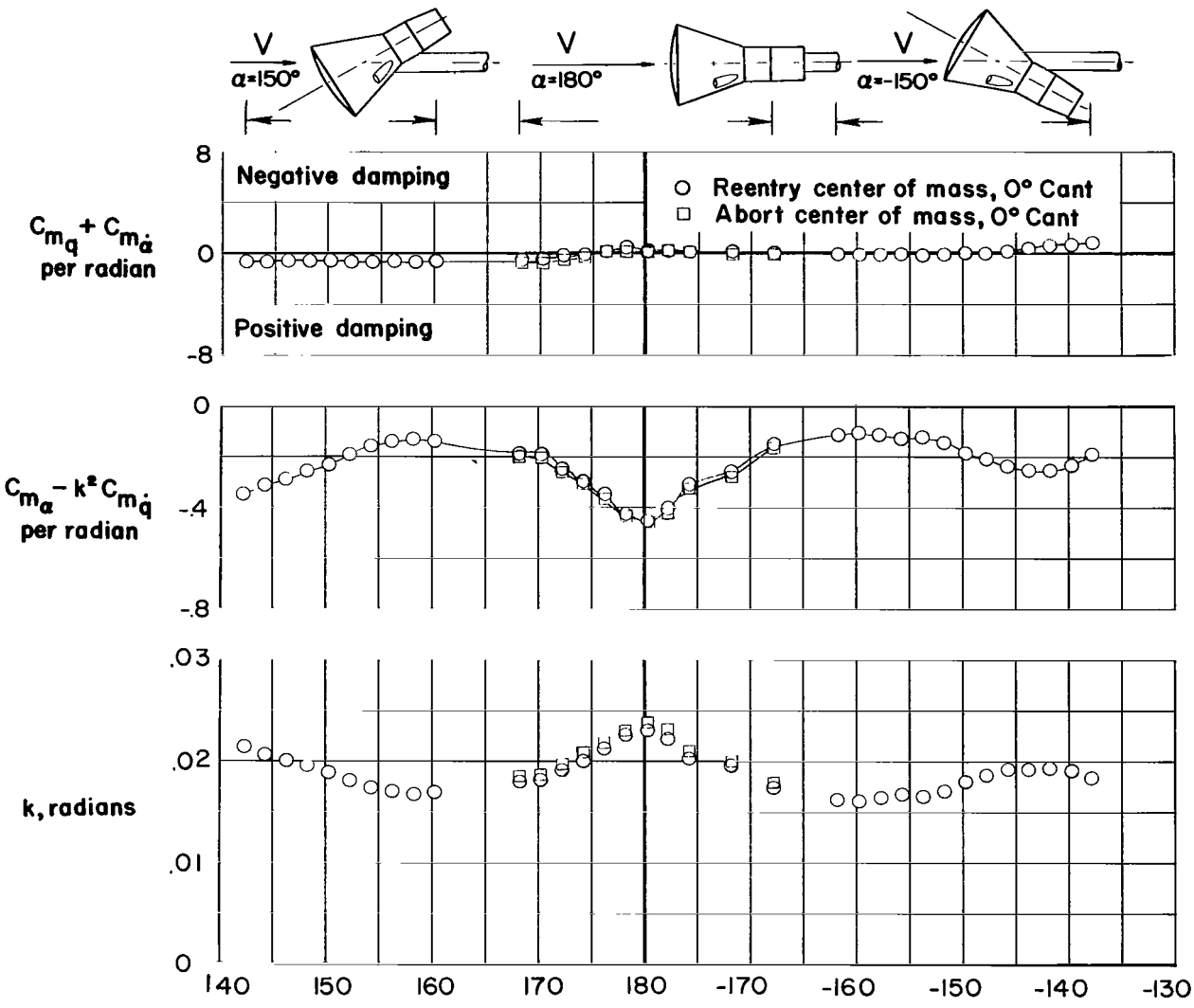

(g) M = 3.00; R = 2.10 × 10^6.

Figure 4.- Continued.

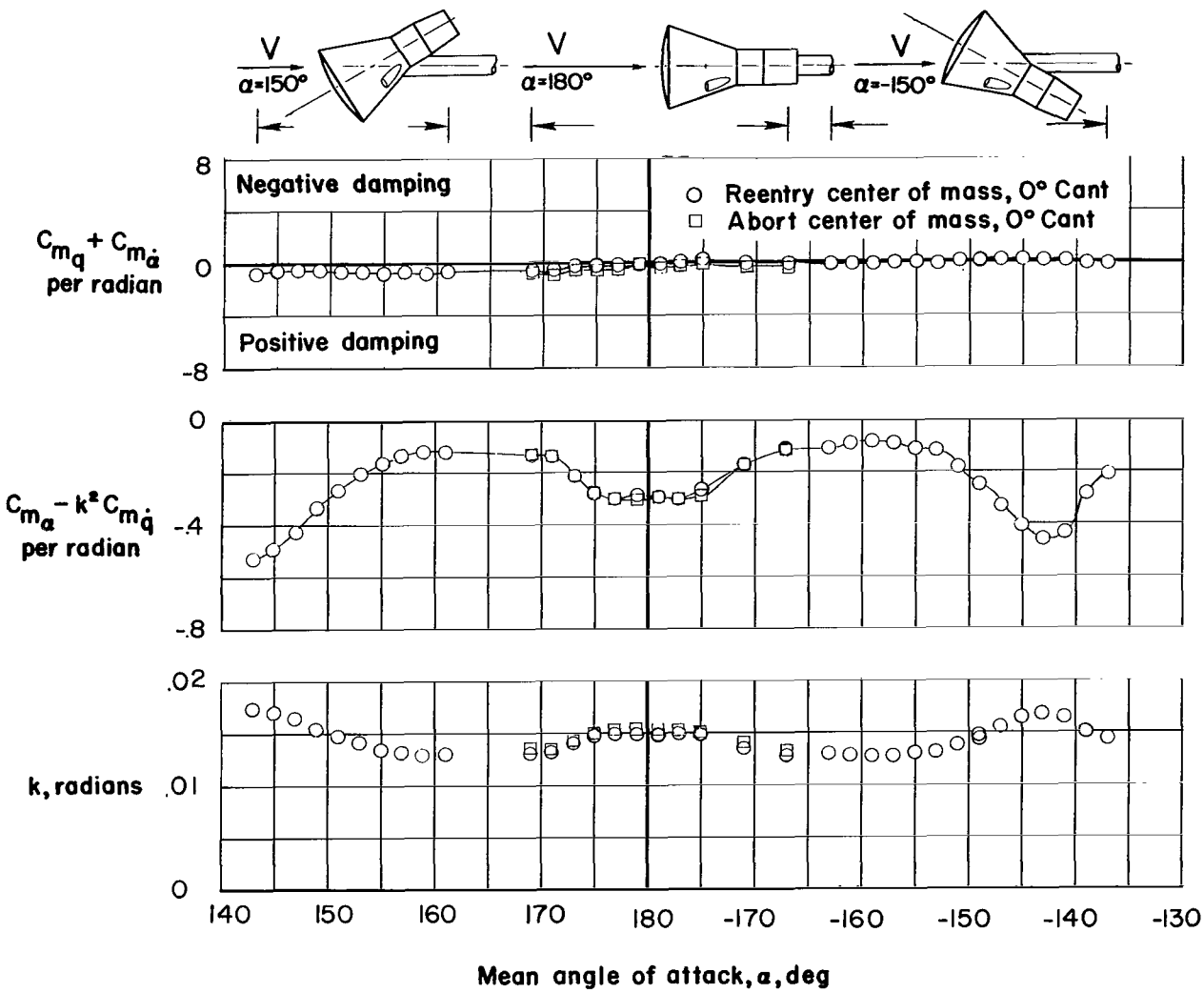

(h) M = 4.63; R = 1.79×10^6.

Figure 4.- Concluded.

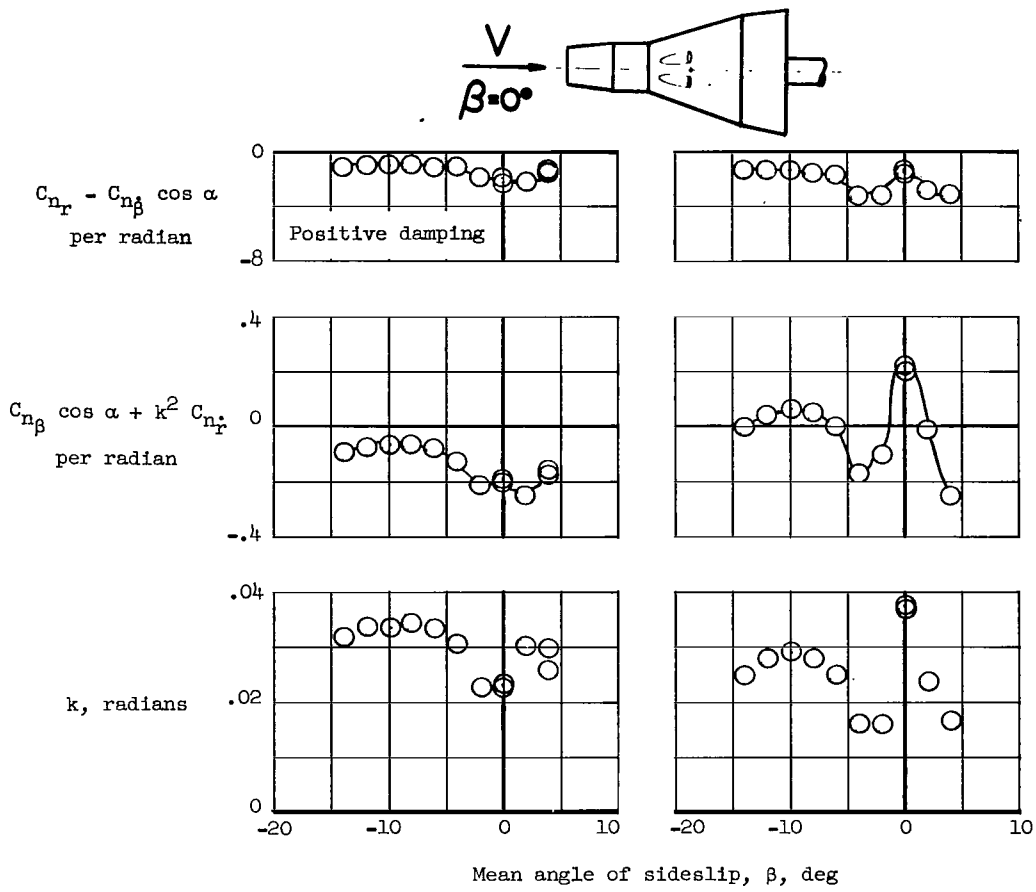

(a) M = 0.50; R = 2.56 × 10^6.

(b) M = 0.80; R = 3.27 × 10^6.

Figure 5.- Variation of damping-in-yaw parameter, oscillatory-directional-stability parameter, and reduced-frequency parameter with mean angle of sideslip for models of Gemini abort configuration with 0^0 cant centered around 0^0 angle of sideslip. $\alpha = 0^0$.

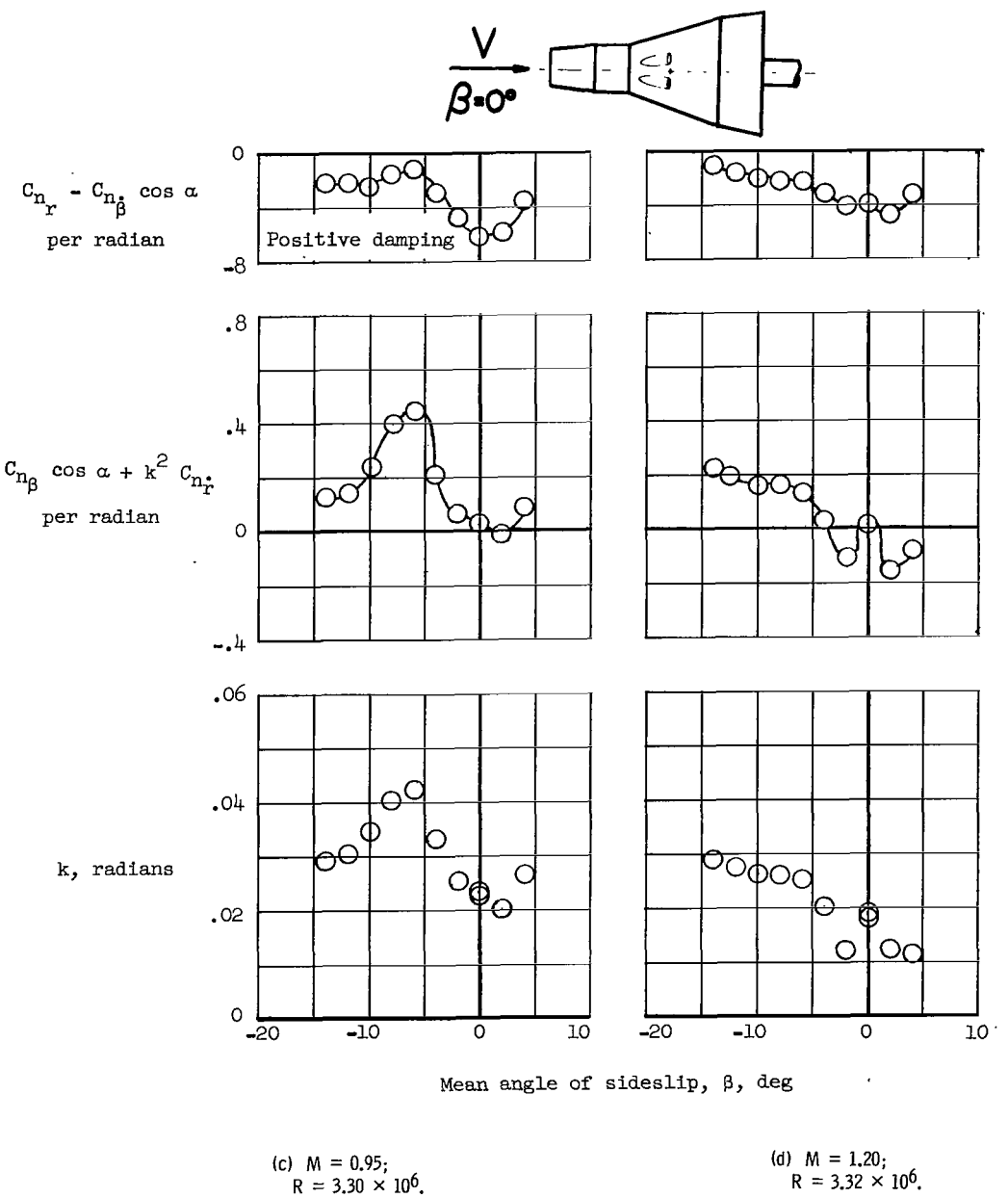

(c) M = 0.95;
R = 3.30 × 10^6.

(d) M = 1.20;
R = 3.32 × 10^6.

Figure 5.- Continued.

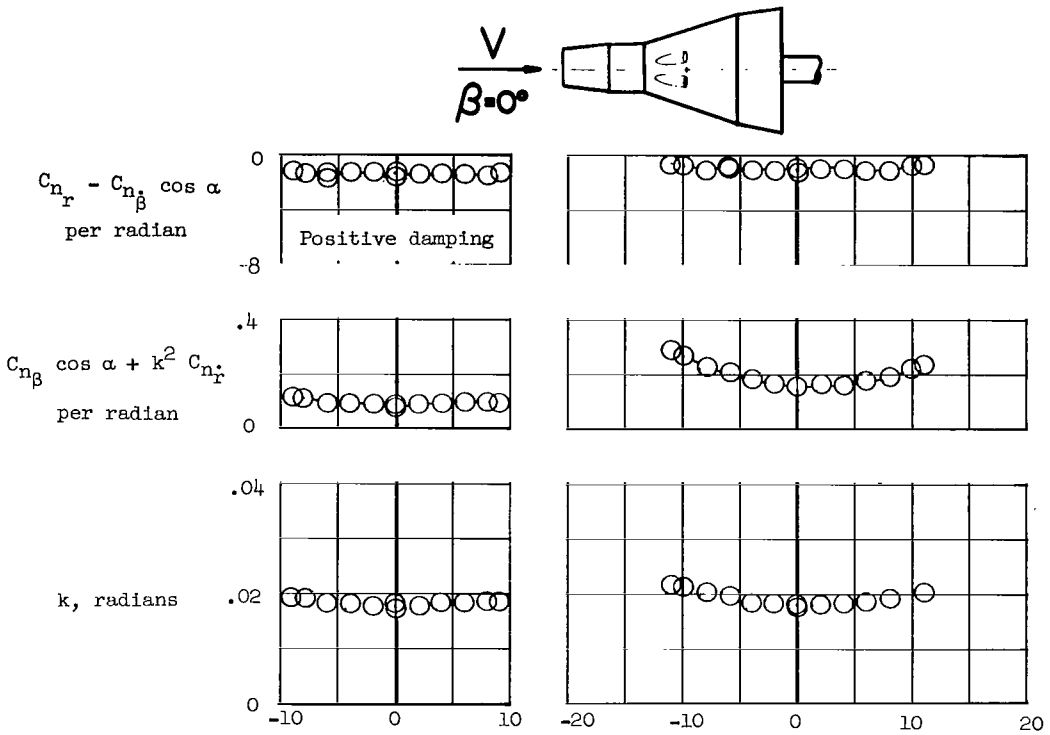

(e) M = 1.70;
R = 3.30 × 10^6.

(f) M = 2.16;
R = 3.36 × 10^6.

Figure 5.- Continued.

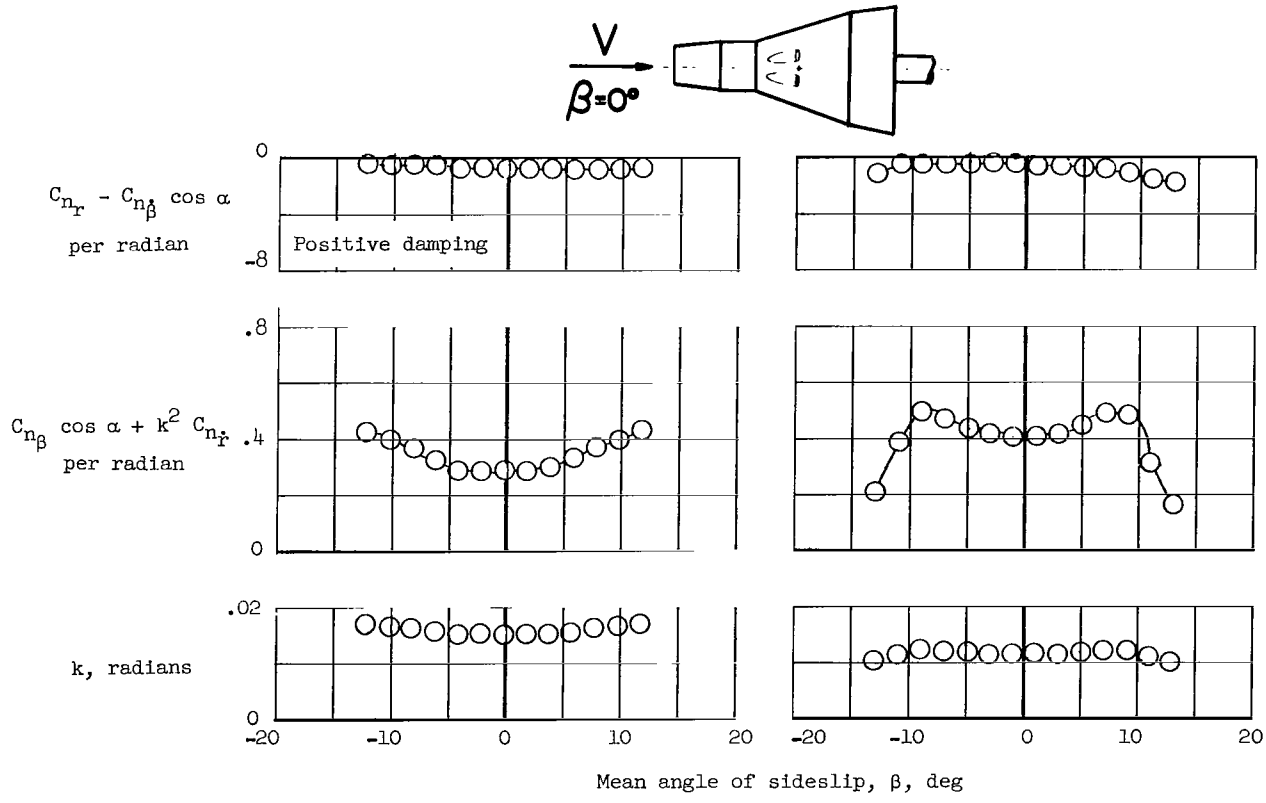

(g) M = 3.00;
R = 2.10 × 10^6.

(h) M = 4.63;
R = 1.58 × 10^6.

Figure 5.- Concluded.

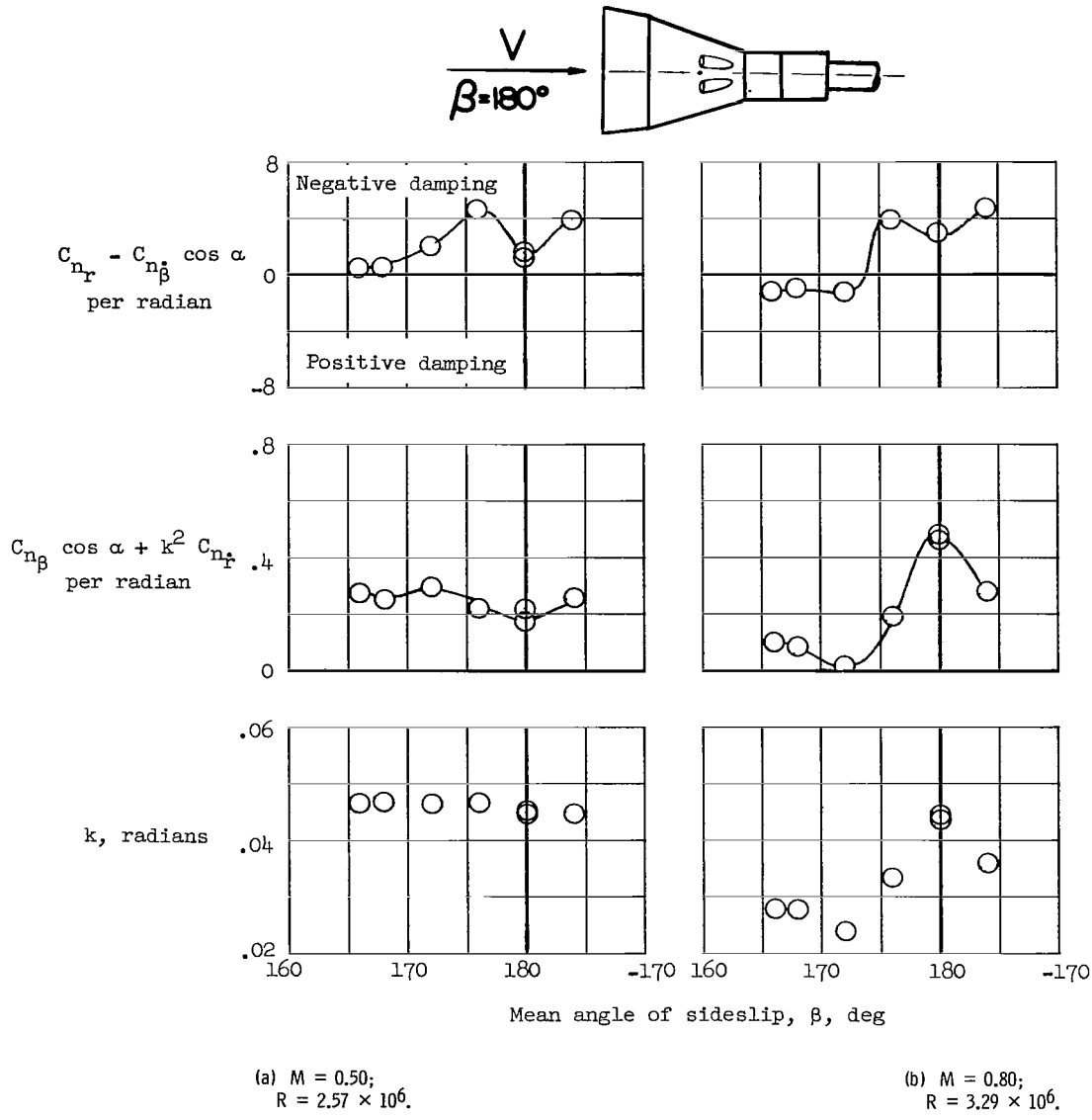

(a) M = 0.50;
R = 2.57 × 10^6.

(b) M = 0.80;
R = 3.29 × 10^6.

Figure 6.- Variation of damping-in-yaw parameter, oscillatory-directional-stability parameter, and reduced-frequency parameter with mean angle of sideslip for models of Gemini abort configuration with 0^0 cant centered around 180^0 angle of sideslip. $\alpha = 0^0$.

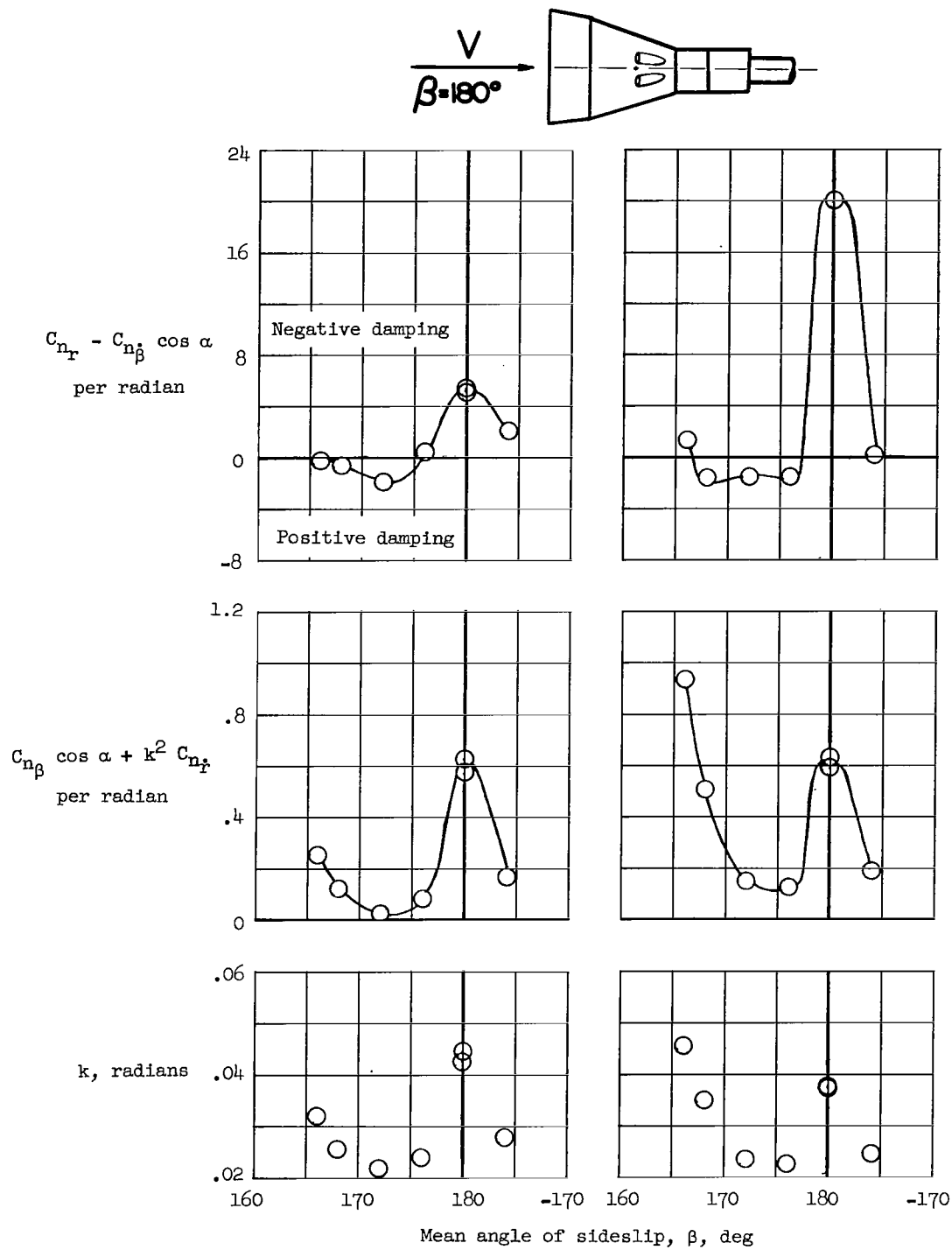

(c) M = 0.95;
R = 3.28 × 10^6.

(d) M = 1.20;
R = 3.24 × 10^6.

Figure 6.- Continued.

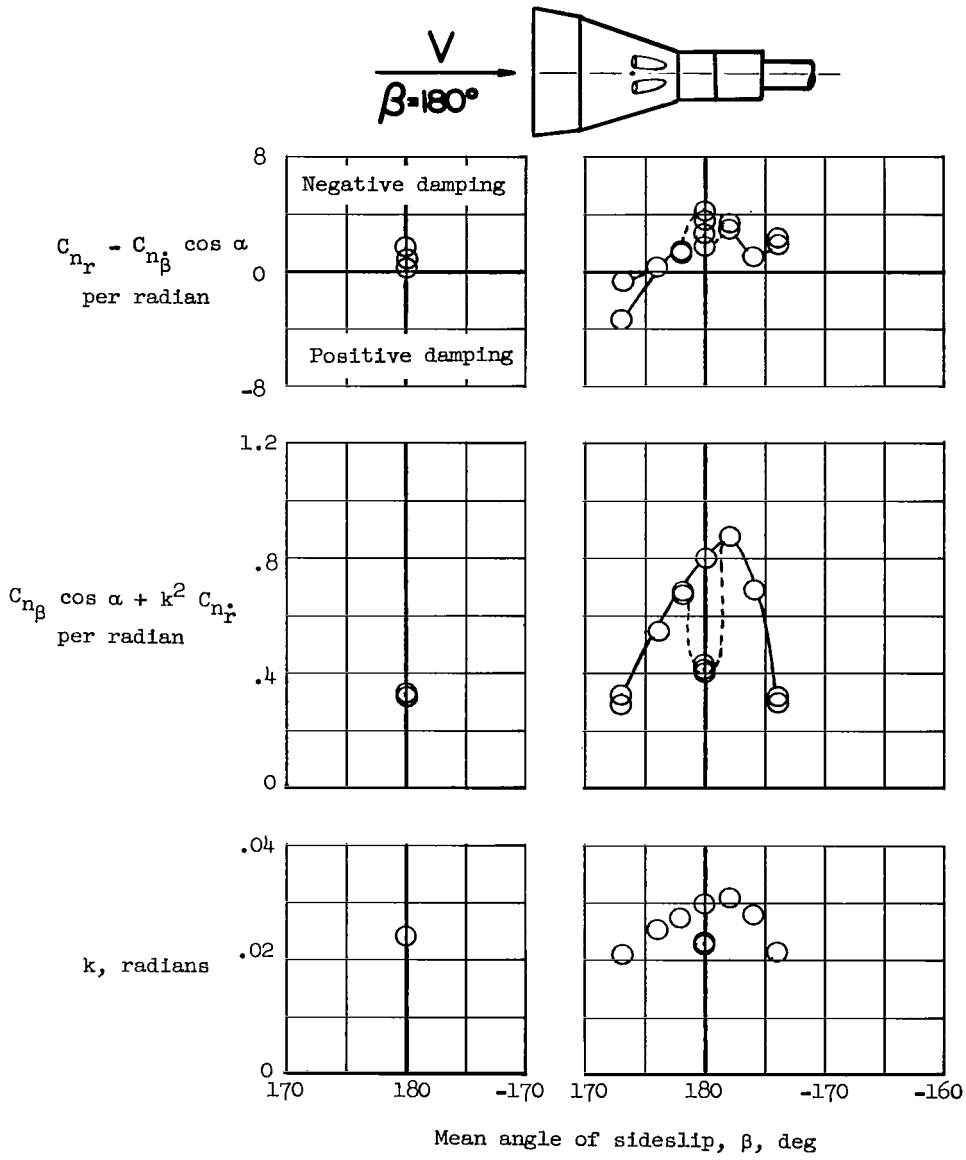

(e) M = 1.70;
R = 3.30 × 10^6.

(f) M = 2.16;
R = 3.36 × 10^6.

Figure 6.- Continued.

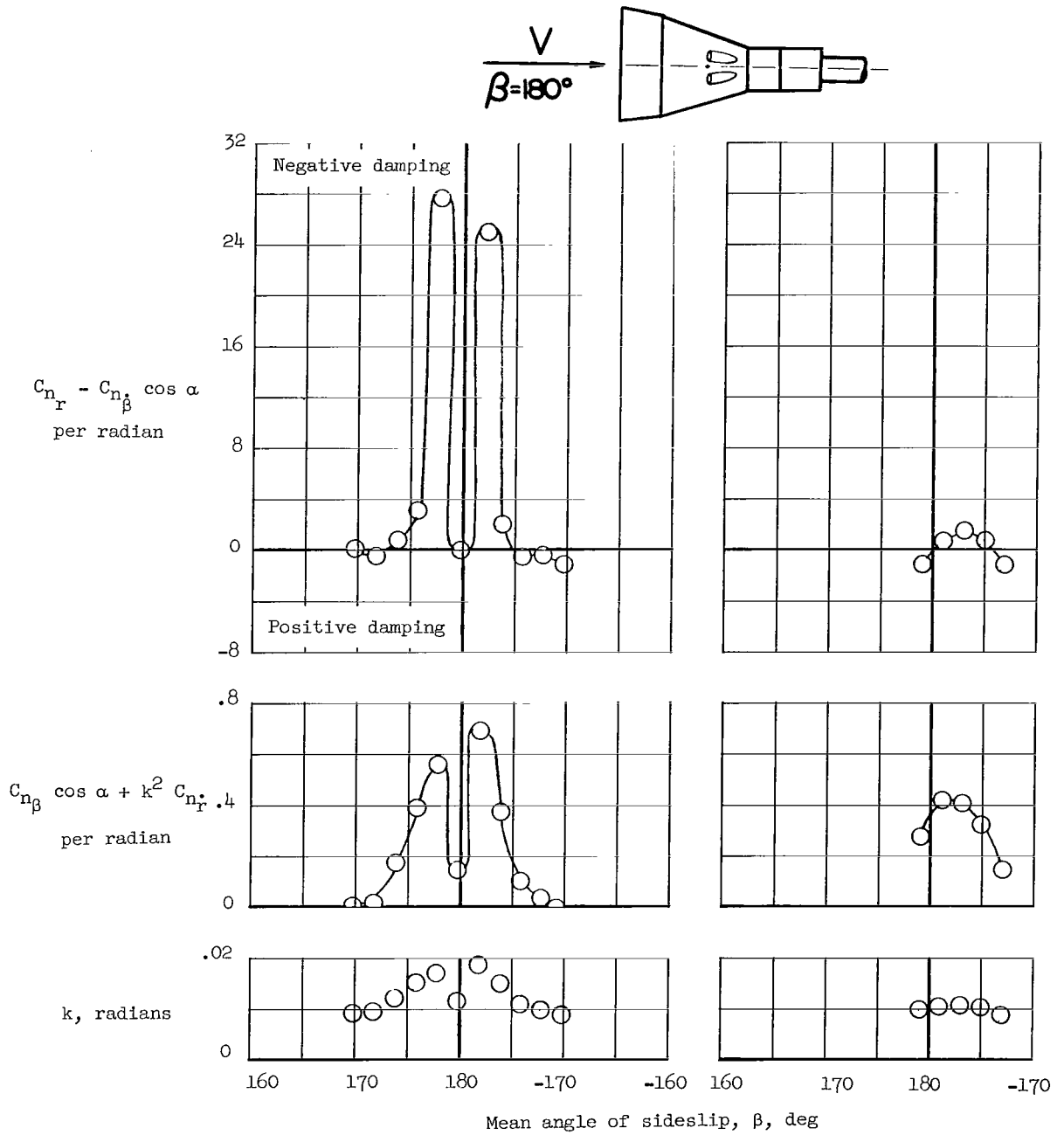

(g) M = 3.00;
R = 2.10 × 10^6.

(h) M = 4.63;
R = 1.58 × 10^6.

Figure 6.- Concluded.

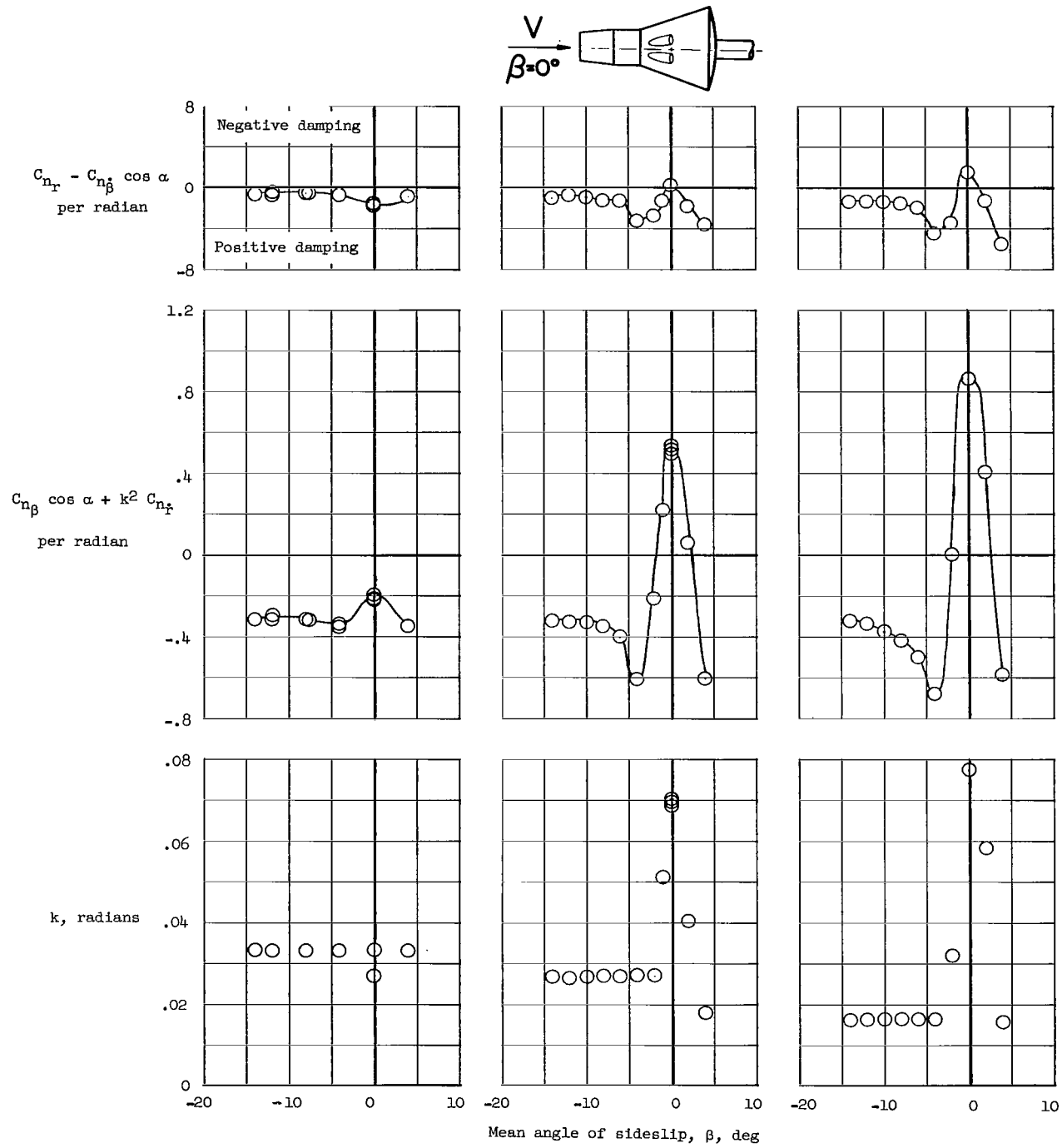

(a) M = 0.50; R = 2.56 × 10^6 to 2.87 × 10^6.

(b) M = 0.80; R = 3.27 × 10^6.

(c) M = 0.95; R = 3.29 × 10^6.

Figure 7.- Variation of damping-in-yaw parameter, oscillatory-directional-stability parameter, and reduced-frequency parameter with mean angle of sideslip for models of Gemini reentry configuration with 0^0 cant centered around 0^0 angle of sideslip. $\alpha = 0^0$.

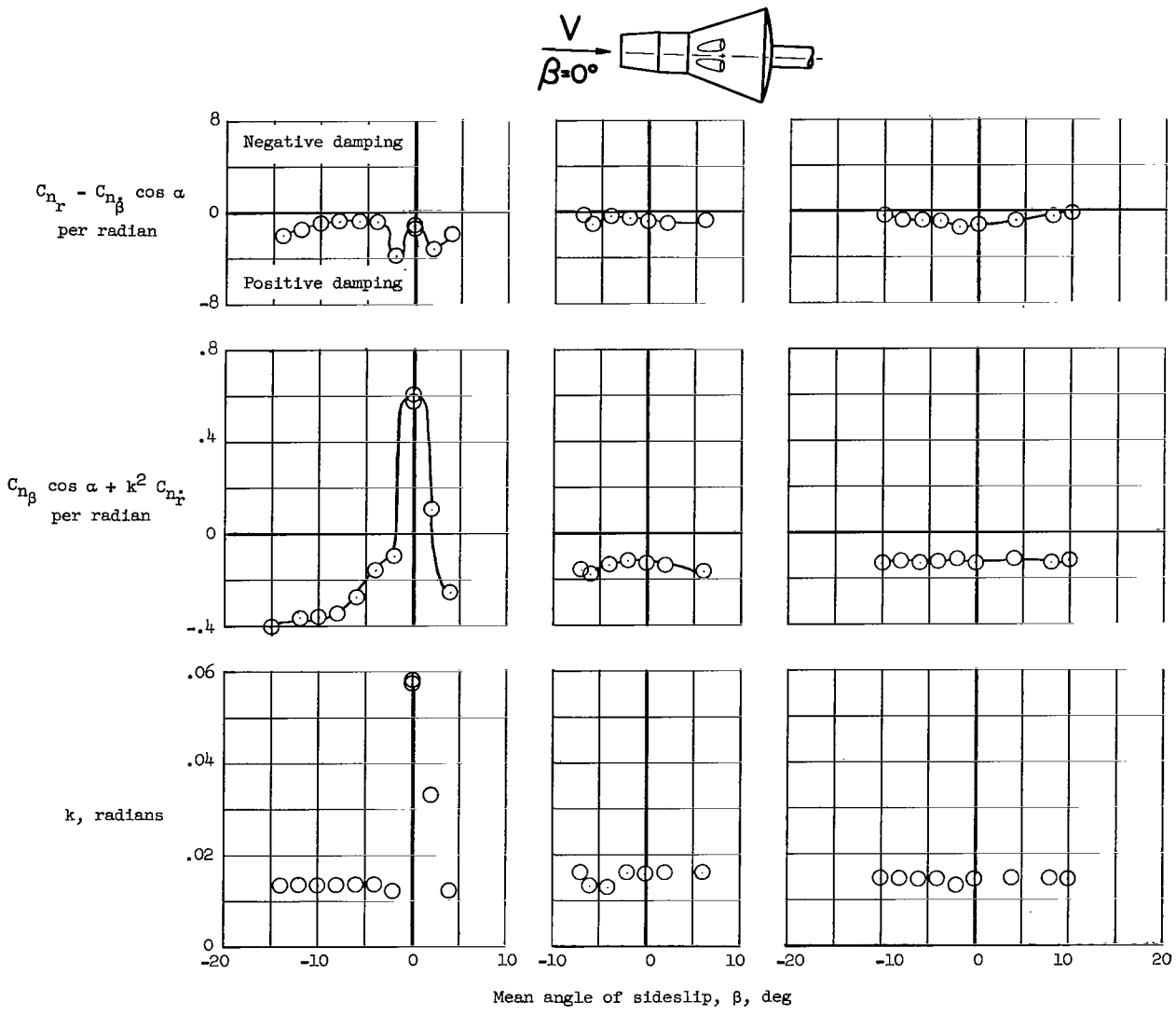

(d) M = 1.20; R = 3.32 × 10^6.

(e) M = 1.50; R = 3.33 × 10^6.

(f) M = 1.70; R = 3.30 × 10^6.

Figure 7.- Continued.

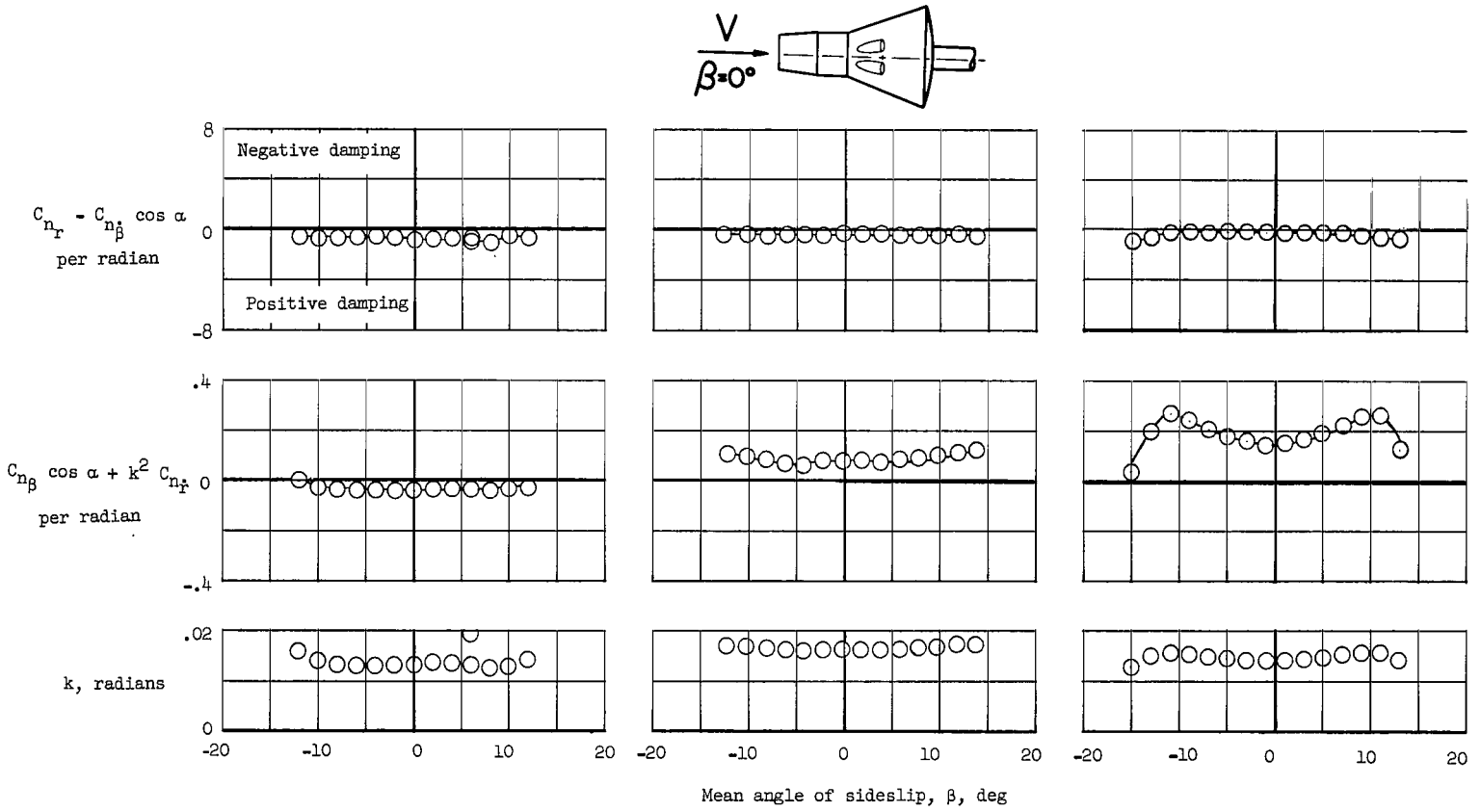

(g) M = 2.16;
R = 3.36 × 10^6.

(h) M = 3.00
R = 2.10 × 10^6.

(i) M = 4.63;
R = 1.79 × 10^6.

Figure 7.- Concluded.

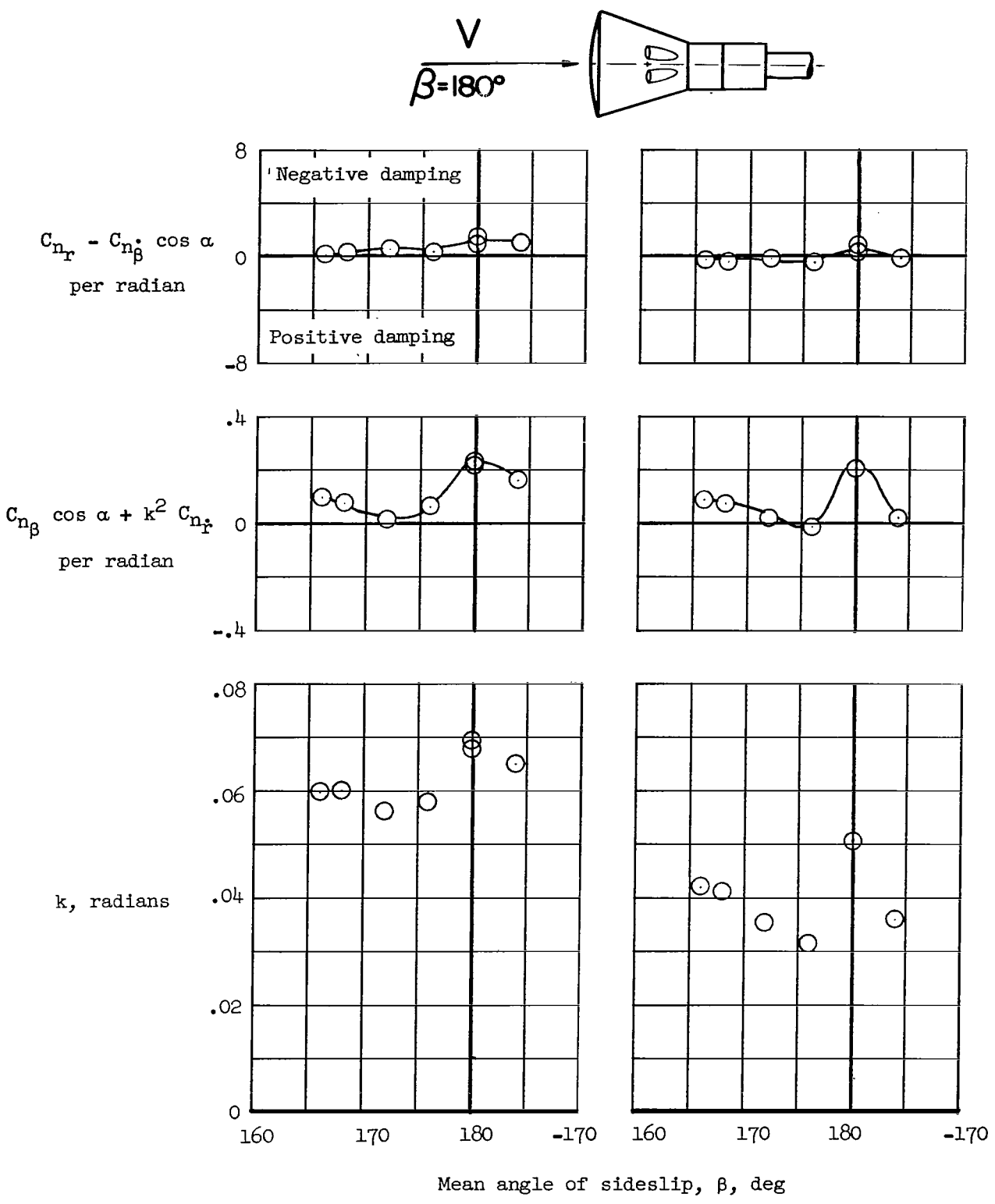

(a) M = 0.50; R = 2.57 × 10^6.

(b) M = 0.80; R = 3.29 × 10^6.

Figure 8.- Variation of damping-in-yaw parameter, oscillatory-directional-stability parameter, and reduced-frequency parameter with mean angle of sideslip for models of Gemini reentry configuration with 0^0 cant centered around 180^0 angle of sideslip. $\alpha = 0^0$.

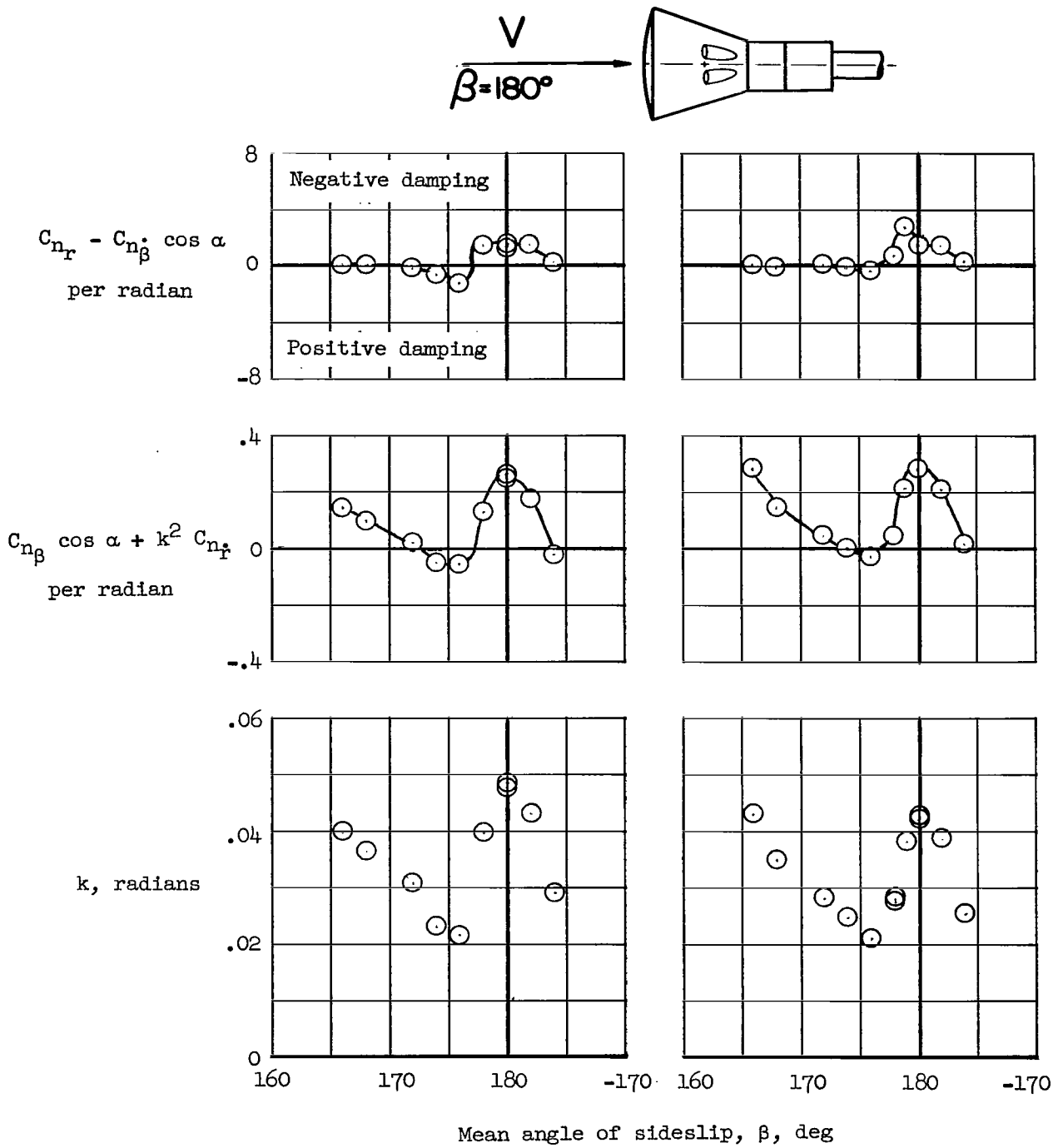

(c) M = 0.95;
R = 3.25 × 10^6.

(d) M = 1.20;
R = 3.25 × 10^6.

Figure 8.- Continued.

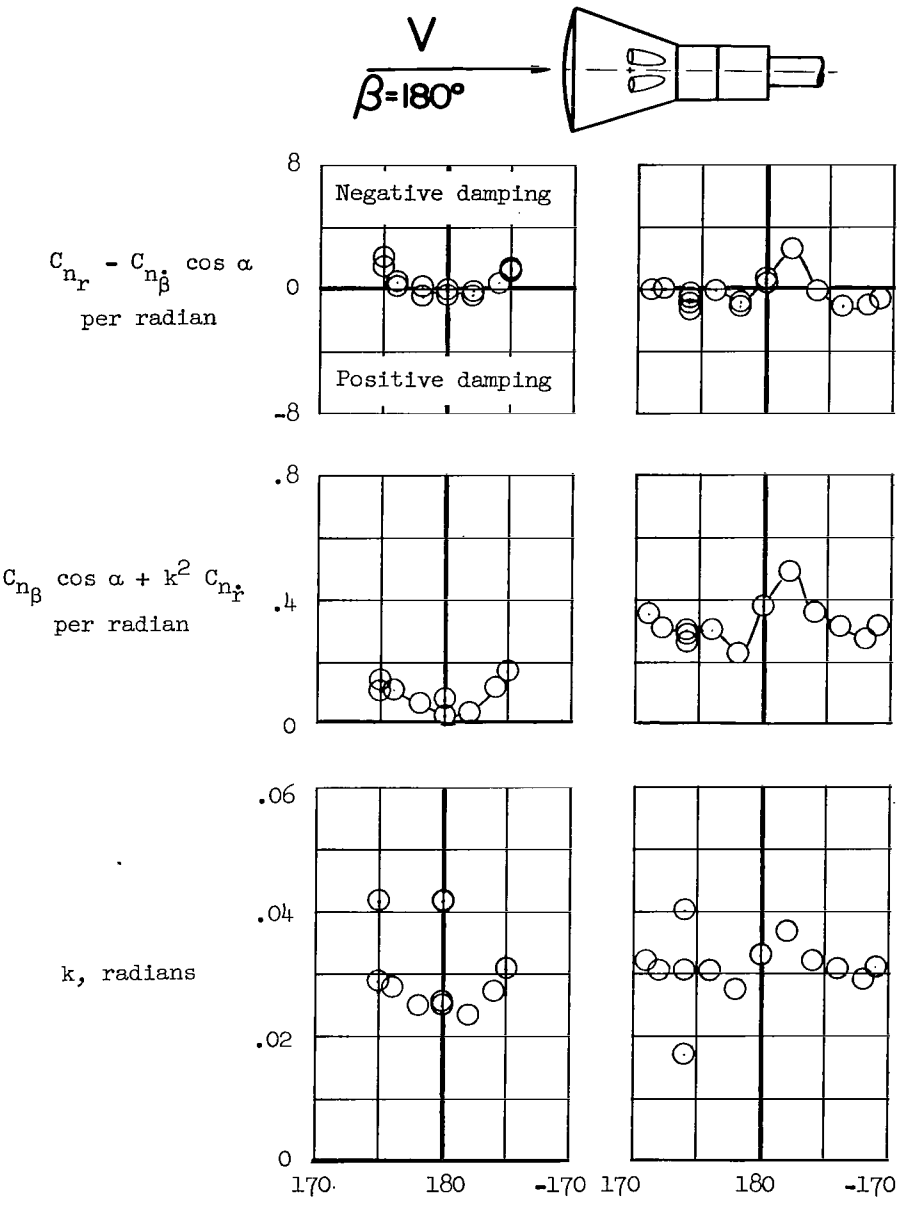

(e) M = 1.70; R = 3.30 × 10^6.

(f) M = 2.16; R = 3.36 × 10^6.

Figure 8.- Continued.

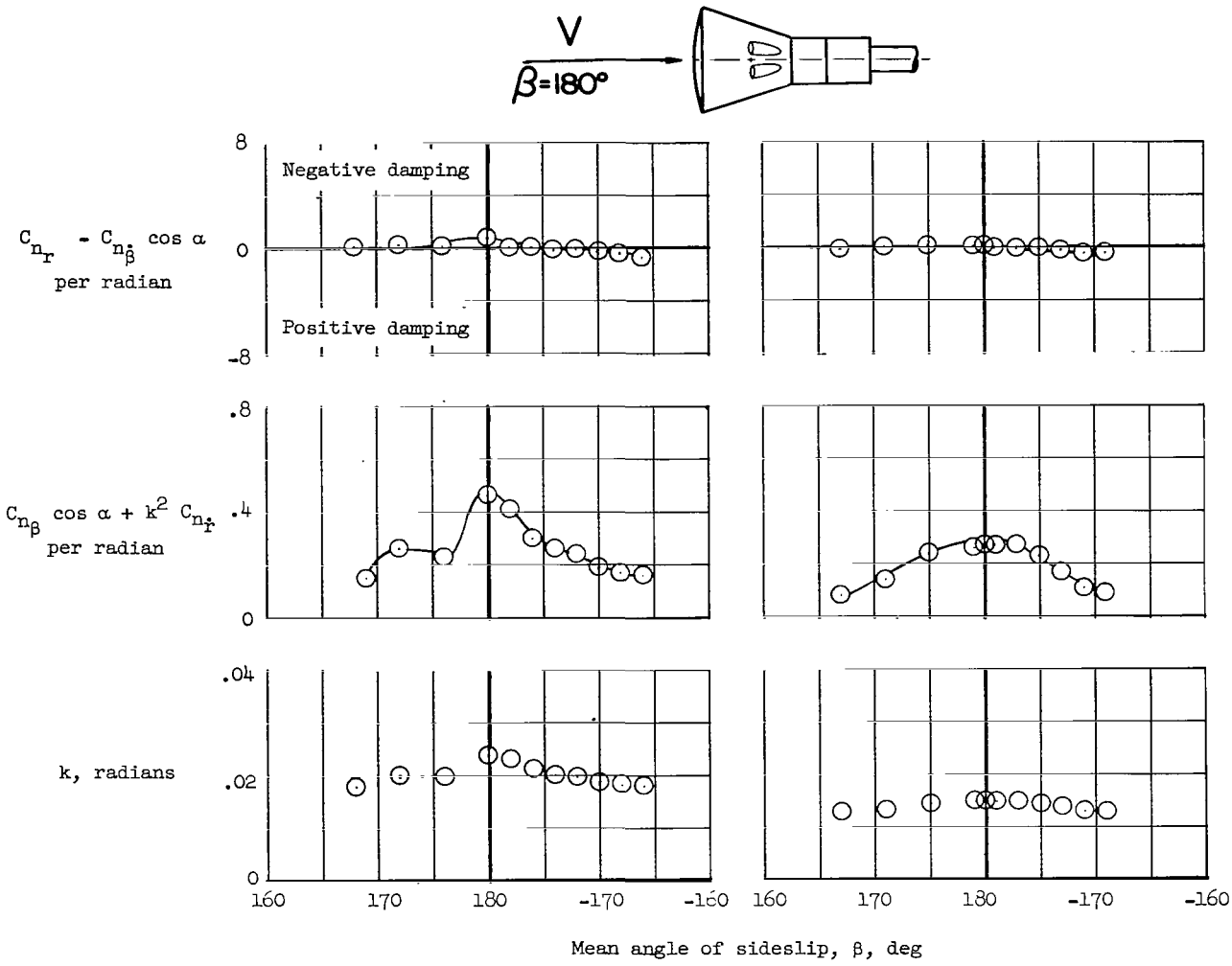

(g) M = 3.00;
R = 2.10 × 10^6.

(h) M = 4.63;
R = 1.57 × 10^6.

Figure 8.- Concluded.

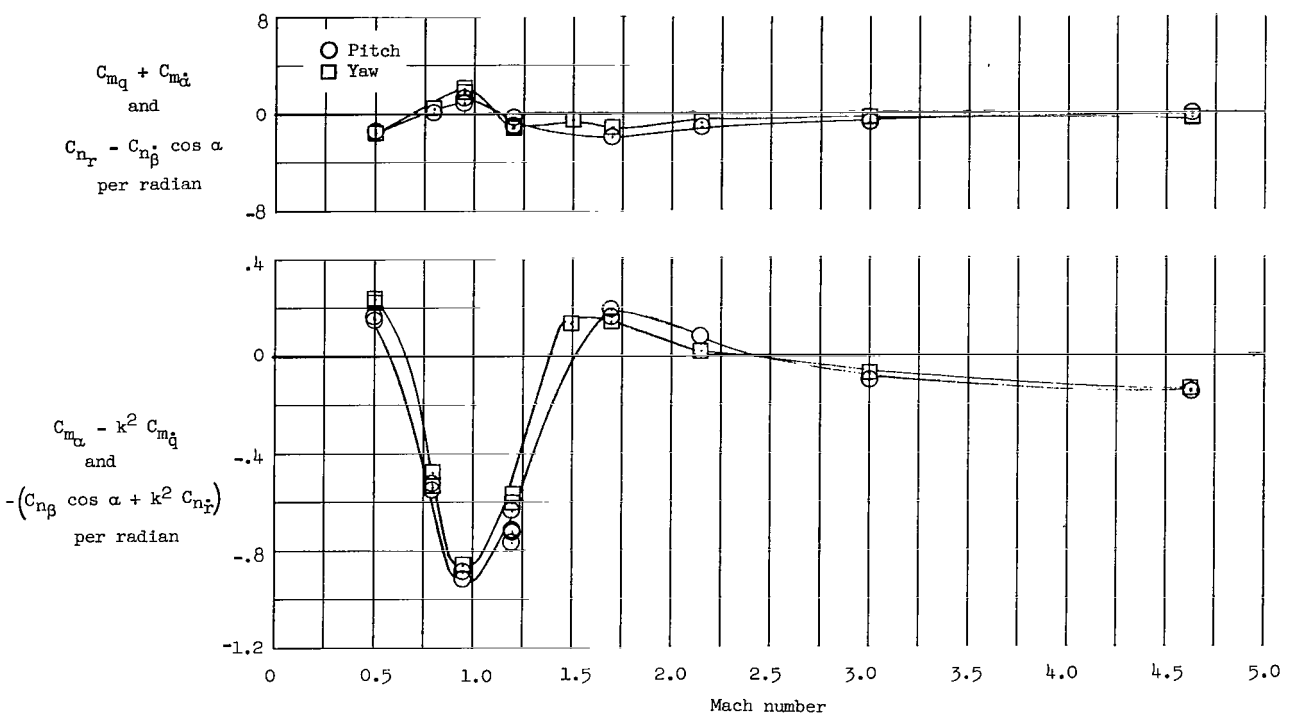

(a) Reentry configuration with 0^0 cant.

Figure 9.- Variation of damping-in-pitch parameter, damping-in-yaw parameter, oscillatory-longitudinal-stability parameter, and oscillatory-directional-stability parameter with Mach number. $\alpha = \beta = 0^0$.

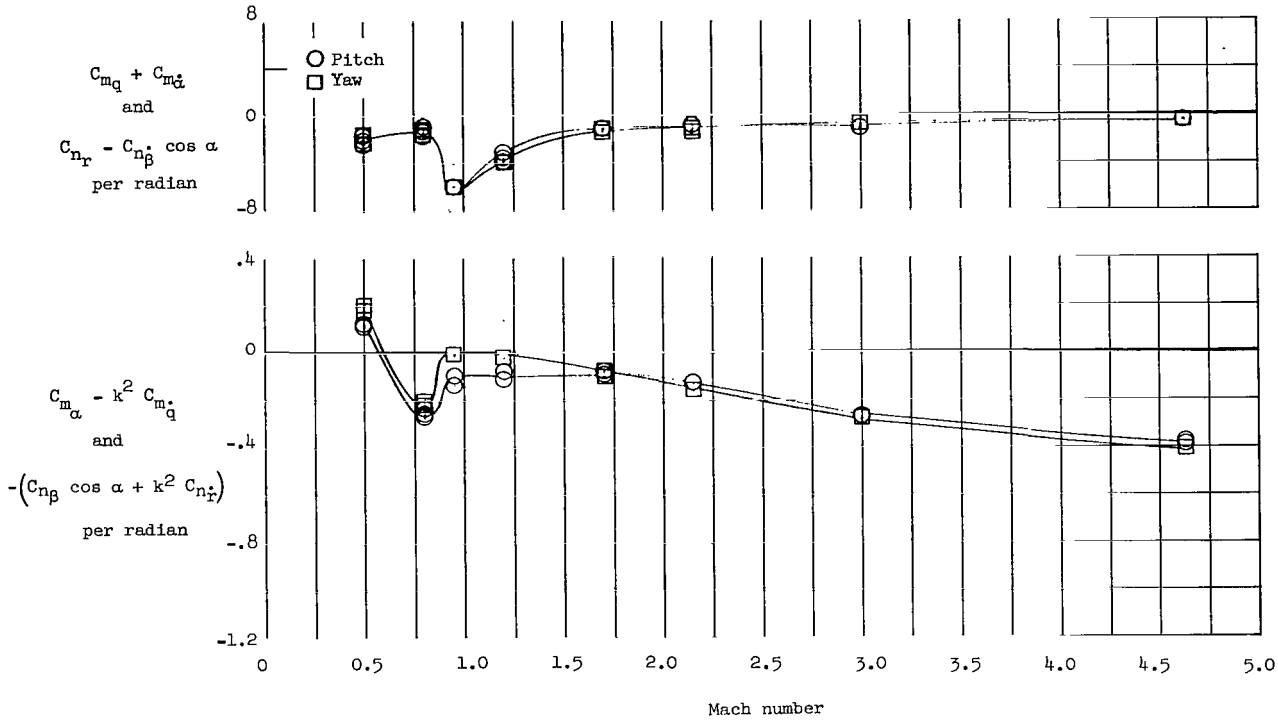

(b) Abort configuration with 0^0 cant.

Figure 9.- Concluded.

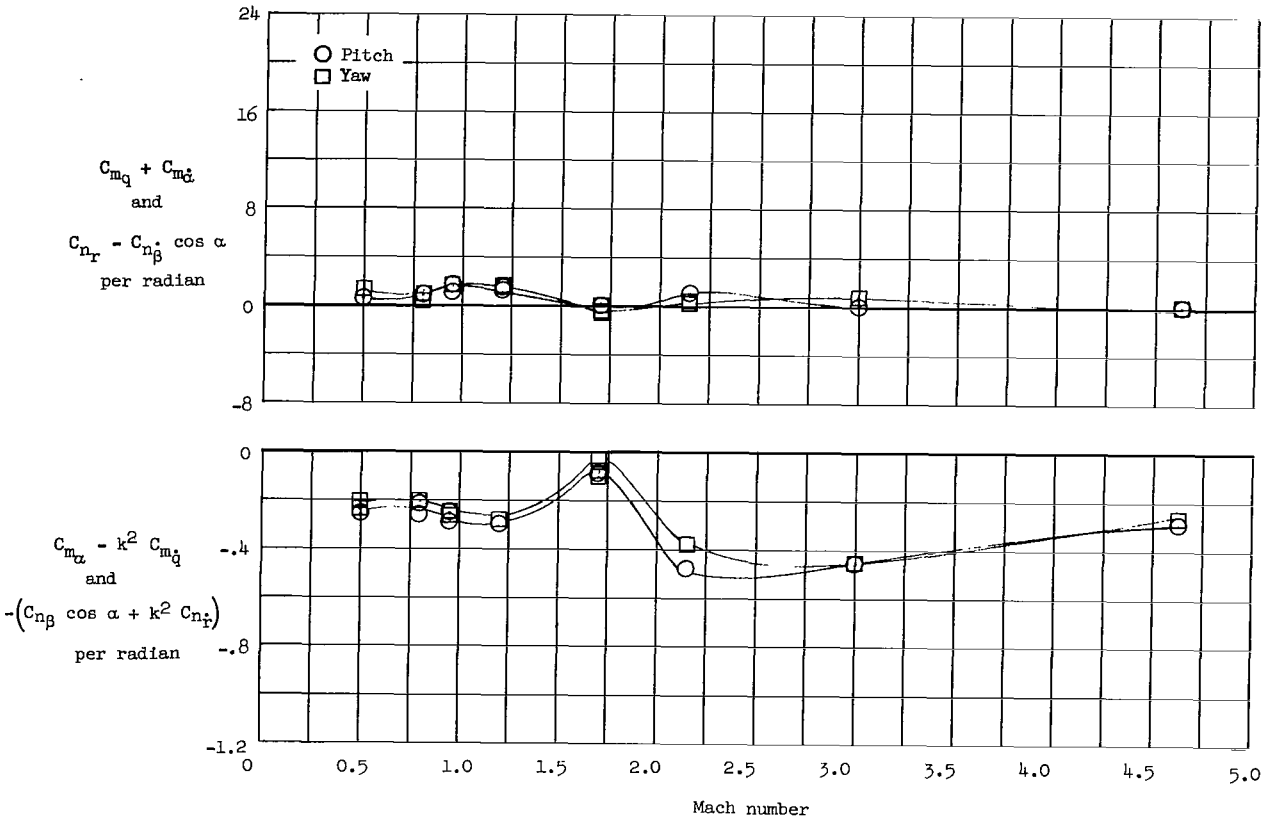

(a) Reentry configuration with 0^0 cant.

Figure 10.- Variation of damping-in-pitch parameter, damping-in-yaw parameter, oscillatory-longitudinal-stability parameter, and oscillatory-directional-stability parameter with Mach number. $\alpha = \beta = 180^0$.

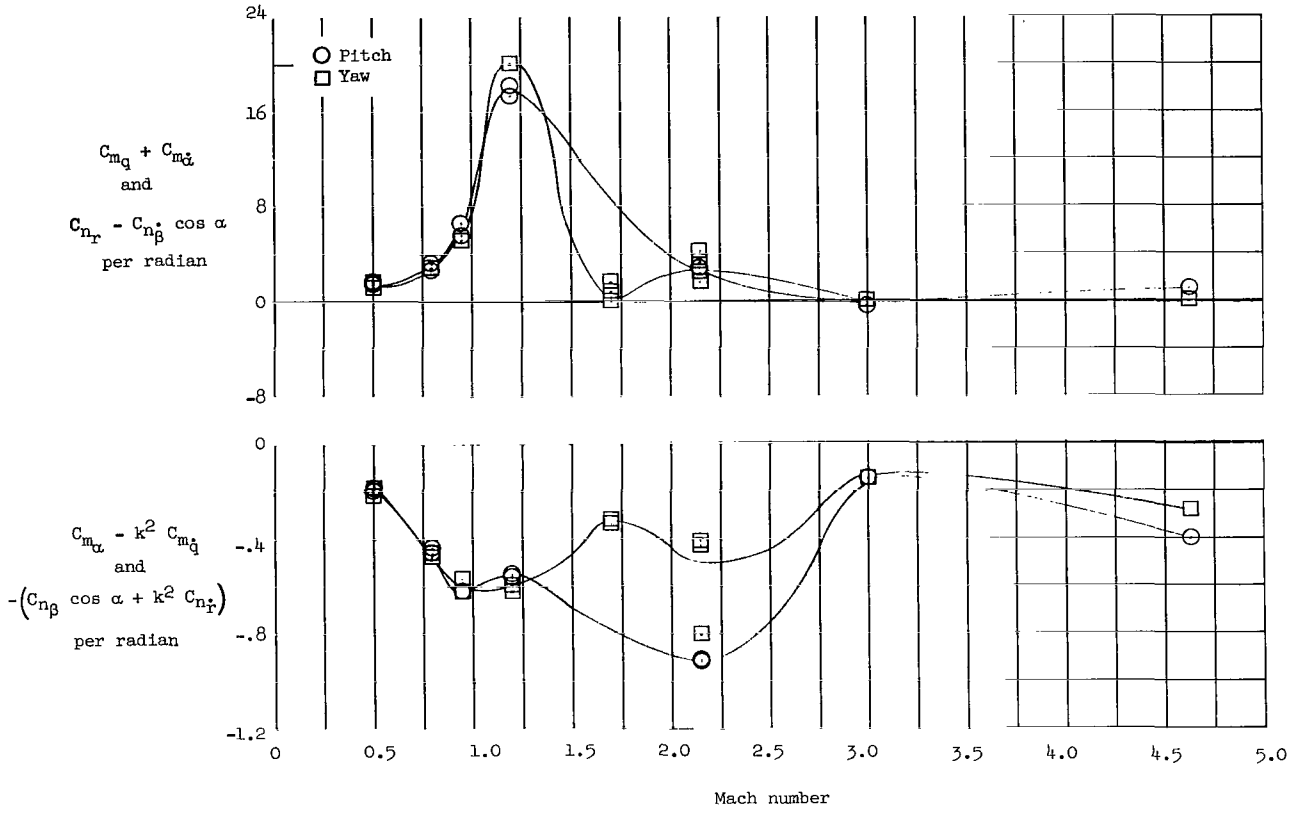

(b) Abort configuration with 0^0 cant.

Figure 10.- Concluded.

"The aeronautical and space activities of the United States shall be conducted so as to contribute . . . to the expansion of human knowledge of phenomena in the atmosphere and space. The Administration shall provide for the widest practicable and appropriate dissemination of information concerning its activities and the results thereof."

—NATIONAL AERONAUTICS AND SPACE ACT OF 1958

NASA SCIENTIFIC AND TECHNICAL PUBLICATIONS

TECHNICAL REPORTS: Scientific and technical information considered important, complete, and a lasting contribution to existing knowledge.

TECHNICAL NOTES: Information less broad in scope but nevertheless of importance as a contribution to existing knowledge.

TECHNICAL MEMORANDUMS: Information receiving limited distribution because of preliminary data, security classification, or other reasons.

CONTRACTOR REPORTS: Technical information generated in connection with a NASA contract or grant and released under NASA auspices.

TECHNICAL TRANSLATIONS: Information published in a foreign language considered to merit NASA distribution in English.

TECHNICAL REPRINTS: Information derived from NASA activities and initially published in the form of journal articles.

SPECIAL PUBLICATIONS: Information derived from or of value to NASA activities but not necessarily reporting the results of individual NASA-programmed scientific efforts. Publications include conference proceedings, monographs, data compilations, handbooks, sourcebooks, and special bibliographies.

Details on the availability of these publications may be obtained from:

SCIENTIFIC AND TECHNICAL INFORMATION DIVISION

NATIONAL AERONAUTICS AND SPACE ADMINISTRATION

Washington, D.C. 20546